Computational methods toward early detection of neuronal deterioration

Seyed-Ali Sadegh-Zadeh

This thesis is submitted in partial fulfilment of the requirements for the degree of

Doctor of Philosophy in Computer Science

Department of Computer Science

The University of Hull

January 2019

Abstract

In today's world, because of developments in medical sciences, people are living longer, particularly in the advanced countries. This increasing of the lifespan has caused the prevalence of age-related diseases like Alzheimer's and dementia. Researches show that ion channel disruptions, especially the formation of permeable pores to cations by Aβ plaques, play an important role in the occurrence of these types of diseases. Therefore, early detection of such diseases, particularly using non-invasive tools can aid both patients and those scientists searching for a cure. To achieve the goal toward early detection, the computational analysis of ion channels, ion imbalances in the presence of Aβ pores in neurons and fault detection is done. Any disruption in the membrane of the neuron, like the formation of permeable pores to cations by Aβ plaques, causes ionic imbalance and, as a result, faults occur in the signalling of the neuron.

The first part of this research concentrates on ion channels, ion imbalances and their impacts on the signalling behaviour of the neuron. This includes investigating the role of Aβ channels in the development of neurodegenerative diseases. Results revealed that these types of diseases can lead to ionic imbalances in the neuron. Ion imbalances can change the behaviour of neuronal signalling. Therefore, by identifying the pattern of these changes, the disease can be detected in the very early stages. Then the role of coupling and synchronisation effects in such diseases were studied. After that, a novel method to define minimum requirements for synchronicity between two coupled neurons is proposed. Further, a new computational model of Aβ channels is proposed and developed which mimics the behaviour of a neuron in the course of Alzheimer's disease. Finally, both fault computation and disease detection are carried out using a residual generation method, where the residuals from two observers are compared to assess their performance.

Acknowledgements

At first, all praise is due to almighty Allah, the lord of the worlds for granting me the ability, strength and determination to complete this PhD. I am profoundly grateful to my supervisor, Dr Chandrasekhar Kambhampati for encouraging and assisting me throughout the PhD. I would like to avail this opportunity to appreciate his support and his advices that helped me to face the challenges more successfully. I think myself fortunate enough to be one of his students.

I would also like to thanks Dr Darryl N. Davis as a chairperson and Dr Yongqiang Cheng as a technical expert of the panel meetings and their friendly advices that helped me to stay positive and more focused. Special thanks go to the staff and technicians of the Department of Computer Science, the University of Hull, for their assistance and providing me with a nice work environment along with the great technical facilities.

Public Outputs

Some of the supporting material used in a number of sections of this thesis were published elsewhere as shown in the following Public Outputs by the author.

1- **SA Sadegh-Zadeh**, C Kambhampati, *Analysing the impact of sodium channels in Alzheimer's disease using a computational model*, 26th Annual Computational Neuroscience Meeting (CNS*2017)

2- **SA Sadegh-Zadeh**, C Kambhampati, *All-or-None Principle and Weakness of Hodgkin-Huxley Mathematical Model*, International Journal of Mathematical and Computational Sciences, Vol: 11, No: 11, 2017.

3- **SA Sadegh-Zadeh**, C Kambhampati, *A Computational Investigation of the Role of Ion Gradients in Signal Generation in Neurons*, Conference: Computing Conference 2018, London, UK

4- **SA Sadegh-Zadeh**, C Kambhampati, *Computational investigation of amyloid peptide channels in Alzheimer's disease*, MDPI Journal, J-Multidisciplinary Scientific Journal, Volume 2, Issue 1, 2019, DOI 10.3390/j2010001

5- **SA Sadegh-Zadeh**, C Kambhampati, DN Davis, *Ionic imbalances and coupling in synchronisation of responses in neurons*, MDPI Journal, J-Multidisciplinary Scientific Journal, Volume 2, Issue 1, 2019, DOI 10.3390/j2010003

List of Abbreviations and Symbols

Abnormal Event Management	AEM
Action Potential	AP
Alzheimer's Disease	AD
Amyotrophic Lateral Sclerosis	ALS
Beta-Amyloid	$A\beta$
Central Nervous System	CNS
Cerebrospinal Fluid	CSF
Chloride	Cl-
Corticobasal Degeneration	CBD
Dementia with Lewy Bodies	DLB
Electroencephalogram	EEG
Fault Detection	FD
Frontotemp Dementia	FTD
Hodgkin-Huxley	HH
Huntington's Disease	HD
Inhibition Neurones	IN
Input/Output	I/O
Magnetic Resonance Imaging	MRI
Mild Cognitive Impairment disease	MCI
Multiple System Atrophy	MSA
Neurodegenerative Disorders	NDDs
Parkinson's Disease	PD
Peripheral Nervous System	PNS

Positron Emission Tomography	PET
Potassium	K+
Progressive Supranuclear Pols	PSP
Sodium	Na+
Spinocerebellar Ataxia Disorders	SCA
Thalamo-Cortical Relay	TCR
voltage-gated calcium channels	CaV
voltage-gated sodium channels	NaV

Content

Figures

Tables

1 Introduction

1.1 Background

Studies on the brain have become a highly interdisciplinary field which is no longer confined to medicine, neurophysiology and related fields. In fact, in our efforts to understand the functioning of the human brain, many concepts are taken directly from physics, mathematics, computer science (especially artificial intelligence, computational biology and computational neuroscience) and related fields. This list is not complete, but it indicates the concepts and computational techniques from these fields which enable a deeper understanding of the behaviour of large networks of neurons.

The term neurodegeneration is an umbrella term for describing progressive disorders which lead to senile neurological disorders. Such kinds of diseases can show a variety of symptoms such as speech difficulties, cognitive impairment, and motor dysfunctions (Andreas & Bowser, 2017). The loss of neuronal populations in the central nervous system is the underlying pathological cause of the diseases. Parkinson's disease (PD), Alzheimer's disease (AD), amyotrophic lateral sclerosis (ALS), multiple system atrophy (MSA), progressive supranuclear pols (PSP), spinal muscular atrophy, front temp dementia (FTD), spinocerebellar ataxia (SCA) disorders, and corticobasal degeneration (CBD) are some of these diseases. This thesis focusses on the development of models which enable us to get an insight into the manner in which neuro-degenerative problems are propagated. The main focus will be on Alzheimer's disease and its cause to opening of extra ionic channels.

Alzheimer's disease is the common neurodegenerative disorder; it is a chronic neurodegenerative disease that accounts for 60% to 70% of cases of dementia (Lewis, et al., 2014); (Serretti, et al., 2017). The disease usually starts very slowly in the onset process and gets worse over the time. The most common early warning sign is difficulty in remembering recent events and loss of the short-term memory (World-Health-Organization, 2015). This stage is usually known as prodromal Alzheimer's disease. Alzheimer's disease affects more than 35 million people worldwide and 5 million people in Europe, with the universal prevalence of Alzheimer's disease predicted to quadruple to more than 106 million by 2050 (Brookmeyera, et al., 2007). A financial review put the total cost of Alzheimer's disease to the economy of Great Britain at over £26 billion per annum (Brookmeyera, et al., 2007); (Andlin-Sobocki, et al., 2005). In 2015, Alzheimer's disease was the leading cause of death in both males and females over 80 years old, in the United Kingdom (Public-Health-England, 2017). Approximately 850,000 British people had Alzheimer's disease in 2014. With the expected ageing of the British population, it is estimated that 2 million older British people will have Alzheimer's in 2050 (Gallagher, 2014). Given the predictions of an increase in cases of neuro-degenerative diseases , it is estimated that total health care costs for Alzheimer's disease will reach £59.4 billion by 2050 (Lewis, et al., 2014).

1.2   Motivation

The neurodegenerative diseases like Alzheimer's disease can be seen as a fault accrued in the nervous system or neurons. In order to early detection of disease the detection of fault is needed. Study on computational model of nervous system can enable scientists to apply fault and fault detection on nervous system. The model of neuron as a basic and fundamental part of a nervous system can help scientist to study on the behaviour of

neuron during the faulty condition. The ability to simulate a neuron under different conditions allows scientists to study different diseases without recourse to the study of real neurons, this however, implies that the computational models are an accurate representation of the real neurons. The reason for this is that laboratory-based experiments can take weeks for the realisation of results, while computational experiments take remarkably less time. In addition computational simulations offer the advantage of flexible adjustment of environment variables to gather a broad range of data.

The model of the neuron can be used to see how action potential will influence the neural signal and signal transaction. In some neurodegenerative diseases, like Alzheimer's disease the disease can be seen as an ionic imbalances in the neuron. An ionic imbalance is the progressive damage of function of neurons, including the death of neurons. In Alzheimer's disease the deterioration of neuronal function is a result of the accumulation of beta-amyloid (Aβ) plaques and neurofibrillary tangles associated protein τ in the some parts of the brain (Perez, et al., 2017). This accumulation causes some pores which are permeable to cations like sodium, potassium, calcium etc (Andreas & Bowser, 2017).

 Today, Alzheimer's disease is clinically diagnosed by complicated examinations and through neuropsychological and cognitive tests. In addition to these facilities, the latest guidelines for the diagnostics of Alzheimer's disease (Frisoni, et al., 2017); (McKhannab, et al., 2011); (Kou & Chen, 2017); (Waldemar, et al., 2007) confirm the important role of several biomarkers. These include measures from Electroencephalogram (EEG), positron emission tomography (PET), magnetic resonance imaging (MRI), and cerebrospinal fluid (CSF) protein profiles, as well as any kind of genetic risk profiles.

Detection of Alzheimer's disease in the early stages is very difficult, because the rate of progression is slow in the early stage (Braak & Braak, 1991) ; (Sierpina & Kreitzer,

2012); (Hampel, 2011). A solution to this problem of early detection is not clear, and requires more extensive studies. This thesis, develops a framework which will enable the development of strategies for early detection. Clinical studies are currently focussing on early detection and preliminary studies are yielding some interesting results. However, the early diagnosis of Alzheimer's disease remains the most important and unresolved issues for national health services.

A key to both understanding of and the development of computational methods for Alzheimer's disease is to understand the various stages of progression. Alzheimer's disease progresses through various stages, early stage, middle stage, and severe or late stage (Hampel, 2011). One possible approach would be to build on the advances in artificial intelligence in healthcare to modify the diagnoses of Alzheimer's (Jiang, et al., 2017). This would make it possible for specialists to use artificial intelligence technologies in their medical develop and decision-making process using for instance pattern recognition through the data obtained from the nervous system to early detection (Obreja, et al., 2017). Since the definitive diagnosis of these diseases can be accomplished by examination of damaged tissues of brain after patient death, thus the research agenda is completely timely and appropriate (Mantzavinos, et al., 2017). There is another problem, as well. Clear symptoms of neurodegenerative diseases (for example, gait disorders) only occurred in the advanced stages of the disease exactly when there is no possible treatment available (Raggi, et al., 2017). This often puts the patient in a wretched state, waiting for his death. Thus, new methods for the early detection of symptoms are needed to either prevent or mitigate the disease process (Awasthi, et al., 2017).

The motivation for this research arises from the existing knowledge of neural modelling, the computational ability to predict a neural response. This research study will contribute to a general foundation for recreating neural functions and the external stimulus with a view towards enhancing our understanding of neuronal degeneration in the case of Alzheimer's disease. It also contribute to the impact of ion gradients in exacerbating neurodegenerative diseases, defining a region for synchronicity in coupled neurons, finding the relation between coupling conductance and synchronisation between neurons, study about the computational model of amyloid channels and applying fault detection to identifying changes in action potential in neural disorder using a computational study of neural functions.

1.3   Context of Research

Computational neuroscience studies the brain function, the properties of information processing and the structures that make up the mechanism of nervous system. Its aim is to illustrate how electrical and chemical signals are used to process information by the neurons and the hence the brain. Despite the advances concerning the structure of the brain at the cellular and molecular levels, including learning and memory, taking place over the last several decades; several significant scientific problems remain to be solved. The first step to achieving diagnostic tools is detecting any faults in order to diagnose changes in the patient's neurological system before prodrome or at most at the beginning of the prodrome. This is because surveys show that usually the disease process has started, long time before any critical damage is done to the brain (Yang, et al., 2003). Therefore, early detection of the disease remains critical to preserving the brain before any severe damage due to Alzheimer's disease occurs.

The neuropathological changes in Alzheimer disease, which include cognitive and behavioural changes in patients, are now well known. Despite this, little therapeutic advance can be found in the research on Alzheimer's disease. One cause for this may be the unavailability of tools or methods for distinguishing other forms of primary degenerative dementia related to senescence from Alzheimer's disease. Unfortunately, as mentioned before, distinct symptoms of Alzheimer's disease are not shown until the course of the disease is relatively far advanced. In this stage, usually, major pathological degradation of the brain has already occurred (Geula, 1998). It is widely thought that early diagnosis of Alzheimer's disease might open the door to specifying drugs to delay the beginning of the disease by even a decade (Awasthi, et al., 2017). On the other hand, the chance of fully curing the disease is not completely denied (Geula, 1998); (Cummings, et al., 1998).

According to research and existing literature (Kumar, et al., 2016); (Perez, et al., 2016); (Arispe, et al., 1993); (Ullah, et al., 2015) there is growing evidence that ion channel dysfunctioning has a direct impact on neurodegenerative disorders (NDDs). Many neurological disorders affecting the central nervous system, are caused due to alteration in the function of ion channels (Kumar, et al., 2016). Here, ion channel dysfunctioning is one of the identifying characteristics of neurodegenerative disorders. Even though it is likely that such dysfunction can be an indicator of underlying pathological deviation associated with other biological disorders, the prodromal stages of neurodegenerative disorders are clearly recognisable from a set of control subjects. Studies show that 28.2% of patients who are affected by Mild Cognitive Impairment (MCI) were diagnosed with Alzheimer's disease in the period of 14.8 months (Soininen, et al., 1992); (Prinz & Vitiell, 1989).This enhances speculation that mild cognitive impairment may be a precursor to Alzheimer's disease (Babilonia, et al., 2009); (Rossini, et al., 2006).

There is a general consensus among experts that ion channels play a crucial role in the maintaining of cell homeostasis. Further, ion channels are very significant as these channels specify the membrane potential and play a critical role in the secretion of neurotransmitter. In addition, ion channel abnormalities produce a range of symptoms which symptoms can include movement disabilities, memory loss, and neuromuscular sprains (Kumar, et al., 2016). A challenging problem for neuroscientists is the implementation of therapeutics for targeting neurodegenerative disorders.

1.4   Aims and Objectives of this Research

Ion channels have been characterized by their functional consequences in neurodegenerative disorders. This study will attempt to detect Alzheimer's disease by applying the potential role of dysfunctions of these channels in the plasma membrane physiology and brain. In the first stage, finding predictive relationships from data plays a key role. For this reason, it is important to produce data which can be done by the Hodgkin-Huxley model.

Since Alzheimer's can be viewed as a fault in the neurons or a faulty signals being propagated, applying the Fault Detection (FD) method may prove that the disease has started, long time before damage is done to the brain. Therefore, in the next part of the research, FD methods will be applied to the data for detecting Alzheimer's disease. Fault Detection has a wide area, and there are many kinds of classification in the literature (Khalastchi & Kalech, 2018). In section 2.5, a brief definition of FD methods is provided. The project aim is to develop accurate computational methods to analyse the effect of ion channel dysfunction and ion imbalances in the neuron, which are known to be directly affected and associated with Alzheimer's disease. Such methods can be very important in studies of the dynamics of ageing and can be applied to support hypotheses that are

gained in experimental models involving patients with Alzheimer's disease. These methods can lead to a better perception of these kinds of neurodegenerative diseases.

The immediate focus of the project is the neurological modelling of ion channel dysfunctions in Alzheimer's disease. To achieve this aim the following objectives are considered:

(a) Investigating the neuron and network of the neuron, looking at the signals being generated and propagated to obtain a better understanding of the neurophysiology model of the neuron. In addition analysing the different levels of ions and ion imbalances in a network and single neuron to understand the feedback mechanism.

(b) Investigating the impact of coupling and synchronization in a neuronal network.

(c) Computational modelling and analysis of the beta-amyloid hypothesis and Alzheimer's disease as an ion channel disease.

(d) Investigating the relationship between fault detection for ion channel dysfunction and Alzheimer's disease. The reason is that, because Alzheimer's can be viewed as a fault in the neurons or a faulty signal being propagated, by applying fault detection methods on the functions of neurons, early detection of Alzheimer's may be possible.

1.5   Thesis Outline

This research has demonstrated an initial framework for the early detection of neurodegenerative diseases using investigation of functional changes of ion channels and the appearance of ionic imbalances. This presented that the origin of these ion changes

in the neuron and, consequently, in the nervous system, is the secretion of Amyloid beta plaques and, consequently, the creation of Amyloid beta channels. This study has mentioned some neurodegenerative disorders like Alzheimer's disease start with epileptic seizures in the nervous system due to abnormal brain functionality. Therefore, this type of disturbance in the brain is considered as the first symptom of Alzheimer's disease as well as other neurodegenerative diseases like Parkinson's.

In order to retain all cases in a normal sequence and to present them so that they are easy to understand, this study divided the thesis into three main parts. The first part was focused on the role of ion channels and ion imbalances and their impacts on neural disruptions. The second part concentrated on the main cause of diseases, i.e. the amyloid beta plaques and their role in creating ionic channels which are permeable to cations such as sodium and potassium. These channel leakages cause ionic imbalances that disrupt the normal cell functions. The third part of the thesis was focused on fault detection. A fault detection approach was selected to complete this project in order to detect disease as a fault in the nervous system. A comparison of linear and nonlinear observers was provided based on visualisation analysis, which helps us to realise the difference between them. A summary of the thesis, along with the extracted results, is are presented briefly by below sections:

Chapter 1: This chapter outlined the potential issues about neurodegenerative diseases along with challenges linked to computational neuroscience, neurology and medicine. This chapter discussed the potential of computational neuroscience to make remarkable advances in the early detection of neurodegenerative disorders. At the end of the chapter, the research aims and objectives are outlined.

Chapter 2: This chapter gave detailed information about the nervous system and its functions. Neurodegenerative diseases were discussed and Alzheimer's disease was selected as an example of these diseases. A brief presentation was provided of its development stages with probable symptoms. The chapter also provided a background and preliminary information about fault detection and residual techniques. Matters like coupling and synchronisation are also discussed.

Chapter 3: In this chapter, using computational modelling, the response of a neurone was investigated for different concentrations of sodium and potassium ions, and the resultant ion gradients, including the combination of imbalances in both sodium and potassium. It was shown that the responses to various concentrations are in line with current clinical thinking. The levels of the ions determine the characteristics of the response, namely, the resting potential, the magnitude of the spikes, and the inter-spike interval. It was shown that sodium and potassium are two physiologically essential electrolytes whose concentrations play an important role in nerve impulses and neurodegenerative disorders that affect the nervous system. The ability to represent changes in ion concentrations and the gradients across membranes will help in developing models for more complex networks of neurones.

Chapter 4: This chapter investigated the dynamics of a coupled neuron as ion changes occur. These changes were incorporated using the Nernst equation. It was shown that within the central and peripheral nervous system, signals and hence rhythms, are propagated through the coupling of the neurons. It is found that under certain conditions the coupling strength between two neurons can mitigate changes in ion concentration. By defining the state of perfect synchrony, it was shown that in coupled neurons the

effects of ion imbalance are reduced, while in uncoupled neurons these changes have a more significant impact on the neuronal behaviour. As most neurodegenerative diseases are a result of changes in the chemical composition of neurons these investigations seem important. For example, Alzheimer's diseases (AD) is the result of Aβ peptide deposition, which results in changes in the ion concentration. These changes in ion concentration affect the responses of the neuron to stimuli and often result in inducing excessive excitation or inhibition.

Chapter 5: This chapter showed that the build-up of Aβ deposits during the onset of Alzheimer's disease has profound effects on the activity of the local community of neurons in the central nervous system. These effects can include enhanced neural activity, spontaneous epileptiform activity, and incidences of epileptic seizures. According to the results of the experiments, it can be well understood that the neurodegeneration observed in Alzheimer's disease is associated with the increase of toxicity of Aβ depositions. Aβ accumulation has been discovered to form large, relatively cation-permeable channels under physiologic conditions. Formation of channel in the membranes of a neuron could cause cell depolarisation, sodium and potassium dysregulation, depletion of neural energy stores, and other types of cellular dysfunction.

Chapter 6: This chapter applied linear and nonlinear filters as an observer to track the dynamic behaviour of a neural model and to estimate the unknown parameters of the neuron. Then, by the residual observer-based method, fault investigation was applied to detect disease in our neuronal model. These three observers were applied both to track the states and estimate the parameters of our neuronal model.

2 Introductory Concepts

2.1 Neuroscience background

The human nervous system is the most complex and highly organized among the systems of the body. Study of neural systems encompasses a wide range of issues about the organization of the nervous system and its functions. These issues can be examined through the use of tools from physiology and biology and their translation to computational processes. The main challenge for a researcher is to integrate the variety of knowledge obtained from these different levels of analysis into a coherent understanding of the nervous system and its functions. This section provides an overview of the nervous system function and the structure of the neuron.

The nervous system consists of two parts. These parts are the the Peripheral Nervous System (PNS) and Central Nervous System (CNS). The CNS includes all the nerves of the brain and the spinal cord. The nerves spreading out from the brain and the spinal cord constitute the PNS. The PNS usually connects the CNS to the organs of the body.
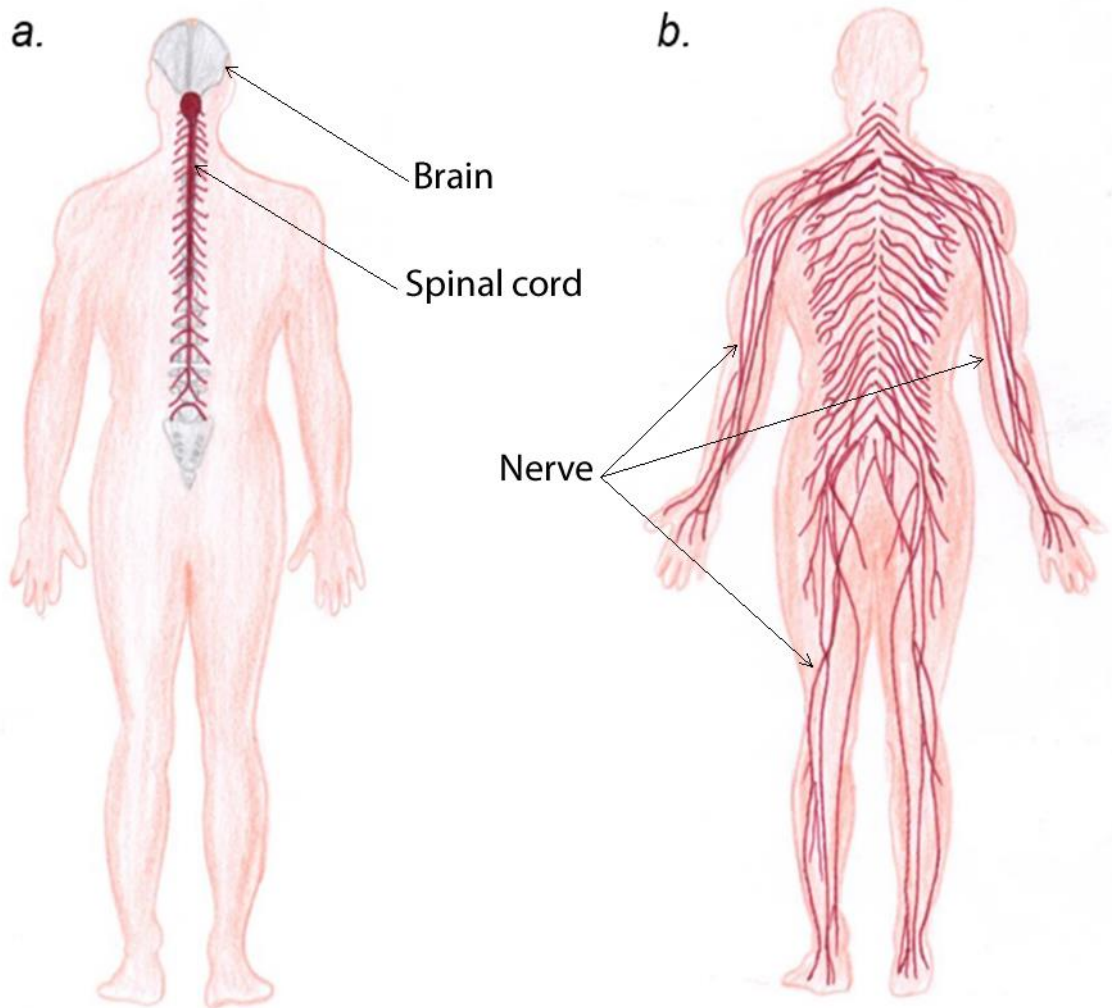
Figure 2.1 – a. the central nervous system. The central nervous system is the basis of all mental and behavioural activity. It consists of the brain and the spinal cord. b. the peripheral nervous system. Peripheral nervous system gets all information into the brain. The peripheral nervous system connects the senses to the central nervous system and also connects the central nervous system to the muscles and glands

The neurons, which make up the neuronal system of human body are responsible for both the processing and transmission of neural messages though the body. Thus knowledge about the structure and the functioning of the nervous system will enable the development of tools to diagnose, manage and treat neurological diseases such as Alzheimer's disease or dementia. A fundamental building block of the nervous system is a neuron the collective properties of these neurons dictate the functioning of the nervous system. This chapter introduces some of the key concepts of neurophysiology and later one the coupling and synchronization phenomena for a collection of neurons are discussed.

2.1.1 Neurons

Neurons are the functional units of the peripheral nervous system and central nervous system and have an ability to send and receive electrical signals. Nerves, which are a collection of neurons that transmit signals from the brain are called motor or efferent nerves, while those nerves that transmit information from the body to the central nervous system are called sensory neurons (Sarangdhar, 2010). Neurons are morphologically and functionally polarized so that information may pass from one end of the cell to the other. The basic neuron structure includes a cell body, axons and dendrites.

The cell body (soma) contains the neuron's nucleus and produces all the proteins for the dendrites, axons and synaptic terminals. The principal function of neurons is to integrate synaptic messages and after that transmit this messages to other neurons which is done by the axon. The axons are usually extensions of neurons. Axon conducts signals away from the cell body to other neurons in nervous system. The original function of axon is to transmit electrical impulses. Another part of a neuron is the axon hillock. The axon hillock is a unique area within the cell body (or soma) of a neuron that connects to the axon. This section of a neuron is the last section of the soma, where membrane potentials propagated by synaptic inputs are aggregated before being transmitted to the next neuron through the axon of the current neuron. One of the important characteristics of the axon hillock is the existence of a specialised membrane that contains many ion channels. These ion channels are responsible for action potential initiation in nervous system. Dendrites which are extensions of neurons are another part of neuron structure. Dendrites receive all signals and lead them toward the cell body. The original function of dendrites is the handling of the signal input into the neuron. It can eventually result in an axon spike. In other words, dendrites generate and integrate postsynaptic potentials and intracellular signalling cascades. Both dendrites and axons can extend far away from the cell body.

Some human axons may reach lengths of more than three feet (Kumar, et al., 2013). The general structure of a neuron is shown in Figure 2.2 and different types of neurons are shown in Figure 2.3.
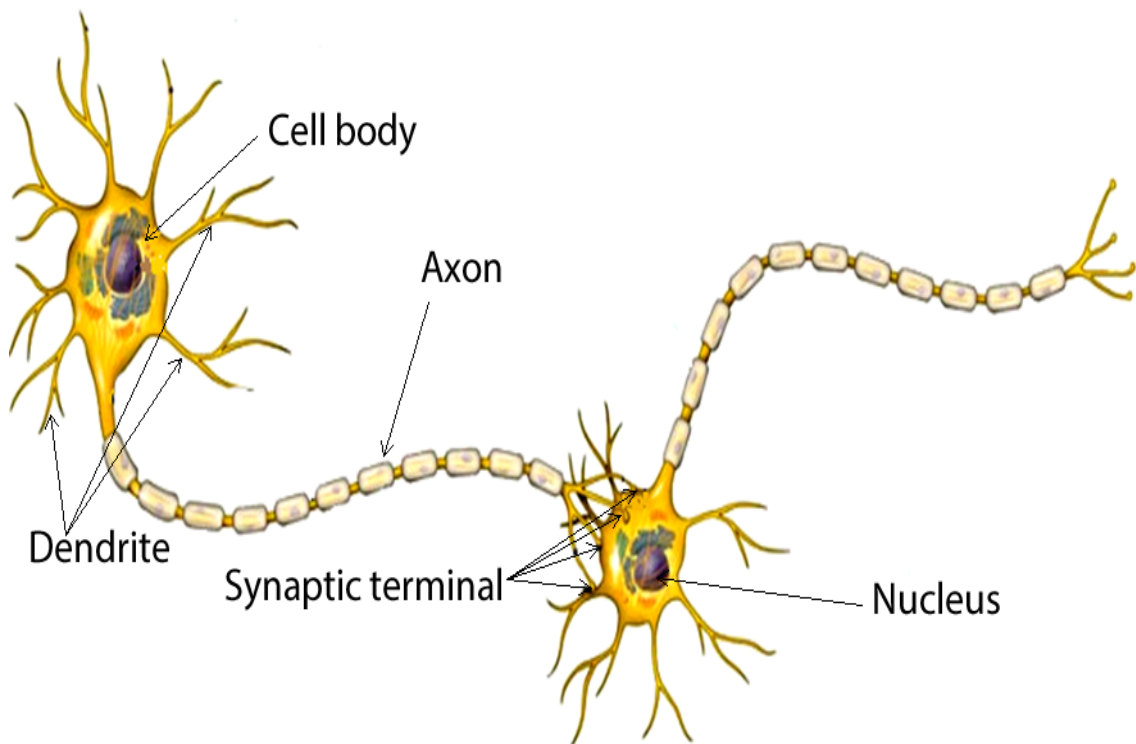
Figure 2.2 – The structure of a neuron. Neurons in the nervous system have the same structure generally. The cell body has the nucleus, axons and dendrites which projected from axons. Axons transmit element of neurons, and they are of different lengths. Some of them are more than 2 m within the body. Both apical and basal dendrites with the participation of the cell body are the input elements of the neuron and receiving signals from other neurons. Adapted from (Barnett & Larkman, 2007)
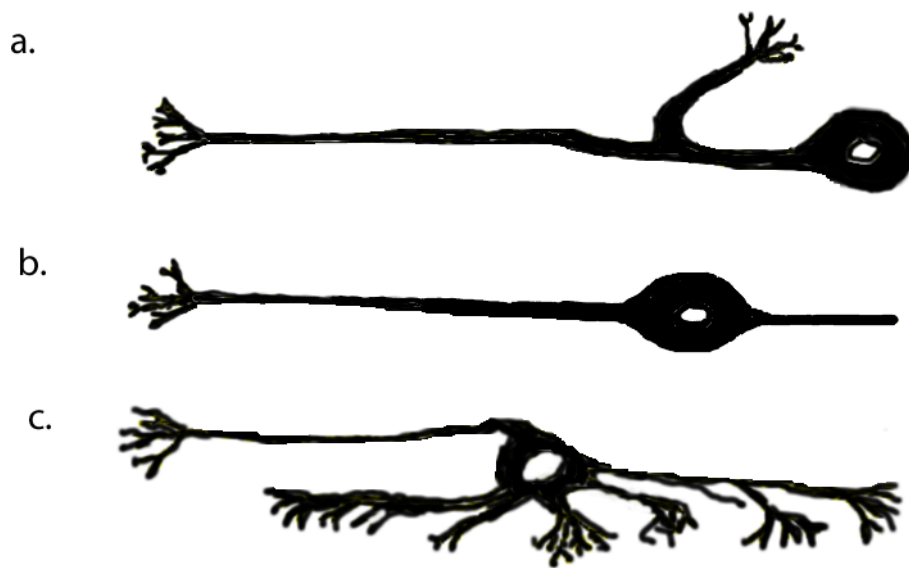
Figure 2.3 – There are three kinds of neurons unipolar, bipolar, or multipolar. **a.** Unipolar cells have a single process and various segments serve. **b.** in the bipolar cells the dendrite receives electrical signals and the axon transmits signals to other cells, so it has two types of processes. **c.** Multipolar cells possess a single axon which is long. In this kind of neurons many dendrites, allow for the integration of a great deal of information from other neurons

2.1.2   Voltage-Gated Channels

The biophysical properties of voltage-gated ion channels is very important as these properties influence the shape of the action potential in nervous system. These channels are a class of transmembrane ion channels. These channels are embedded in a plasma membrane of a neuron. Changes in membrane potential activate voltage-gated ion channels. These types of ion channels open for few values of membrane potential, but for other values are closed (Brenowitz, et al., 2017). When the membrane potential is hyperpolarized, the gates of both channels are closed. Voltage sensors allow the channel gates to open just in the case of potential depolarization. Sodium channels are inactivated during prolonged depolarization. Voltage-gated ion channels play an important role in the process of action potential of the neuron. By the opening of ion channels, the membrane conductance changes to ionic current flow. Any change in membrane potential will open voltage-gated ion channels, increasing membrane conductance.

The electrochemical gradient will be changed by the inflow or outflow of ions which causes changes in membrane potential, and results in a change in ion current. An action potential occurs only if the potential of membrane reaches to a certain level. This is called 'threshold potential'. Threshold level is the critical level at which the membrane potential rapidly increases.

The schematic neuron shown in Figure 2.2, is an electrically excitable cell which is found in the nervous system. Nervous cells have three essential functions: a) to receive signals, b) integrate incoming signals and, c) to transfer signals to target neurons. In a neuron, signals are generated by a variety of membrane-spanning ion channels. These channels allow ions, mainly potassium, sodium, and chloride, to move in and out of the cell. These ionic channels can control the flow of ions by rapidly opening and closing in answer to changes of voltage in plasma membrane of neuron. The voltage changes are a result of both external stimuli and internally generated spikes. The electrical signals of relevance to the nervous system are the difference in potential between the enclosing extracellular medium and the interior of a neuron.

Figure 2.4 shows the different phases of the membrane potential of a neuron. These phases are (a) resting potential phase, where the effects of the stimulus is not seen, (b) a depolarisation phase where the effect of the stimulus is such that the neuron acts like a capacitor storing charge, (c) a repolarisation phase where the neuron is discharging its potential, and (d) a recovery or hyperpolarisation phase where the neuron having discharged itself is returning to the rest state. The changes in the potential are controlled by the ionic gradients, which in turn are regulated by the ion pumps. Sodium has a higher concentration outside the neuron than inside. Against, the concentration of potassium is significantly higher inside the neuron. Therefore, ions flow into and out of a neuron because of voltage and concentration gradients. The process in which negatively charged

ions flow into the cell and positively charged ions flow out of the cell via open channels creates a current. This current causes to makes the membrane potential more negative. Generally, this process called hyperpolarization. Flowing of current into the cell changes the membrane potential to less negative and this process called depolarisation (see Figure 2.5).
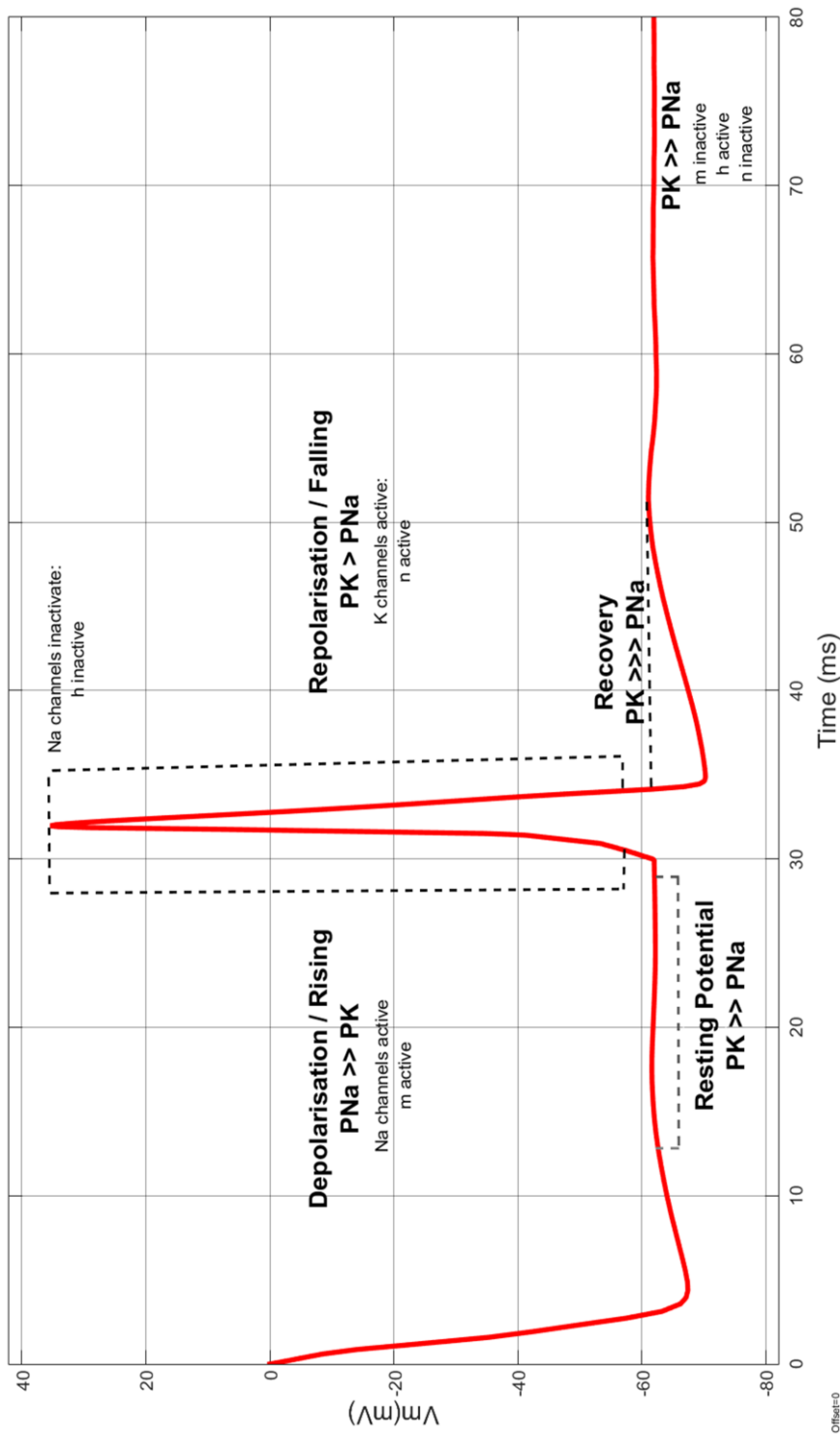
Figure 2.4 – Recording a transmembrane potential during depolarisation and repolarisation of a nerve fibre. The membrane contains channels. These channels open or close and allow the polarity of the membrane to change as ions pass through the channel. A stimulus causes sodium channels to open. There are lots of sodium ions on the outside, and the inside of the neuron is negative about the outside, sodium ions rush into the neuron. For the potassium, it takes the longest time to open channels. When the potassium channels to open, potassium rushes out of the cell, reversing the depolarisation and at this is the time that sodium channels start to close. The different phases of the action potential have presented. Vm transmembrane voltage; PNa membrane permeability to sodium; PK membrane permeability to potassium. The relative membrane permeability relationships between potassium and sodium ions associated with each of the phases. For instance, PNa>>PK means that permeability for Na is greater than permeability for K where > means greater and >> means much greater.

35

By depolarising a neuron and bringing the membrane potential above a threshold level, a positive feedback process initiates. In this condition the firing neuron as shown in Figure 2.5 generates a spike. Generation of the spike is very dependent on the recent history of firing of neuron. Just the few milliseconds after a spike, it may be impossible to initiate a next spike. This called the refractory period. Spikes then regenerate actively along axon processes. Spikes can travel fast over long distances and without any attenuations. The role of ions in neural communication is critical, and any imbalances can have harmful effects on the nervous system. Section 2.1.9 deals with ionic imbalances in the nervous system. Biologists such as Andrew Huxley and Alan Hodgkin (Hodgkin & Huxley, 1952) have mathematically modelled the electrical process of the nervous system with a set of differential equations, which deals in section 2.3.

2.1.3 Ion Pumps

A mechanism is needed to maintain a different ion concentration during the resting state. Ion pumps achieve this mechanism. Ion pumps are another types of transmembrane protein channel (See figure 2.5). The extracellular and intracellular environment have different ionic composition. The movement of ions is from areas of high concentrations to areas of low concentrations, and is so-called 'diffusion'. Diffusion will continue until equalisation of concentration on both sides (He, 2006).

Just as Ion Pumps deal with ions of the same type, there is also the effect of the differences in electrostatic charges between positive and negative ions outside and inside the cell. This allows movement of ions in a opposite direction which gives rise to the Nernst Potential. The ionic balances and the electrostatic charges which give rise to the potential is called the NERST effect.
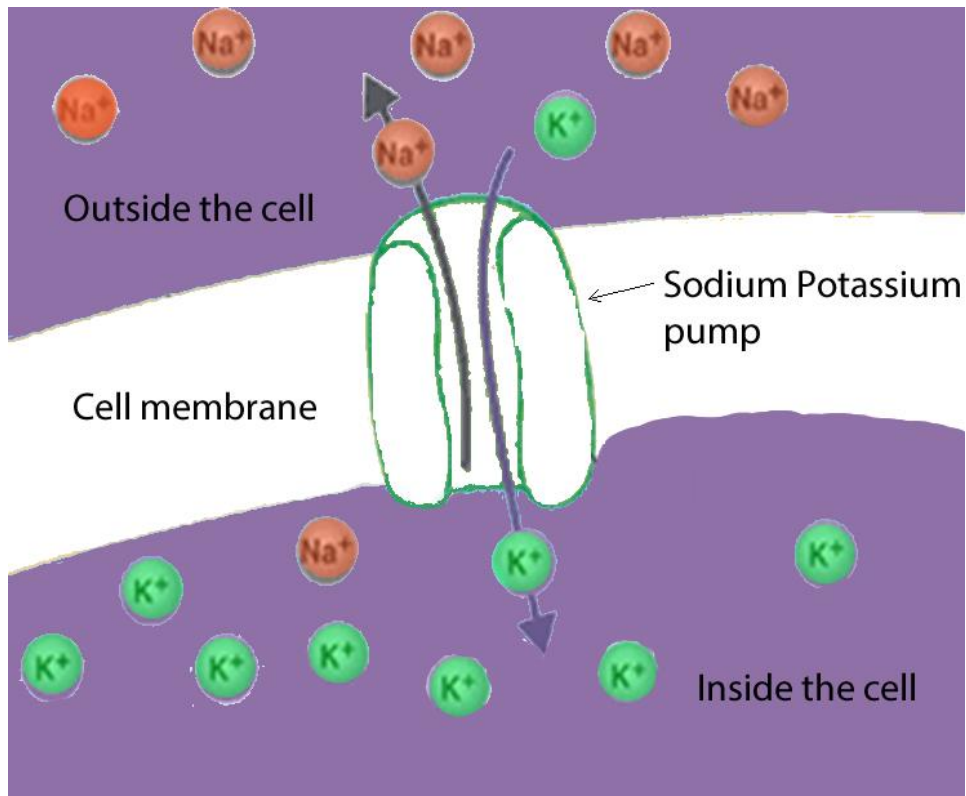
Figure 2.5 – Ion Pump. Ion composition outside the cell differs from that inside. Adapted from (Barnett & Larkman, 2007).

2.1.4   Ion Channels

In the nervous system, action potential and consequently, membrane potential is regulated by the voltage-gated sodium and potassium channels during a neuronal action potential. Sodium and potassium ions, along with other cations such as magnesium, calcium are responsible for the generation of the action potential in the neuron. In the main however it is the Sodium and Potassium ions which are responsible for the potentials.

The nervous system consists of a vast number of interconnected neurons, which transmit signals using ion channels to generate potentials across membranes. As a result, the chain of neurons is activated by electrical signals generated at various points. When a stimulus occurs, the activation of the neuron results in an internal change in concentration of the

ions. These changes lead to a membrane voltage, which is dependent on the threshold for the particular cell. The first stage in this change is known as depolarization, after which an action potential is triggered (Frohlich & Jezernik, 2005). In response to depolarization in transmembrane voltage, ion channels allow an inward flow of sodium ions. This changes the electrochemical gradient, which in turn produces a further rise in the membrane potential, causing more channels to open and to generate further electric current throughout the cell membrane. The firing process continues until all of the available ion channels are open, causing a significant expansion in membrane potential. The rapid influx of sodium ions causes ion channels to rapidly deactivate because it reverses the polarity of the membrane (Figure 2.6.b phase 2 of action potential).
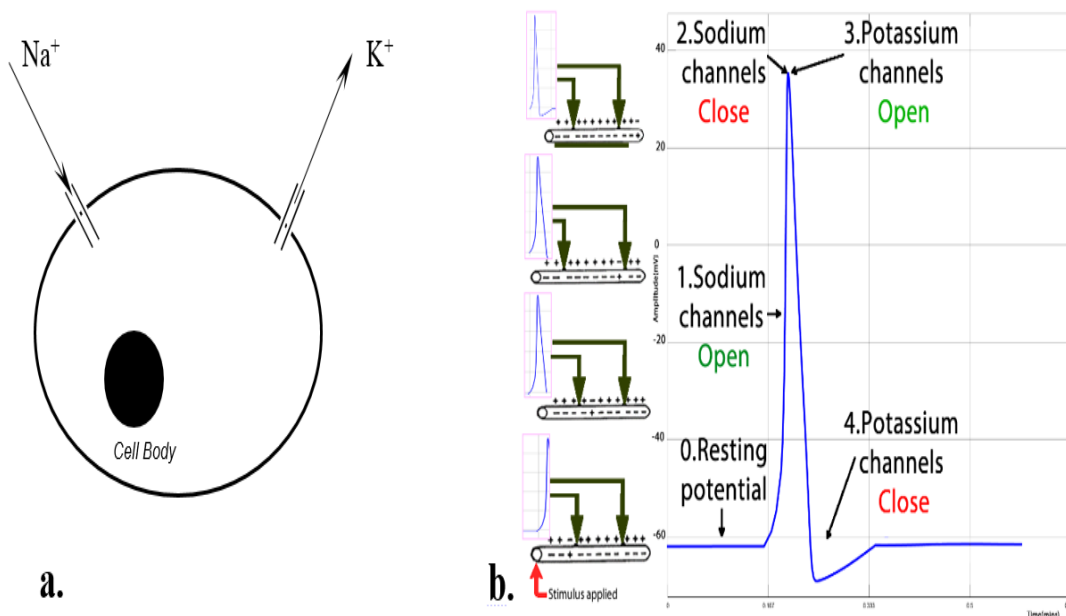
Figure 2.6 – **a.** The membrane includes open or closed channels. These channels allow the polarity of the membrane to change near to -70 mV. The action potential passes -70 mV (a hyperpolarization) as the potassium channels stay open a bit too long. As ions pass through the channel. **b.** A stimulus forces sodium channels to open. About the potassium, it takes more time to open channels. When the potassium channels do open, reversing the depolarization and this is the time that sodium channels start to close. This leads the action potential to return.

These changes are shown in Figure 2.6.b. It shows the various stages of the response of a neurone to a stimulus. In the first instance, when a stimulus occurs, the sodium channels open, which results in depolarization and an increase in membrane potential. The rate of depolarization is dependent on the difference in sodium concentration inside and outside the cell. The magnitude of the response is also dependent on the concentration of these ions. The second stage occurs when the sodium channels close (Chappell & Payne, 2016). As a result, sodium ions can no longer enter the neurone, and then they are transported back out of the membrane. Then the potassium ions affect the remainder of the response (Chappell & Payne, 2016). By activation of potassium channels and outward current of potassium ions, the electrochemical gradient returns to the resting state (Figure 2.6.b phases 2 and 3 of action potential). The action potential flows along the length of the axon by changing the states of the ionic channels in the membrane of the axon.

2.1.5   Synapse

Synapse structure allows a neuron to transmit a chemical or electrical signal to another neuron or an efferent cell. Nerve cells are not continuous entire the human body but they have communication with each other (Lorin & Deborah, 2006). This idea is known as neuron doctrine. This doctrine puts the neurons under the wider cell theory. For neuronal function, synapses are essential. In the nervous system structure, neurons are cells that transmit all neural signals. In the synaptic space, the presynaptic neuron comes into close apposition with the postsynaptic cell. Presynaptic and postsynaptic sites have a wide range of arrays of molecular machinery. These arrays link both membranes together and perform the signalling process. There are two different types of synapses: chemical

synapse and electrical synapse. Electrical activity in the presynaptic neuron in the chemical synapse changes into the release of the neurotransmitters, complex chemical messengers that transfer signals from one neuron to another neuron (Odish, et al., 2000). On the other hand, in the electrical synapse, both membranes are connected by gap junction that is capable of transiting the electric currents. This causes voltage changes in the presynaptic cell and as a result, induce electrical changes in the postsynaptic cell. Prompt transfer of signals from one neuron to another is the important advantage of the electrical synapse (Silverthorn, 2007). The neurotransmitter systems may be affected by neurological disorders, especially, certain neurodegenerative diseases. For instance, in one neurodegenerative disorder, like Parkinson's disease, there is a problem related with the predictive and secretion of a neurotransmitter which is called dopamine. This disease affects the ability of movement and its symptoms include stiffness, tremors or shaking (Lindemann & Hoener, 2005).
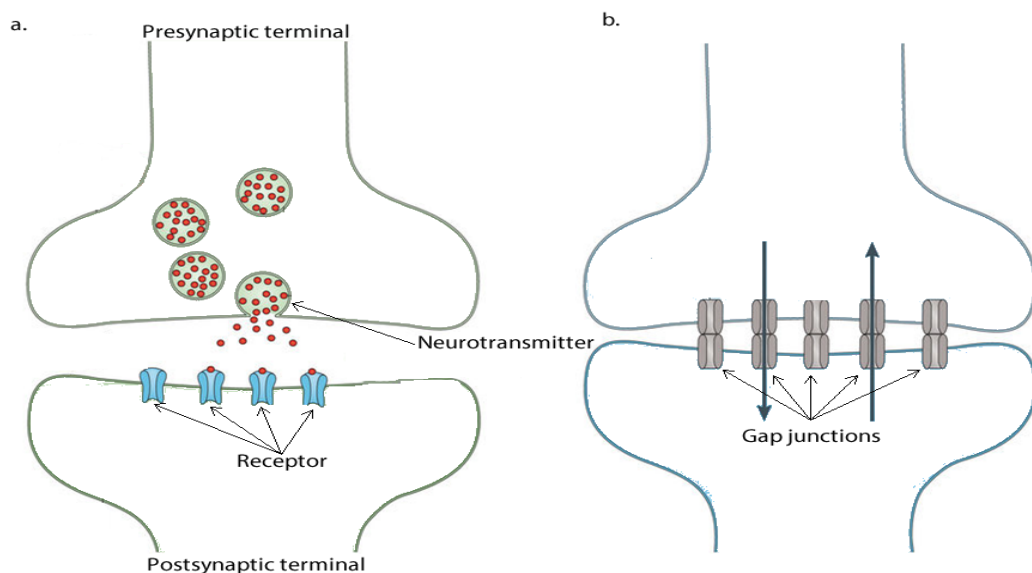
Figure 2.7 – a. chemical synapse. A gap between two neurons. Information can only pass in the form of neurotransmitters b. electrical synapse is a gap which channels connect the two neurons. In this connection, the electrical signal can pass straight over the synapse. Adapted from (Barnett & Larkman, 2007)

2.1.6   Inhibitory and excitatory neurons

Stimulus can generally be categorised as either being excitatory or inhibitory. All neurons can transmit either signal, but those that transmit the inhibitory signals are called inhibitory neurons and the others are called excitatory neurons. The neuron is called excitatory if the presynaptic neuron has excitatory behaviour that is it is transmitting an excitatory stimulus and it is called inhibitory if the presynaptic neuron has inhibitory behaviour. The main mechanism is the action of membrane potential of the target neuron in a positive (excitation) or negative (inhibition) direction. Its direction depends on the specific transmitter which opens or closes ion channels in the postsynaptic neuron. For instance, as sodium ions have a positive charge, they will change the membrane potential of that neuron in the positive direction and as a result, the neurotransmitter that opens the sodium channel would be an excitatory neurotransmitter. Similarly, the neurotransmitter that opens the chloride channel is an inhibitory neurotransmitter.
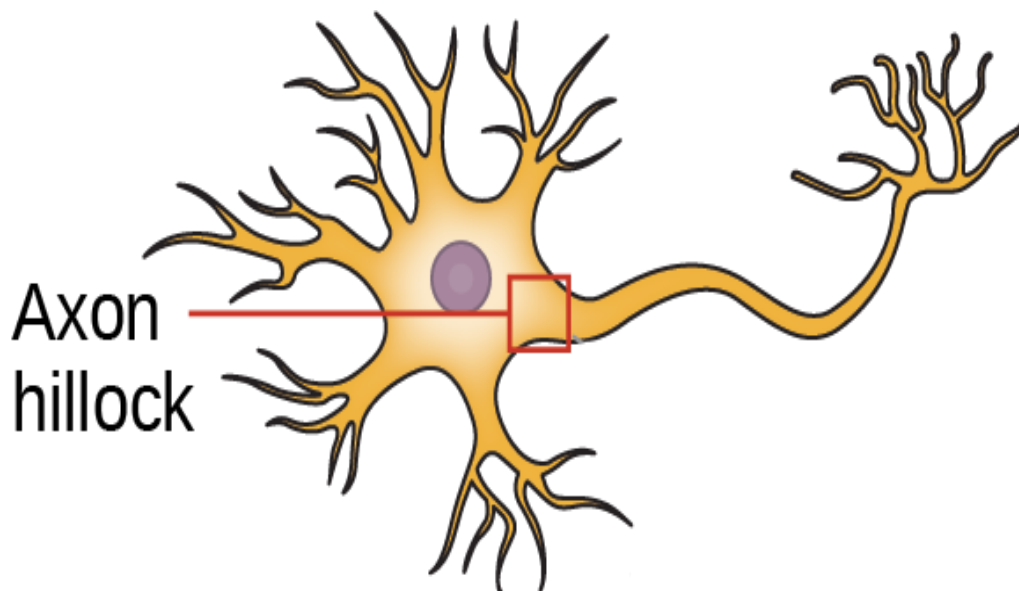
Figure 2.8 – Axon hillock. The place of Axon hillock in the structure of a neuron. The last site in the soma is called the axon hillock. Adapted from (Boundless, 2105)

Axon collateral or recurrent inhibition is a particular case of postsynaptic inhibition. As shown in the Figure 2.9, the output of neuron 1 is conducted along its axon and out one axon collateral to excite an interneuron that inhibits another neuron of the same type, neuron 2. Neurons inhibit other neurons of the same kind. Therefore, neuron 2 is inhibited by neuron 1 and vice versa. This is a form of feedback inhibition in which the output of a neuron inhibits another point in the earlier route.
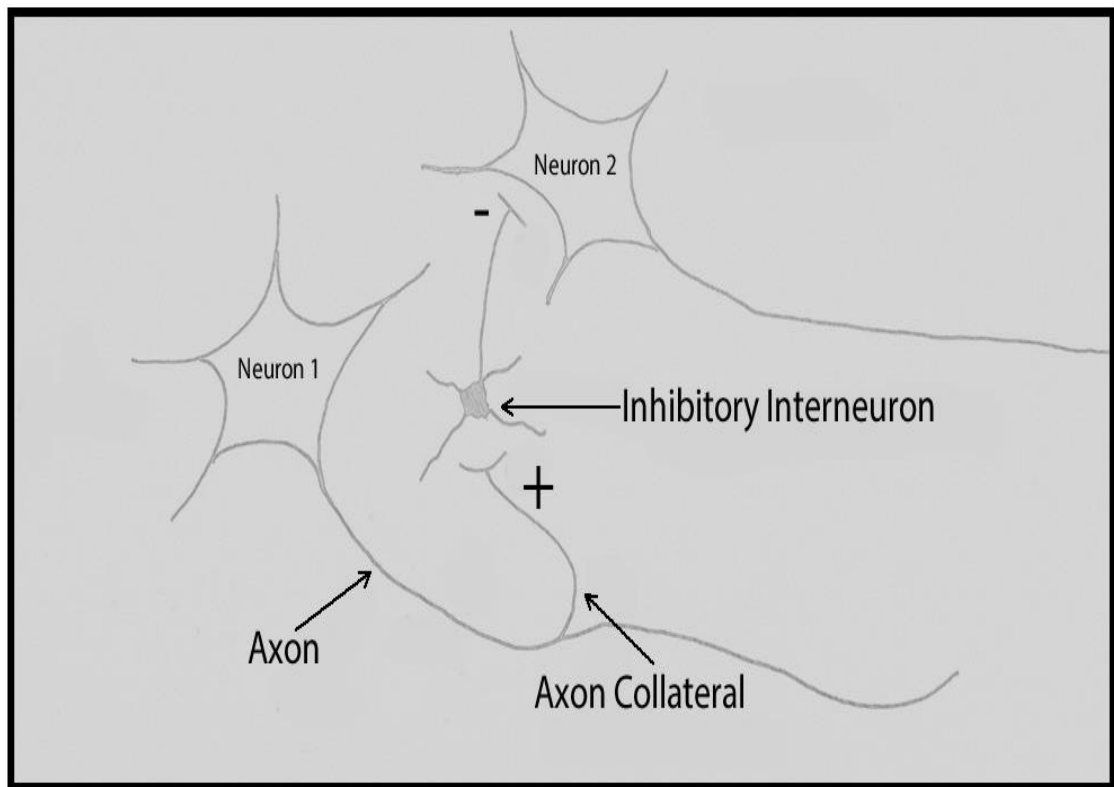
Figure 2.9 – Axon collateral. The output of a neuron 1 is conducted along its axon and out one axon collateral to excite an interneuron that inhibits another neuron of the same type, neuron 2. Neurons inhibit other neurons of the same type.

2.1.7 Action Potential

A spike of action potential is an electrical impulse. In the action potential, the electrical membrane potential of a neuron rapidly rises and then falls. The action potential is generated by a series of events and occurs in some cells, called excitable cells. An important features of the action potential is its initiation at a specific membrane potential, called the threshold.

The Action potentials are divided into two types: (a) voltage-gated sodium channels (NaV) and (b) voltage-gated calcium channels (CaV). The main difference between these two types of action potentials is duration. Sodium based action potential lasts for a very short period, less than a millisecond, while the calcium-based action potential may last over a period of 100 milliseconds or even longer (Plonsey & Barr, 2007). The focus of this thesis and its modelling effort is on action potentials generated by voltage-gated sodium channels.

The potential of membrane is measured in millivolts. The static potential during the resting state of a cell, when potential of membrane is at equilibrium, is approximately -70mV. This means the inside of excitable cells is approximately 70mV more negative than the outside of it. This value varies depending on neuron types and the species (Boundless, 2105).

Action potentials only happen in the depolarising stimulus that starts the membrane potential to a particular value. Many different factors such as the type of neuron, temperature, location and many other parameters determine the threshold level. This is why that there is no particular level of membrane potential that specifies the threshold for a specific neuron in all circumstances (Carlson, 2007).

The action potential is a single, transient reversal of membrane polarity. It is also an explosive all-or-none event with a threshold. The initiating current does not determine

the duration and amplitude of an action potential. The action potential has several phases

or components (see Figure 2.10).
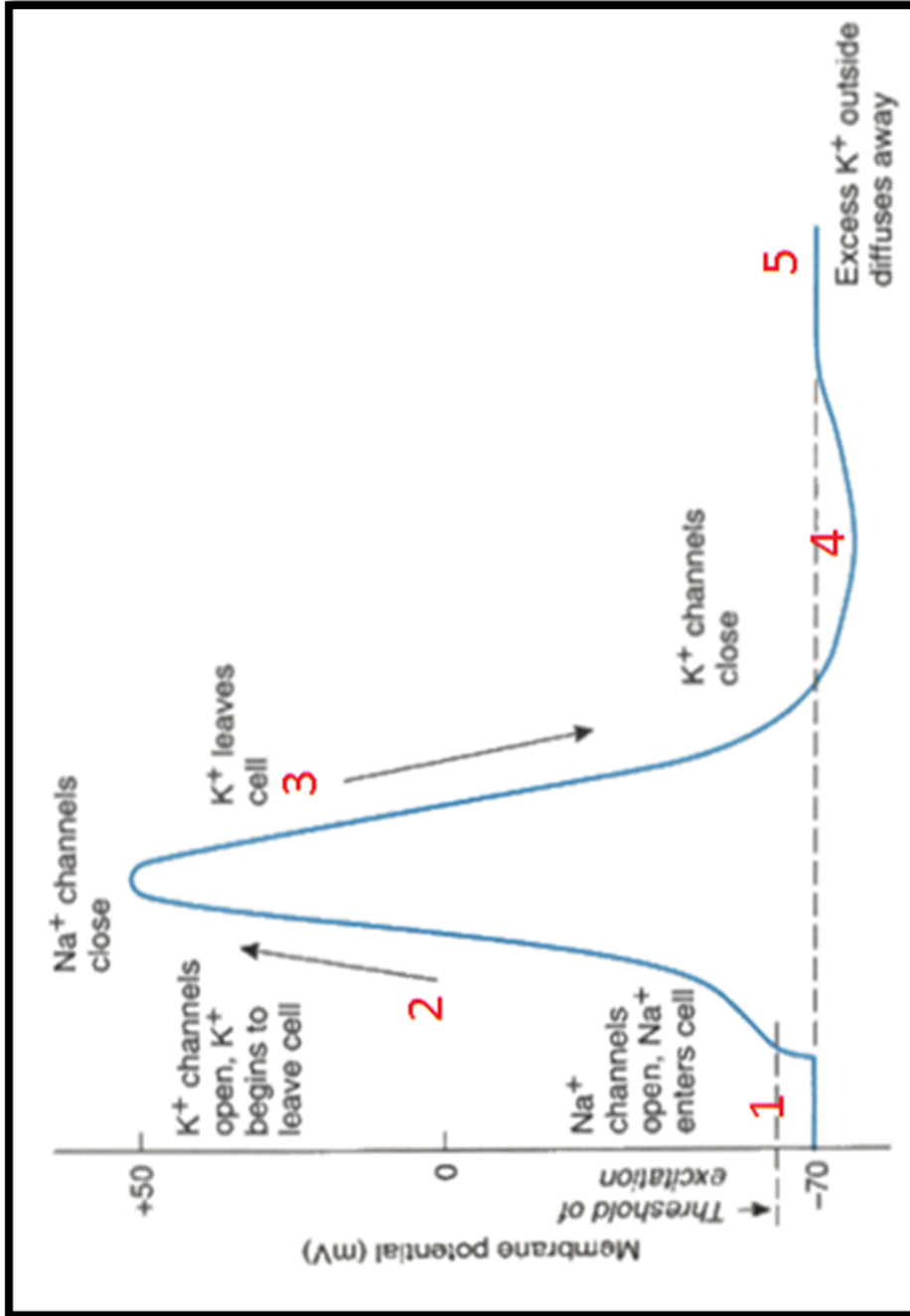
Figure 2.10 – Ion Flow in Action Potential. The phase 1 is resting state. In this phase all gated Sodium and Potassium channels are closed. The phase 2 is depolarizing Sodium. Channels open. In this phase action potential begins just only when the neuron is depolarized around its threshold potential. The potential rapidly becomes positive. Phase 3 is repolarization. Sodium channels inactivated and Potassium channels open. Once the cell reaches its peak positive potential, it repolarizes, returning to negative membrane potential. In phase 4 hyperpolarizing occurred. Potassium channels remain open and Sodium channels inactivated. In phase 5 eventually the membrane returns to its resting state. Adapted from (Barnett & Larkman, 2007)

Depolarization is only possible when membrane potential reaches a certain threshold. Potential greater than 0 mV is termed the overshoot. This called repolarization. In this condition, the membrane potential returns to negative values, which frequently become a little more negative than the resting potential of the axon membrane; so-called hyperpolarization. At resting potential state, the membrane is usually more permeable to potassium than to sodium. In initial depolarization of action potential and just before reaching the threshold, sodium channels open more rapidly than potassium channels. It means sodium permeability is greater than potassium permeability. Therefore, sodium ions move inside the cell and decrease the negative electrical potential inside the neuron.

2.1.8 All-or-none law

The all-or-none principle first time was established by physiologist, Henry Pickering Bowditch (Adrian, 1914) ; (Sadegh Zadeh & Kambhampati, 2017). The all-or-none principle in cell neurophysiology states that the strength with which a neuron responds to stimulus is fully independent of the strength of that stimulus. It means that the amplitude and velocity of an action potential are completely independent of the stimulus that created it. This law states that if the stimulus was greater than the threshold potential, then the neuron will give a full spike to that stimulus, whereas the exciting stimulus under threshold strength fails to draw out a propagated action potential (Adrian, 1914).
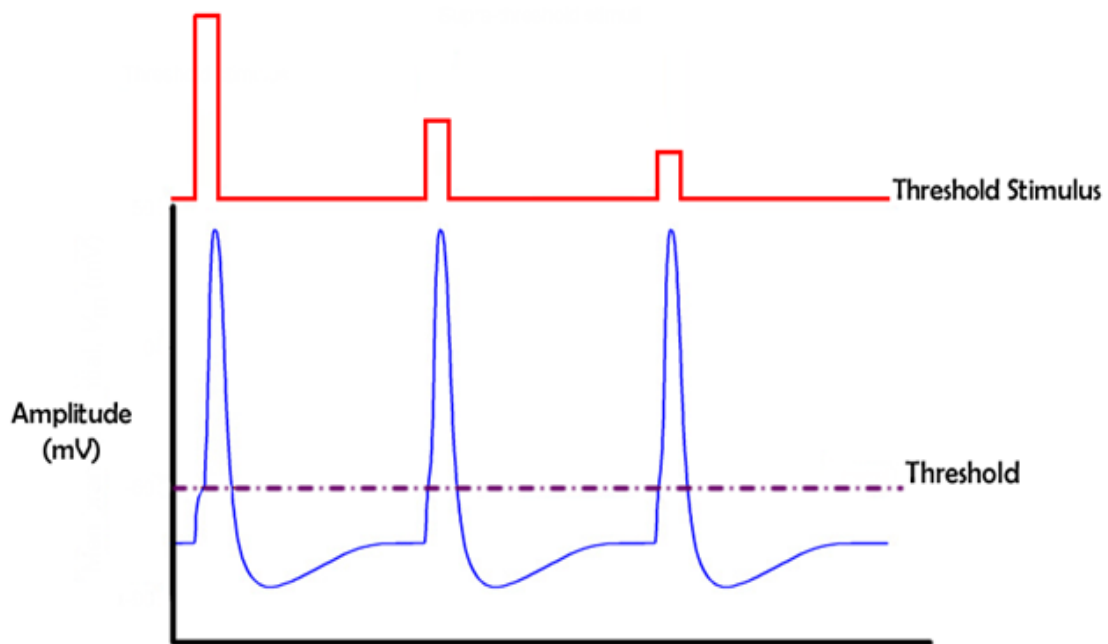
Figure 2.11 – According to the all-or-none principle further increase in the stimulation current does not cause an increase in the strength of the spike. The other traces are on the same time scale. The dashed line shows the threshold voltage of the recorded neuron

Despite the fact that the amplitude, velocity, and shape of an action potentials are consistent over a time period for a given axon, they differ from one neuron to another neuron. Thicker axons allow for faster conduction velocity of an action potential, which means the neuron can convey more action potentials per second. The all-or-none principle puts constraints on how an axon can convey a signal. Figure 2.11 describes the concept of this principle more.

2.1.9   Ionic Imbalances

Ions play an especially critical role in lots of neuronal functions, from the largest to smallest scales. Ionic imbalances strongly affect neuronal activity and are a cause of cell death. Sodium and potassium ions are responsible for the generation of the action

potential and transmitting signals in the neuron. An imbalance in sodium and/or potassium, especially hyponatremia and hypokalaemia, are a common challenge in clinical practice (Whelton, 2016) . Excess of sodium ion concentration is known as hypernatremia and the converse is called hyponatremia. Similarly, excessive potassium ion concentration creates the situation known as hyperkalaemia, and the opposite is defined as hypokalaemia. These disorders are also commonly referred to as electrolyte disorders in the setting of CNS disease (Silva, et al., 2016). Ionic imbalances have a broad range of neurological effects. In these disorders, epileptiform seizures, muscle rigidity and tremor may occur. Imbalances depress the central nervous system and producing lethargy that progresses to coma. Permanent brain damage may result from severe imbalances, especially in children and other impacts of the disease may occur as a consequence of the ion imbalances.

2.2   Ion channels in neurodegenerative disorders

There is growing evidence that confirms the effect of ion channels disorder on dysfunctioning in neurodegenerative diseases. Some neurological diseases and age-related disorders like Parkinson's disease, Alzheimer's disease, are caused by change of function in ion channels. Ion channels are large membrane protein which play a crucial role in determining the membrane potential and secretion of neurotransmitters. Faulty ion channels and losses of pathological proteins have been found to be a major cause of neurological disorders (Kumar, et al., 2016). The dysfunction of ion channels also causes some symptoms, including neuromuscular sprains, memory loss, and movement disabilities. However, the receptor and other factors in such disorders remain elusive because of the possible mechanistic played acted by aberrant ion channels. Therefore,

designing therapeutics for targeting or even treating neurodegenerative disorders is a challenging problem for the neuroscientist.

Thus, it is necessary to understand how changes in the functioning of the ion channels lead to the development of diseases. In this thesis, the potential role of the ions and ion channels in the nervous system is addressed. Moreover, the role of disturbed ion channels in a common neurodegenerative disorder, Alzheimer's disease are discussed.

2.2.1   Ion channels and the physiology of membrane

Ion channels for ions such as potassium, calcium, sodium, and chloride make a passage to move through the lipid bilayer. In addition, they regulate various physiological functions including, the release of neurotransmitters, electrical conduction in the neurons (Lodish, et al., 2000). The ion channels control the four leading roles in membrane physiological regulation (Barnett & Larkman, 2007); (Strange, 2004); (Gouaux & Mackinnon, 2005): 1- Adjusting the potential of the membrane of cells, which is the movement of ions from the membrane. Ion channels determine the resting potential of the membrane and create the action potential. 2- Fast transmission of signals, which means closing and opening ion channels and creating action potentials. 3- Maintaining the electrolyte balance inside and outside the cell membrane to adjust the cell volume. 4- Producing regulatory signals in cells. Ion channels generate the signal flow in order to create electrical signals which result in the release of intracellular signalling cascades associated with neuronal release, hormonal secretion, and muscle contraction. Therefore, the study of ion channels will help to improve our understanding of cellular function in normal and diseased conditions.

2.2.2 Ion channels and brain homeostasis

Homeostasis refers to stability and balance. This physical process correctly compensates for environmental stress to maintain internal consistency. Therefore, homeostasis keeps the balance of the body. It is the brain that performs this function. To keep physiological balance of the nervous system, appropriate ion channel functions are required. For example, retaining the balance of ions among postsynaptic the membrane of neuron. In addition, ion penetration through the channels adjusts several processes, including synaptic plastic and neural diffusion. Moreover, cell responses to synaptic inputs are specified by many ionic channels represented by a particular cell (Kurachi & North, 2004). Activities of ion channels are adjusted by neurotransmitters. Neurotransmitters are involved in regulating the metabolism of the brain (Sohn, 2013); (Madry, et al., 2010); (Weilinger, et al., 2013). Since ion channels are involved in regulating neuronal signalling, therefore, any changes in the structure of the ion channels have harmful results on the activity of the neurons. Therefore, increasing the level of intracellular ions frustrates the brain homeostasis and result in the development of neurological disorders.

2.2.3 Impact of Ion channels on gap junctions

Almost all multicellular organisms keep their homeostasis using cellular communication and they respond completely differently to any changes in any conditions. This cellular connection involves gap junctions. Gap junction is intercellular channel in the certain areas in the membrane of nervous cell (Mes¸e, et al., 2006). The channels of gap junctions mediate cytoplasmic connections between neurons. These channels prepare a medium for forwarding of different ions (Kanno & Loewenstein, 1964) (Lawrence, et al., 1978). The communication in gap junction controls many physiological processes like cell differentiation, cell synchronization, cell motility, and etc. (Vinken, et al., 2006) (White

& Paul, 1999). In a complicated system like the neuronal networks, gap junctions rectify electrical coupling upon different neuronal damages.
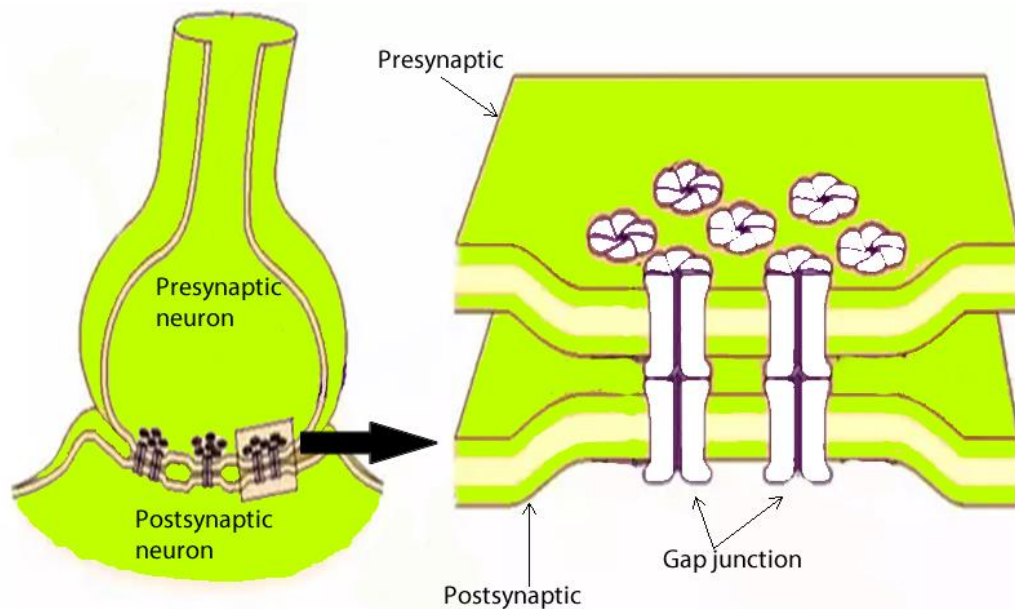
Figure 2.12 – Electrically link in neurons. It is formed at a gap junction. Adapted from (Kurachi & North, 2004)

The channels of gap junctions are responsible for the cytoplasmic link between neurons. They synchronize their electrical activities and they provide a diffusion pathway for ions (Figueroa, et al., 2014). Structural aberrations in the gap-junctional channels have been presented in different neurodegenerative diseases especially Alzheimer's disease (Mylvaganam, et al., 2014); (Quintanilla, et al., 2012); (Vega, et al., 2013).

2.2.4 Alzheimer's disease and ion channel hypothesis

The hypothesis of ion channel first time was suggested by Arispe in 1993. He found that Aβ can form unregulated cation-selective channels in the plasma membrane of neurons (Arispe, et al., 1993). Subsequent research showed that Aβ (25-35) inserts into planar lipid bilayers (Mirzabekov, et al., 1994). This membrane insertion situates irreversibly

along with a broad range of oligomer (Hyunbum, et al., 2013);(Suresh, et al., 2018). It is estimated that about 70% of the risk of Alzheimer's disease is genetically related to the many genes that are commonly involved (Ballard, et al., 2011). There are other factors such as a history of head injuries, hypertension, or depression (Burns & Iliffe, 2009). The process of the disease is accompanied by the accumulation of large amounts of plaques and tangles in the synaptic spaces (Ballard, et al., 2011). Currently, detection is based on the history of the disease and cognitive testing along with medical imaging, as well as blood tests (NICE, 2018). Early signs of disease are often mistaken for natural ageing but for a definite diagnosis, examination of the tissues of the brain is required (Ballard, et al., 2011). There is no treatment to stop or reverse the progress of the disease; however some treatments can improve the symptoms temporarily (Burns & Iliffe, 2009). The course of the disease can be divided into four separate stages, with a progressive pattern of functional and cognition disorders:

1- Mild cognitive impairment (MCI)

2- Early

3- Moderate

4- Advanced

In the early stage, the first symptoms are often mistakenly associated with stress or normal ageing. At this stage, very accurate neuropsychological tests can show mild cognitive impairments. Although these symptoms are very mild, these early and very critical symptoms affect the many activities of everyday life. In the next stages, with the deterioration of the disease process, ultimately the patient will not be able to perform everyday activities. In the final stages, the patient is entirely dependent on the caregiver. Speech will be limited to very simple phrases and ultimately it will lead to a complete loss of speech (Frank, 1994).

The main cause of Alzheimer's disease is still mostly unknown. However, in 1% to 5% of cases with genetic differences have been recognised (Reitz & Mayeux, 2014). On the other hand, there are various competing hypotheses which seek to explain the cause of Alzheimer's disease. These hypothesises are the genetic, the cholinergic hypothesis, the amyloid hypothesis, the tau hypothesis, and the neurovascular hypothesis (Reitz & Mayeux, 2014).

The ion channel hypothesis proposes that the influx of cation ions interrupts cation ion homeostasis and finally induces apoptosis in nerve cells. The extracellular deposition of Aβ fibrils is not adequate to predict the onset of Alzheimer's disease. Moreover, so far, all clinical trials to target the Aβ fibrillization process have broadly failed. However, this hypothesis proposes novel molecular targets for Alzheimer's disease therapies and great understanding of the mechanism underlying the progression of Alzheimer's disease (Hyunbum, et al., 2013).

The mechanism of action of Aβ ion channel is divided into three parts:

1- Channel formation, which forms channels permeable to cations.

2- Ionic leakage, which degrades membrane potential in neurons and rapidly disrupts cellular homeostasis.

3- Mitochondrial pathway of apoptosis which triggers apoptosis through insertion in mitochondrial membranes (Kagan, et al., 2002).

2.3 The dynamics of membrane potential

In recent decades, much has been learned about the behaviour of biological neurons. Due to the electrical response of the mechanisms of processing the nerve impulses through the neural cells in the CNS, applying extracellular stimulation to affect the activity and

the responses of the human nervous system has been extensively explored. Activation of sodium channels leads to changes in the membrane potential in around 10^-3 second, and this sharp change of voltage causes an action potential. Action potentials are the method by which the nervous system receives, analyses, and transfers information. The core mathematical framework for advanced biophysically based neural modelling was developed half a century ago by Alan Hodgkin and Andrew Huxley.

Several types of neurons have been studied and modelled e.g. squid axons (Hodgkin & Huxley, 1952a), frog (Dodge, 1967), dog (Matsuda, et al., 1958), rabbit (Amthor, et al., 1984), cat (Ahmed, 1997) and purkinje cell (Raman & Bean, 1999). The common specification of the models is that they are based on the membrane potentials of the cells, and the ion channel dynamics, originally formulated by Hodgkin and Huxley.

There are many models to represent the excitable membrane of the neural cells. Including Izhikevich, CRRSS (He, 2005), Frankenhaeuser (FH) and Hodgkin–Huxley (HH) (Hodgkin & Huxley, 1952 a), most of which are developed based on the Hodgkin–Huxley and Frankenhaeuser. The Frankenhaeuser model is based on the cell's ionic permeability, while the Hodgkin–Huxley model is based on the electrical conductance of the ion channels of the excitable membrane. While, the Frankenhaeuser model was extracted from electrophysiological experiments on the myelinated fibres of the frog while that the Hodgkin–Huxley model was achieved by an elegant series of experiments on the nerve fibre of a giant squid. The unique feature of the axon of giant squid is its remarkable large diameter, is approximately 0.5 mm (He, 2005). This large size of axon lets the nerve fibre conduct the action potentials quickly.

Since this vast diameter of nerve fibres is much thicker than other nervous systems, Hodgkin and Huxley were able to study and manipulate their model more easily than with other neural cell models. They applied voltage-clamp methods to collect large

quantitative experimental results. They presented a system of four-dimensional differential equations containing nonlinear functions. This model not only provides voltage-clamped experimental data but also is outstandingly successful in simulating the responses of action potential. It describes observed phenomena exactly and quantitatively analyse the change of currents and voltages on the membrane of cell. The Hodgkin–Huxley equivalent electrical circuit is shown as follows. It is well known that the signals of neurons communication are achieved through electrical potentials. The cell membrane of a neuron creates an ionic potential by separating various ions across its membrane. Any construct that can separate an electric charge can be considered a capacitor, even the lipid bilayer membrane of a neuron. Various ion channels are utilized by neurons to maintain a transmembrane ionic gradient, which produces electric potential which assumed as a battery. The pumps can be described as the electrical properties of a neuron membrane in the physical terms of resistors.
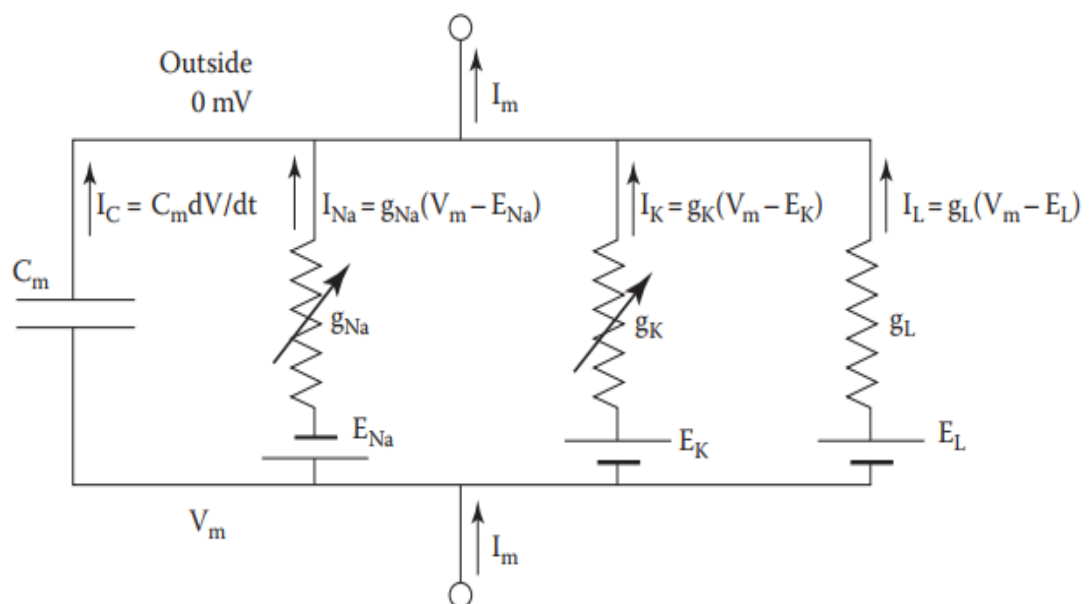
Figure 2.13 – Equivalent circuit of Hodgkin and Huxley. This circuit is a short segment of squid giant axon. Adapted from (Barnett & Larkman, 2007)

55

In general these models take the form

$$C_m \frac{dV}{dt} = I - f(\theta, \bar{V}) \qquad (2.1)$$

C_m is the capacitance of membrane, I is the current, V is the potential of membrane in mV, t is time. The various forms of the mathematical models are based on the structure and form of $f(\theta, \bar{V})$. This term is a function of (a) the probabilities of opening and closing of an ion channel, (b) the conductivity of the ion channel and (c) the potential difference between the membrane and the ion channel (given by V). In general, $f(\theta, \bar{V})$ is an algebraic sum of the currents associated with the various ion channels, and thus for a specific ion, i, this would take the form

$$f_i(\theta_i, V_i) = g_i(V - \bar{V_i}) \qquad (2.2)$$

$$(\theta, \bar{V}) = \Sigma_i f_i = \Sigma_i g_i(V - \bar{V_i}) \qquad (2.3)$$

The variables g_i are functions of the probabilities of the opening and closing of channels, and the conductance of that particular channel. $(\theta, \bar{V})$ is an algebraic sum of the currents associated with the various ion channels. The membrane potential dynamics around the activation and deactivation of the channels. Thus if the neuron dynamics are restricted to sodium and potassium channels, these become

$$\frac{dn}{dt} = \alpha_n(V)(1-n) - \beta_n(V)n \tag{2.4}$$

$$\frac{dm}{dt} = \alpha_m(V)(1-m) - \beta_m(V)m \tag{2.5}$$

$$\frac{dh}{dt} = \alpha_h(V)(1-h) - \beta_h(V)h \tag{2.6}$$

Where *n, m, h* (with range between 0 and 1) are representations of the properties of the open and closed channels for the different ions. Thus the membrane potential based model takes the form

$$\frac{dV}{dt} = I_{inj} + \sum_{i=1}^{N} g_i \psi_i(y_i)(V - V_i) \tag{2.7}$$

where ψ are given by *n, m, h.*

This model, based on the Hodgkin-Huxley membrane dynamics, essentially describes the time behaviour of the intracellular membrane potential and the currents through the channels. For the channels under consideration, the parameters given in (2.4) to (2.6) are given by the following

$$\alpha_n(V) = \frac{0.01\,(V+55)}{1 - \exp[-(V+55)/10]} \tag{2.8}$$

$$\beta_n(V) = 1.125\exp\left[-\frac{V+65}{80}\right] \tag{2.9}$$

$$\alpha_m(V) = \frac{0.01\,(V+40)}{1 - \exp[-(V+40)/10]} \tag{2.10}$$

$$\beta_m(V) = 4\exp[-(V+65)/18] \tag{2.11}$$

$$\alpha_h(V) = 0.07 \exp[-(V+65)/20] \tag{2.12}$$

$$\beta_h(V) = \frac{1}{1 + \exp[-(V+35)/10]} \tag{2.13}$$

Based on the relationships between permeability and conductance within the neuron (Hodgkin & Huxley, 1952a), the following can be obtained for the current generated within a particular ion channel:

$$I_{ion} = g_{ion} \cdot (V_m - V_{ion}) \tag{2.14}$$

Therefore, the three states, for sodium, potassium and leakage are given by the following algebraic equations:

$$I_{Na} = g_{Na} m^3 h (V - V_{Na}) \tag{2.15}$$

$$I_K = g_K n^4 (V - V_K) \tag{2.16}$$

$$I_L = g_L (V - V_L) \tag{2.17}$$

These equations represent a time-invariant system. In these equations, V is the trans-membrane potential. I_{inj} is the sum of external and synaptic currents. I_{Na} is the current in the sodium channel, I_k in the potassium, I_L is the leakage current. $0 \le m \le 1$ and $0 \le h \le 1$ are the gating variables indicating inactivation and activation of sodium ion current, respectively. $0 \le n \le 1$ is the gating variable showing activation of potassium ion current. g_{Na}, g_K, and g_l represent the maximal conductance of corresponding currents. $C_m = 1.0$

μF/cm^2 is membrane capacitance. I_{inj} is the current injected into the neuron. V_{Na} and V_K are the equilibrium potentials for the sodium ions and potassium ions. For channels that transfer a single type of ion, the potential of equilibrium can be computed easily. This equilibrium potential point has a direct relation with the ionic species, and it can be given by the Nernst equation. This equation can be used to predict the membrane voltage of a cell in which the plasma membrane is permeable to only one ion only.

$$V_{ion} = \frac{RT}{zF} \ln \frac{[C]_o}{[C]_i} \tag{2.18}$$

where V is the potential for both sodium and potassium which measured in volts. R is the universal gas constant which is 8.314 joules·K^{-1}·mol^{-1}, T is the temperature measured in Kelvins K$^\circ$ = 273.16+C$^\circ$; F is the Faraday constant which is $96,485$·mol^{-1} or J·V^{-1}·mol^{-1} ; z is the valence of the ion i.e. for Na$^+$, z = 1 and K$^+$, z = -1; and [C]$_i$ and [C]$_o$ are concentrations of the ions inside and outside the cell, respectively. In equilibrium, the Nernst potentials of all the diffusing ionic species are the same and equal to the membrane potential. By internal and external ion concentrations, equation (2.18) and its properties it is easy to calculate the sodium, potassium and leakage potential at equilibrium point (i.e. V_{Na}, V_K and V_L). This study supposes V_{Na} =50 mV, V_K=-71 mV, V_L=-51 mV. The ions concentration at the equilibrium point can be calculated by equation (2.14). This study supposes g_{Na} = 120 mS/cm^2, g_K = 36mS/cm^2, and g_l = 0.3 mS/cm^2, which are the ideal experimental data.

The Hodgkin-Huxley model is a phenomenological model of the generation of action potentials in neurons as a function of current injection or stimulus. The Hodgkin-Huxley model has a broad range of applications, for example, study of the impacts of ion

imbalances on a single neuron and its influences on synchronization in coupled neurons. The original Hodgkin-Huxley equations is a system with two channels, corresponding to Na^+ and K^+ ions and three gating variables for activation and inactivation for sodium and potassium ion currents.

2.4 Coupling and synchronization phenomena

Synchronization is effective in several fields of science. Generally, synchronization phenomenon is an adjustment of rhythms of oscillating objects because of their very weak interaction (Pikovsky, et al., 2003). Seventeenth-century, Christiaan Huygens first discovered the synchronization phenomenon (Pikovsky, et al., 2003). Huygens found that a couple of pendulum hanging from a common support area had synchronized. He observed that the oscillations of the pendulums coincided perfectly and they always moved in opposite directions. This discovery had a high impact on science and increased the accuracy of time. He discovered that the compatibility of the rhythms of the two pendulums was created by the invisible motion of the beam. What is really critical is that each pendulum moves through the supporting structure to the other pendulum. It means that both pendulums can feel each other. This phenomenon would mean that the clocks were synchronized because of coupling through the beam.

Suppose that there are two no identical pendulums that interact weakly and are not independent and have different oscillation periods. Assume that the two pendulums are fixed on a common support, and it is not a rigid beam. Experiments prove that even a loose action can synchronize both pendulums. Then this coupling adjusts their rhythms so they begin to oscillate with a common period. In general, the phenomenon is explained in terms of coincidence of different frequencies.

2.4.1   Synchronization in the neural system

The brain of human is the most complex system has been known. This system contains about 100 billion neurons that cooperate with a very complex complexity. In this project, the brain has been imagined as a physical system. This project, studies the neural network behaviour in the face of ionic imbalance. Neurons are nonlinear dynamical systems. They are able to transmit information between neurons by generating signals. An observable empirical phenomenon is the synchronization between the "firing" of neurons. It is now widely believed that correlation between spike trains plays a significant role in brain function. Synchronization is an essential mechanism that explains how our complex brain solves the problem. However, it should be noted that synchronization among a wide group of nervous cells can be harmful to healthy behaviour. For example, it is believed that tremor in Parkinson's or epileptic seizures is caused by such a mechanism. However, understanding the concept of synchronization and desynchronization is a major concern in modern brain research.

2.4.2   Synchronization of two coupled neurons

The Chapter 4 will analyse the synchronization phenomenon in systems of coupled neurons. The synchronization between the two self-excited oscillatory systems is a classical problem in synchronization theory. For coupled neurons in a relaxation regime, mutual synchronization of two coupled cells was investigated as well. Although the issue of coupled oscillators was studied in the first of the twentieth century, various new studies demonstrate a serious interest in many open issues on this subject (Osipov, et al., 2007).

2.5   Fault Detection

As the complexity of a system increases, the application of fault diagnosis methods to ensure tolerance to faults and reconfiguration becomes important (Isermann, 2005); (Poon, et al., 2017). The fault is the primary cause of changes in the structure or parameters of the system which finally leads to degraded system performance or even the loss of the system function. A fault is any external or internal event which changes the behaviour of a system, such that the system can no longer satisfy its purpose. In large systems, each component is designed to perform a particular function and the whole system works adequately only if all elements provide the service for which they are designed. Hence, a fault in a single component typically changes the performance of the whole system. To avoid any damage in the system, faults have to be found as soon as possible, and all decisions that stop the propagation of fault effects have to be made. These actions can be performed by control equipment, whose purpose is to make the system fault tolerant. In the case of success, the system function is satisfied also after the appearance of a fault, possibly after a short period of degraded performance. The control algorithm adapts to the faulty plant, and the overall system satisfies its function again. Generally, a fault in a dynamical system is a deviation of the system structure or the system parameters from the normal situation. In all these circumstances, the set of interacting components is changed by the fault. All these faults yield deviations of the dynamical input/output (I/O) properties of the plant from the normal ones and, hence, change the performance of the closed-loop system, which further results in a degradation or even a loss of the system function.

In statistics, an observation point which is distinct from other views is called an outlier (Grubbs, 1969). In data mining, the identification of observations that do not conform to

an expected pattern in the dataset is called outlier detection (or anomaly detection) (Chandola, et al., 2009).

Fault and anomaly detection

System model based methods (Control Model-Based)		Data model based methods (Artificial Intelligence Model-Based)	
	System Model	Quantitative Model	Qualitative Model
Signal Model	Most disciplines of the engineering profession require a sound understanding of the techniques used in the modelling and control of dynamic, multi-domain physical, and other, systems. For example: $\begin{cases} \dot{x} = f(x) + g(x)u \\ y = h(x) \end{cases}$	Some methods like Neural Network (NN) Networksk Bayesian (BN), Principal Component Analysis (PCA), Support vector machine (SVM), and so on	Some methods like Expert systems, Fault Tree Decision, and so on
The idea of signal modelling is to represent the signal via (some) model parameters. $x(t) = A\,Cos\,(\omega t) + noise.$			

Table 2.1 – Classification of fault detection.

Researchers have purposed different concepts from several fields such as statistics, machine learning, data mining, spectral theory, and information theory. They have applied them to particular problem formulations. An anomalous observations can be applied to various problems such as a structural defect, medical conditions, finding errors in text, bank fraud, etc.

One such concept is abnormal event management (AEM), an execution flow that diagnoses and corrects abnormal conditions of faults in a process which requires accurate fault diagnosis and also a complete supporting system for making the right decisions. Another related concept is fault detection. Fault detection ensures continual acceptable function of a system when a fault occurs through fault detection. Fault detection also provides controller reconfiguration in response to the particular fault after detection. Fault detection makes a binary decision as to whether something has gone wrong or is operating normally, determining the location and nature of the fault. Specifically, fault detection techniques take advantage of the concept of redundancy which can be divided into two kinds. They are analytical redundancy and hardware redundancy.

There are many kinds of classifications of fault detection in the literature, (Hwang, et al., 2010); (Hodge & Austin, 2004); (Chandola, et al., 2009); (Isermann & Balle, 1997); (Venkatasubramaniana, et al., 2003); (Kleer & Williams, 1987), but this research need to summarise the models in order to choose a correct direction. The suggested classification of diagnostic methods is presented as Table 2.1. In this classification, fault detection methods are divided into two types: system model based methods (or Control Model-Based) and data model based methods (or Artificial Intelligence Model-Based). Detecting faults in a system using a system model based methods is divided into two

categories, signal model and system model. On the other hand, there are data model based methods that deal with faults and outliers by two methods quantitative and qualitative models.

2.5.1   Generation of residuals for fault detection

The most recent fault detection methods apply system models for producing residuals (Korbicz, et al., 2012). A diagram for fault detection using residual generation is shown in Figure 2.16. The process of fault detection using this method consists of two parts.

Figure 2.14 – Fault diagnostic diagram using residual generation

In the first part, the residual value is generated according to a model of the system and in the second part the value is defined and finally, the diagnostic signal is produced by the algorithm. The residuals can be calculated as follows:

1. The measured value obtained by using the difference between a process variable and its value estimated based on the model.

2. The measured value obtained by using the difference between the right-hand and the left-hand sides of the system equation (Frank, 1990).

3. The measured value obtained by using the difference between estimated and nominal values of the parameter of the model.

Among the group of analytical methods used for detection of faults, the following diagnostics can be obtained (Korbicz, et al., 2012):

1- Diagnosis using physical models

2- Diagnosis using linear input-output-type models

3- Diagnosis using state observers or Kalman filters

4- Diagnosis using online based identification

Residual generation methods and the algorithms for the evaluation the value of residual to making a decision on fault detection are briefly explained below.

There are several methods for residual generation. These methods are as follows:

1- Residual generation based on physical equations

2- Residual generation based on system transmittance

3- Residual generation based on state equations

4- Residual generation based on state observers

5- Residual generation based on neural and fuzzy models

As this project has been used residual generation based on state observers this method is described in the below.

2.5.1.1   Residual generation based on state observers

Residual generation techniques based on Luenberger observers were developed by Clark (Clark, 1978), Frank (Frank, 1990) and Patton (Patton & Chen, 1993). In this technique, the output signal of the observer is compared with the real signal. The difference is considered as the residual (see Figure 2.15).
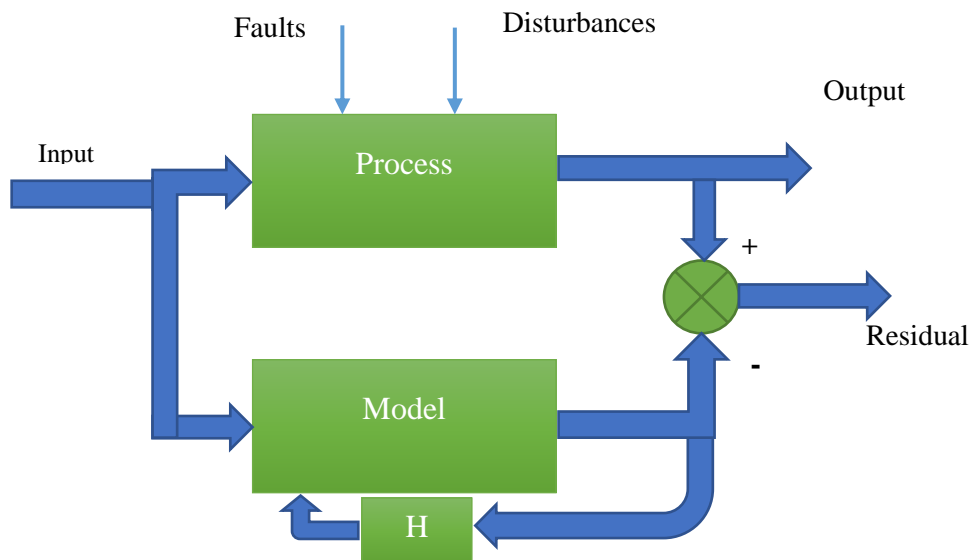
Figure 2.15 – Fault detection using state observer

Use of observers in order to generate residuals has a wide range of applications from typical observer to automatic control and its task is the recreation of immeasurable state variables, not output signals. In the classical of residual generation, the system output is approximated based on the input signals (Korbicz, et al., 2012). In addition to input signals, measurable outputs are also applied by the observer to estimate outputs. An important idea in using observers is applying feedback from the difference between the estimated outputs and real outputs of the system in order to improve of the model by defining a suitable feedback matrix like *H*. Feedback is needed to compensate different initial conditions and to stabilize the observer of unstable systems. The observer guarantees estimation error convergence to zero for any initial conditions.

2.5.1.2 Algorithms for deciding on fault detection using the evaluation of the residual values

Each fault detection algorithm contains a decision section in which the evaluation of the residual value takes place and the decision to detect the fault is made with the possible indication of the event in the form of an alarm. The simplest and most widely used decision algorithm is the comparison of the absolute residual value with its threshold value (Korbicz, et al., 2012). A diagnostic signal like *d* takes the value "1" if the threshold value *T* has been exceeded and it means the fault symptom is detected.

$$d(residual_j) \begin{cases} 0 \ if \ |residual_j| \leq T \\ 1 \ if \ |residual_j| > T \end{cases} \tag{2.19}$$

2.6 Summary

The neuron forms an important unit of the nervous system, so its understanding is significant for neural processing. The reaction of a neuron to external stimulation is in the form of spikes. The spikes present the basis of neuronal functions and activities. It is thought that the train of spikes plays an important role in neural processing. A neuron can be classified into three parts:

1- The soma

2- The axon

3- The dendrites

There is a synaptic transmission which occurs due to the release and binding of neurotransmitters. These neurotransmitters release between the pre-synaptic and post-synaptic neurons which causes the neuron to generate spike. The study of neurophysiology showed that this electrical activity is due to the movement of charge

across the neuron plasma membrane. This flow in the membrane of a neuron is due to the ions that act as carriers of charge.

A number of different types of neurons have been studied and modelled. The common feature of these models is that they are based on the membrane potentials of the cells, and the ion channel dynamics, originally formulated by Hodgkin and Huxley. There are many models to represent the excitable membrane of the neural cells and most of which are developed based on the Hodgkin–Huxley. The Hodgkin–Huxley model is based on the electrical conductance of the ion channels of the excitable membrane.

The coupling and synchronization phenomena have discussed in this chapter as well. Synchronization is an adjustment of rhythms of oscillating objects because of their weak interaction. These phenomena occur in the neural activities when two neurons are coupled with each other and have interactions.

The concept of fault was also discussed in this chapter. A fault is an internal or external event which changes the behavior of a system, such that the system can no longer satisfy its purpose. The faults are the primary cause of changes in the parameters of the system which finally leads to degrade the performance of system or in some condition the loss of the system function. Since neurodegenerative diseases are a dysfunction in the function of neurons, it can be interpreted as a fault in the neuron.

3 The role of ion gradients in signal generation in neurons

3.1 Introduction

Description of a system using mathematical concepts and language called a mathematical model (Melnik, 2015). Applying the mathematical models in the experimental analysis has increased in recent years and they have many advantages (Mazur, 2006). Meanwhile, computational modelling is applying the mathematical model to computational science which needs considerable computational resources to investigate the behaviour of a complex system with a simulation (Melnik, 2015). Basically, models can be categorized into several classes. First of all, a model can be static or dynamic (Winkler, 2014). The static model defines the structure of a distributed parameter system which means that the system describes it in a specific time instant. In contrast, a dynamic model describing the behaviour of a system over time. This kind of model is applied when the behaviour of a system described as a set of conditions and this conditions occur in the sequences (Kemmetmüller, 2008). The mathematical equations of a model divide to linear and non-linear. Research activities in the field of nonlinear models are very important, as the more demanding performance required in practical applications. Moreover, in the real world, the majority of systems are nonlinear in nature (Kugi, 2001). This chapter applied neuronal mathematical modelling along with computational modelling to investigate the electrolyte dysfunction following ionic channels disease.

Electrolyte dysfunctions cause abnormal electrical conduction in the excitable cells of the heart and in general the nervous system. These disorders can result in neurologic impairment and extreme cases cause death as a result of osmotic demyelination (Bacak, et al., 2016). Of the many electrolytes present in these cells, sodium (Na+) and potassium (K+) are two essential electrolytes which play a role in the generation of synaptic signals. Since the first publication of a neurone model (Huxley, 1952a), some simulated studies have been carried out investigating the various properties of the neurones. These studies range from modelling of potassium in the cells (Jensen, 2012); ion channels (E. Schneidman, 1998) (Izhikevich, 2003), the effect of noise on the dynamic behaviour (Kang, et al., 2016). The key elements of these studies are based on the initial Hodgkin-Huxley model (LuWang, et al., 2016) (Mahmud & Vassanelli, 2016) (Brette, 2007), and the simulation of both the neurone and spiking neurones which are a simplified version (Izhikevich, 2003) (Brette, 2007) (Nygren, 1998). However, most of these studies, often separate ion imbalances from other effects and often do not investigate the combined effect of ion imbalances.

The advantage of using a Hodgkin–Huxley model is that the dynamics are fast, and also it is a phenomenological model of action potential generation in nerve cells as a function of a given current stimulus. In this chapter, using the Hodgkin-Huxley model, the electrolyte imbalances are investigated from the tremors and seizures point of view. A result of this study is to determine if there is a limiting point that is a point beyond which there is no response to the stimulus. At the same time, an investigation is carried out to determine the combinatorial effect of ion imbalances. The simulation studies show that the change in response is such that both the inter-spike interval and magnitude of the spikes change. These changes are different when a single ion imbalance occurs, and when combined ion changes occur it will be seen that the response is similar to the response

when there is an imbalance in the potassium ion. An important consequence of these imbalances is that the responses of individual cells, when combined, are reflected in the manner in which muscles respond signals from the brain or external stimulation. Understanding the mechanisms underlying this type of the response of a neurone could contribute to early detection or even the treatment of some neural deterioration diseases and further promote the clinical application. Simulation analysis of ion channels using computer models gives some tools to uncover the potential unknown causes of ion channels related diseases and may help to design new experiments to further improvement or even curing. In this regard, recent research findings indicate that it may be possible to target the certain ion channel that drives specific disease and providing an illustration of the impact of the Hodgkin–Huxley model in the clinical domain (Waxman, 2012). So, it will be increasingly beneficial for clinical scientists to keep in touch with biologists who studies on ion channels.

3.2   Ion channels for generating signal

In the nervous system, action potential and consequently, membrane potential is regulated by the voltage-gated sodium and potassium channels during a neuronal action potential. Sodium and potassium ions are responsible for the generation of the action potential in the neurone. The nervous system consists of a vast number of interconnected neurones, which transmit signals using ion channels to generate potentials across membranes. As a result, the chain of neurones is activated by electrical signals generated at various points. When a stimulus occurs, the activation of the neurone results in an internal change in concentration of the ions. These changes lead to a membrane voltage, which is dependent on the threshold for the particular cell. The first stage in this change is known as depolarization after which an action potential is triggered (Frohlich &

Jezernik, 2005). In response to depolarization in transmembrane voltage, ion channels allow an inward flow of sodium ions. As a result of these changes the electrochemical gradient, which in turn produces a further rise in the membrane potential. It then makes more channels to open and to generate further electric current throughout cell membrane. The firing process continues as long as all of the existing ion channels are open. Therefore a significant expansion is caused in membrane potential. The mentioned process proceeds, explosively until all of the available ion channels are open, and thus significant increase is due to membrane potential. The rapid influx of sodium ions causes ion channels rapidly inactivate because it reverses the polarity of the membrane. When a stimulus occurs, the sodium channels open, which results in the depolarization and an increase in membrane potential. The rate of depolarization is dependent on the difference in sodium concentration both inside and outside the cell. The magnitude of the response is also dependent on the concentration of these ions. The second stage occurs when the sodium channels close (Chappell & Payne, 2016). As a result, sodium ions can no longer enter the neurone, and then they are transported back out of the membrane. Then the potassium ions effect the remainder of the response (Chappell & Payne, 2016). By activation of potassium channels and outward current of potassium ions, the electrochemical gradient returns to the resting state.

3.3   Build the computational model

As most models of neurones are phenomenological in that they often model flows of currents through, an ideal yet realistic representation of these neurones in the Hodgkin-Huxley model. Here the flow of currents through ion-selective channels in the neural membrane allows us to investigate the effect of changes in the concentrations of various ions in the neurone. In this model, action potentials are generated as a function of current

injection or stimulus. Hodgkin-Huxley model has a broad range of clinical applications, for example, in the study on impacts of electrolyte diseases on nervous system using ion channels and different ion concentrations. Another key feature of this model is that it also describes the time behaviour of the intracellular membrane potential and the currents through potassium (K^+) and sodium (Na^+) channels. As a result, it allows for an accurate explanation of the observed phenomena and enables the quantitative analysis of the effects of change of voltages and currents on the nerve cell membrane. The model consists of the four equations (2.4), (2.5), (2.6), and (2.7). The three states presented by the algebraic equations in the equations (2.15), (2.16), and (2.17). Where the nonlinear functions of V are as equations (2.8), (2.9), (2.10), (2.11), (2.12), and (2.13).

3.4 Ion gradient and potential

Currents are generated when ions flow across a membrane, from the higher concentration to the lower concentration. In other words when there is a concentration gradient. This process makes a voltage across the membrane that opposes the motion of ions. The flow of ions stops when the voltage reaches an equilibrium value. This process is usually called electrochemical gradient. A key element of this study is to investigate the effect of changing ion concentrations. These concentrations affect both the currents and the voltages in the model. The effect of the concentration of the ions on the voltages is given by the Nernst equation (Rossetto, 2016) and are as follows.

$$V_{Na^+} = \frac{RT}{zF} \ln \frac{[Na^+]_o}{[Na^+]_i} \tag{3.1}$$

$$V_{K^+} = \frac{RT}{zF} \ln \frac{[K^+]_o}{[K^+]_i} \tag{3.2}$$

V is the potential for both sodium and potassium which measured in volts. R is the universal gas constant which is 8.314 *joules·K⁻¹·mol⁻¹*, *T* is the temperature measured in Kelvins*; z* is the number of elementary charges of the ion; Faraday constant *F* is *96,485·mol⁻¹* or *J·V⁻¹·mol⁻¹.* The extracellular concentration of potassium is *[K+]ₒ* which measured in *mol·m⁻³* or *mmol·l⁻¹*. Intracellular concentration of sodium is *[Na⁺]ᵢ* . Extracellular concentration of sodium is *[Na⁺]ₒ* which measured in *mol·m⁻³* or *mmol·l⁻¹*. *[K⁺]ᵢ* is the intracellular concentration of potassium. Therefore, increasing / decreasing the V, has direct relation with increasing/decreasing the $[Na^+]_o$ and $[K^+]_o$. Hypernatremia (hyponatremia) and hyperkalemia (hypokalemia) are a high (low) serum sodium and potassium levels, respectively, so changing the potential of sodium and potassium means changing the $[Na^+]_o$ and $[K^+]_o$ as in equations (3-1) and (3-2) $[Na^+]_o$, $[K^+]_o$ have direct relation to V_{Na^+} and V_{K^+}.

3.5   Simulation

As mentioned above, the Hodgkin-Huxley model can be used to simulate and study the impact of electrolyte imbalances on the nervous system. In this project, this is carried out using the ode45 algorithm. The accuracy provided by this method is one of the main reasons for its use in the simulation of neurones, more specifically the Hodgkin-Huxley neurone (Dormand & Prince, 1980). Ode45 is based on an explicit Runge-Kutta method, and is essentially a one-step solver, in other words, it needs the numerical solution at the time, y (t_{n-1}) to determine y (t_n).

Two sets of experiments have been carried out. In the first set, an assessment of effect different single ion concentrations is made. The second set of experiments the combinatorial effect of different ion concentrations is studied. In general, the outputs of neurones are a set of spikes over a period of time, and a spike train can be characterised

by both the intervals between spikes, and the magnitude of the spikes (Sarangdhar & Kambhampati, 2008) (Sarangdhar & Kambhampati, 2011). Thus the analysis and assessment carry out in this project, is based on the changes in the mean interspike intervals and mean of the magnitude of the spikes trains.

One of the key findings is that often the neurone responds in a zero stimulus condition when there is a particular concentration of ions present in the cell. This is a phenomenon seen in everyday situations; there is the tremor in the muscles even when there is no stimulus (Ha, et al., 2016). This then enables a proper analysis of the neuronal responses under a variety of different situations. Thus the stimulus current is not applied for the first 50 seconds of all tests.

3.6 Results

Figure 3.1 shows the responses of the neurone for the nominal set of values mentioned earlier. It can be seen that there is no response between 0 second and 50 seconds, and then once the external stimulus is applied the neurone response. There is no response between 0 second and 50 seconds to consider the behaviour of system during the non-stimulating time. It can be seen that the response is a series of spikes, which have two characteristics, one is the magnitude of the spike and the other is the time between spikes, known as the inter-spike interval. This response is taken to the ideal response, and all comparisons are made to this response. The comparison is carried out for four different electrolyte diseases, i.e., hypernatremia, hyponatremia, hyperkalaemia, and hypokalaemia and combinations there off.
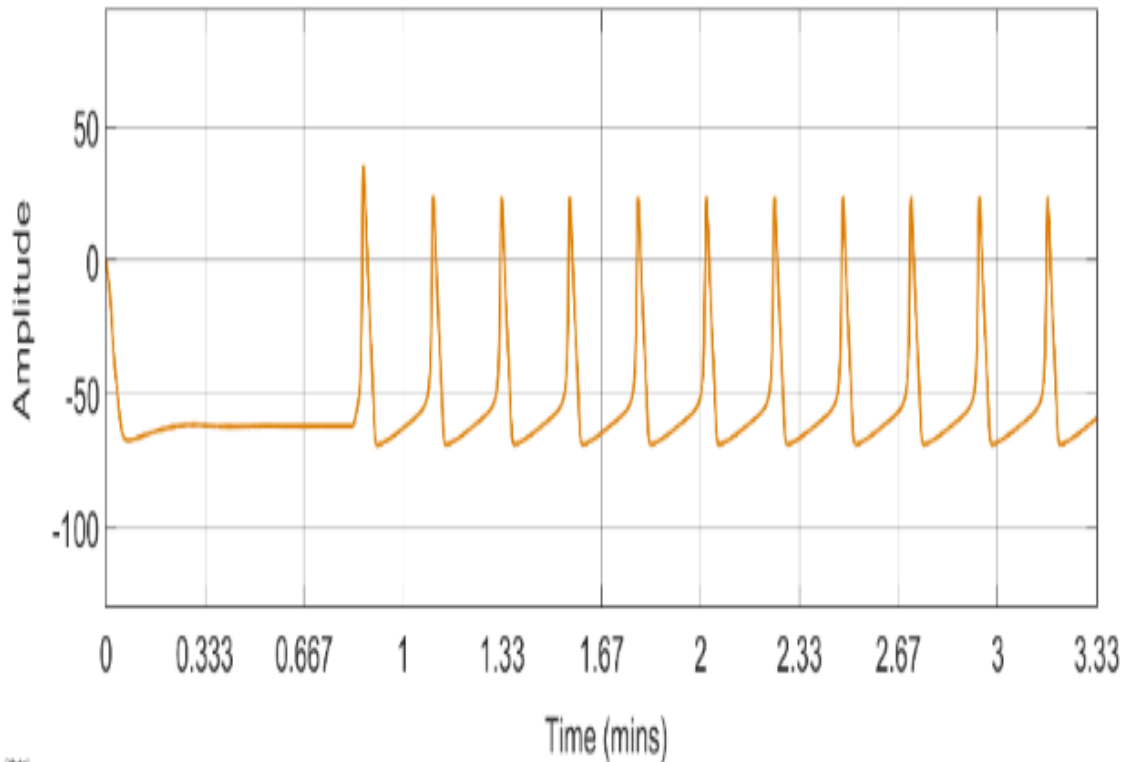
Figure 3.1 – The running of experiments for three neurones without any changes. All three graphs have been overlapped. V_{Na}=50 mV, V_K= -71 mV.

3.6.1   Changes in sodium ion concentration

The first set of results show the responses of the neurone to different levels of sodium

ion concentrations in the neurone. The values were changed so that both Hyper and

Hyponatremia are present. These are shown in Figure 3.2 below. The nominal values for

V_{Na}=50 mV, V_K= -71 mV which its result is presented in Figure 3.2. The sodium

potential was changed in stages from 80 mV to 2o mV, with the nominal value of 50 mV

being the median value. The graphs show the responses the nominal values in Figure 3.1

and those for the different value of sodium Figure 3.2. It can be seen that as the sodium

ion concentration is increased from its nominal value, the magnitudes of the spikes

increase, while the inter-spike interval is reduced. In other words, neurone responds with

larger spikes at a more rapid rate. As the sodium concentration is decreased, it can be

seen that the magnitude of the spikes is suppressed to a point where there is no response

from the neurone.
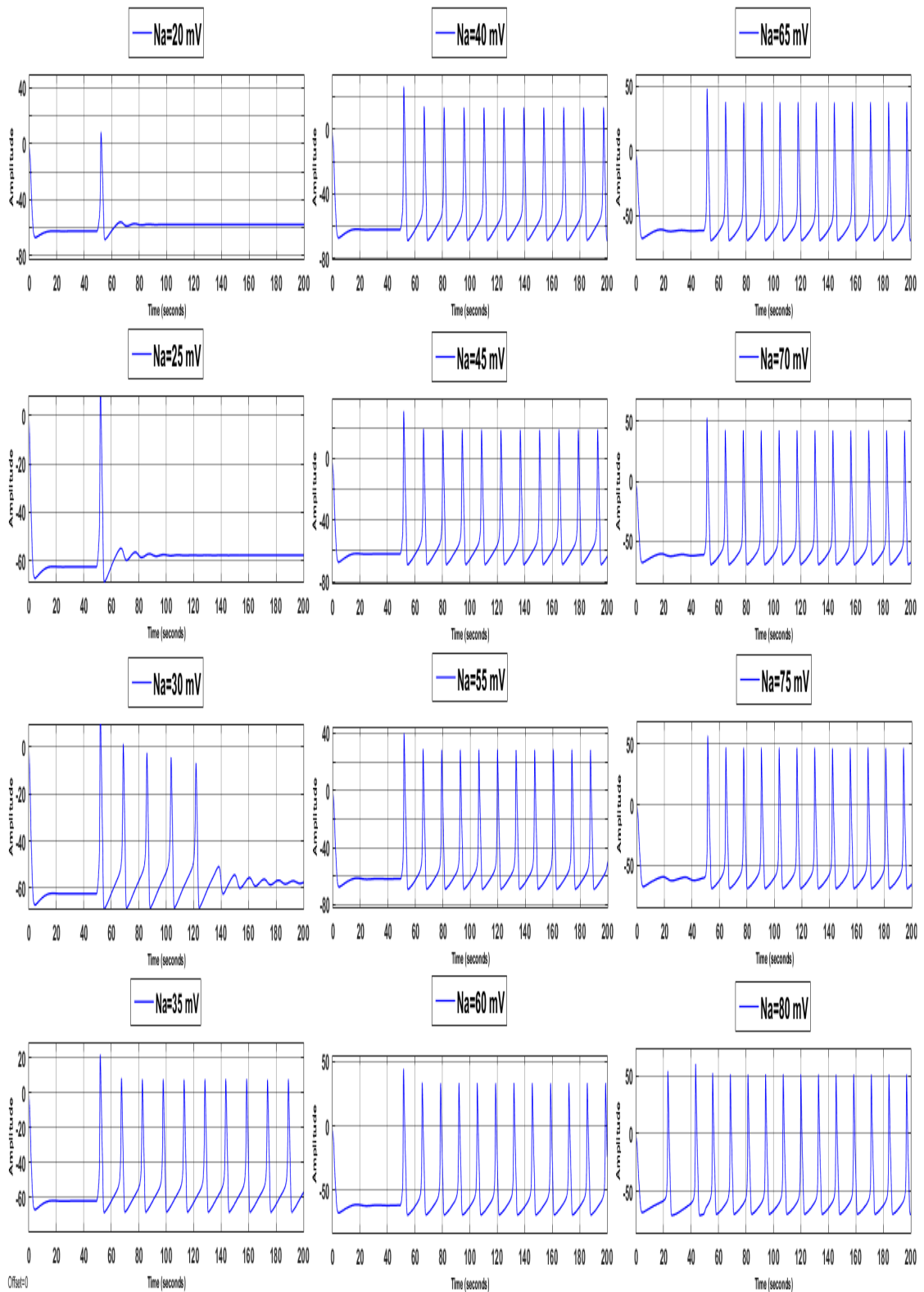
Figure 3.2 – Sodium changes and the responses of neurone in the course of hypernatremia and hyponatremia. The potassium value for all of these experiments remained as normal, V_K= -71.

3.6.2 Changes in potassium concentration

A similar set of results were obtained for the potassium ion concentration. These are shown in Figure 3.3. In the experiments, the effect of changes in potassium ion concentrations is more pronounced. Both a little increase and decrease in potassium ion concentration leads to no responses from the neurone. Thus, when V_K is -51 mV the magnitude of the spikes is zero, and there is no discernible interspike interval. A similar situation arises when V_K is below -76 mV. It should be noted that these values are not that far from the nominal values of potassium which is -71 mV. This indicates that the neurone is more sensitive to potassium ion changes than to sodium ion changes. Of course, the limits of these ranges can change if the parameters of the neurone are modified.

Deficiency of potassium typically occurs when the body loses a lot of fluid. Common signs and symptoms of potassium deficiency include weakness and fatigue, muscle cramps, muscle aches and stiffness, tingles and numbness, heart palpitations, breathing difficulties, digestive symptoms and mood changes. Signs of a potassium overdose include muscle weakness or paralysis, irregular heartbeat, confusion, tingling sensation in the limbs, low blood pressure, and coma.

3.6.3 Combination of changes

The next set of results is meant to changes combination of sodium and potassium in a single neurone. To investigate this particular situation, two different comparisons were carried out. In the first part, the sodium potential was changed at different stages from 61 mV to 41 mV and the potassium potential was decreased from -61 mV to -81 mV, stage by stage. These results are shown in Figure 3.4 and Figure 3.5 below. From the results in these figures, it is apparent that the still it is clear that the both sodium and potassium

changes at the same time affected almost every element of the action potentials, i.e. interspike interval and magnitude of the spikes. Results from these two figures can be compared with the results in Figure 3.2 and Figure 3.3 which shows when combined ion changes occur in the neurone it can be seen that the response is similar to the response when there is an imbalance in the potassium ion.
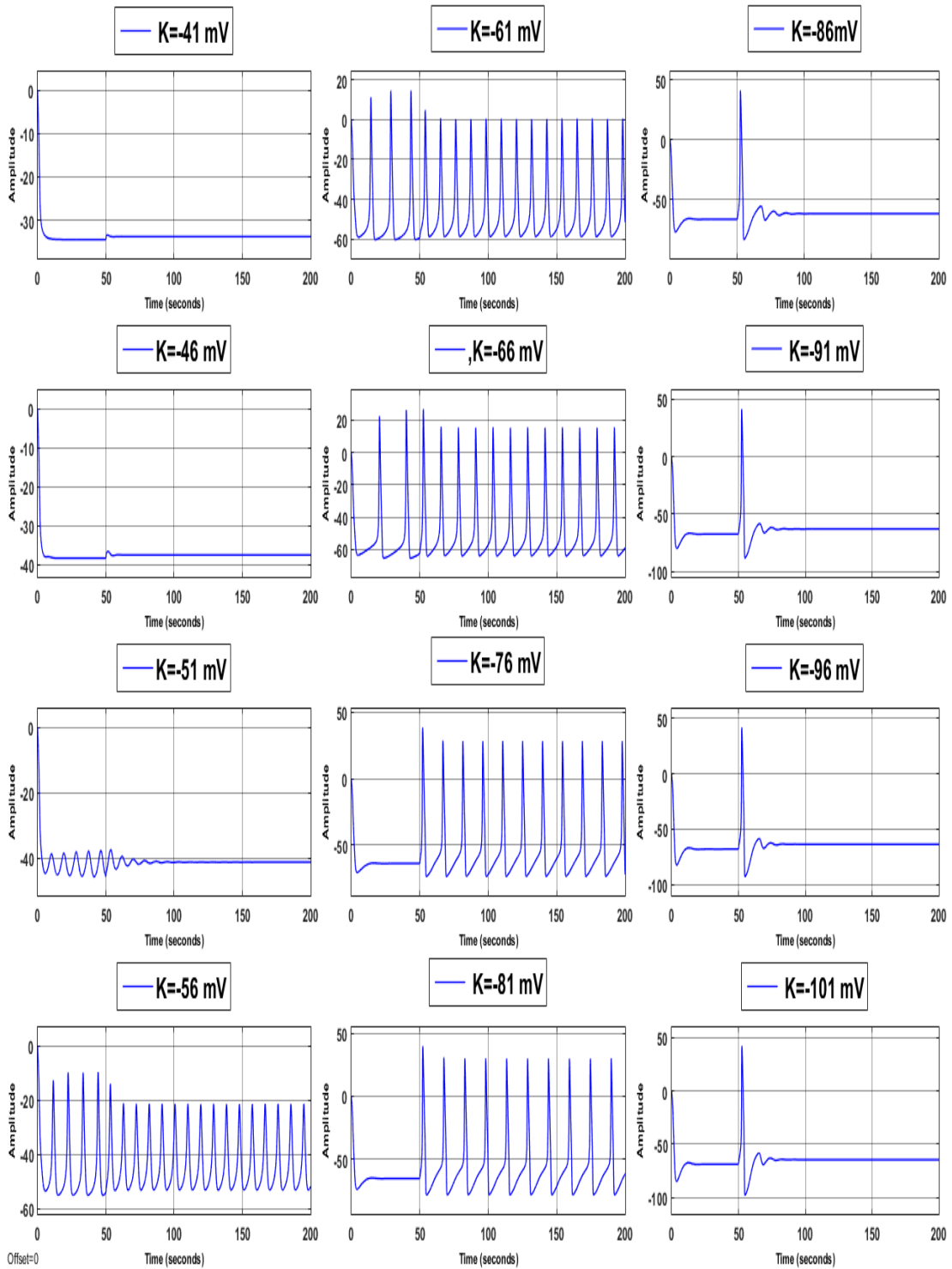
Figure 3.3 – Potassium changes and the responses of neurones in the course of hyperkalaemia and hypokalemia. The sodium value for all of these experiments remained as normal, V_{Na} =50.
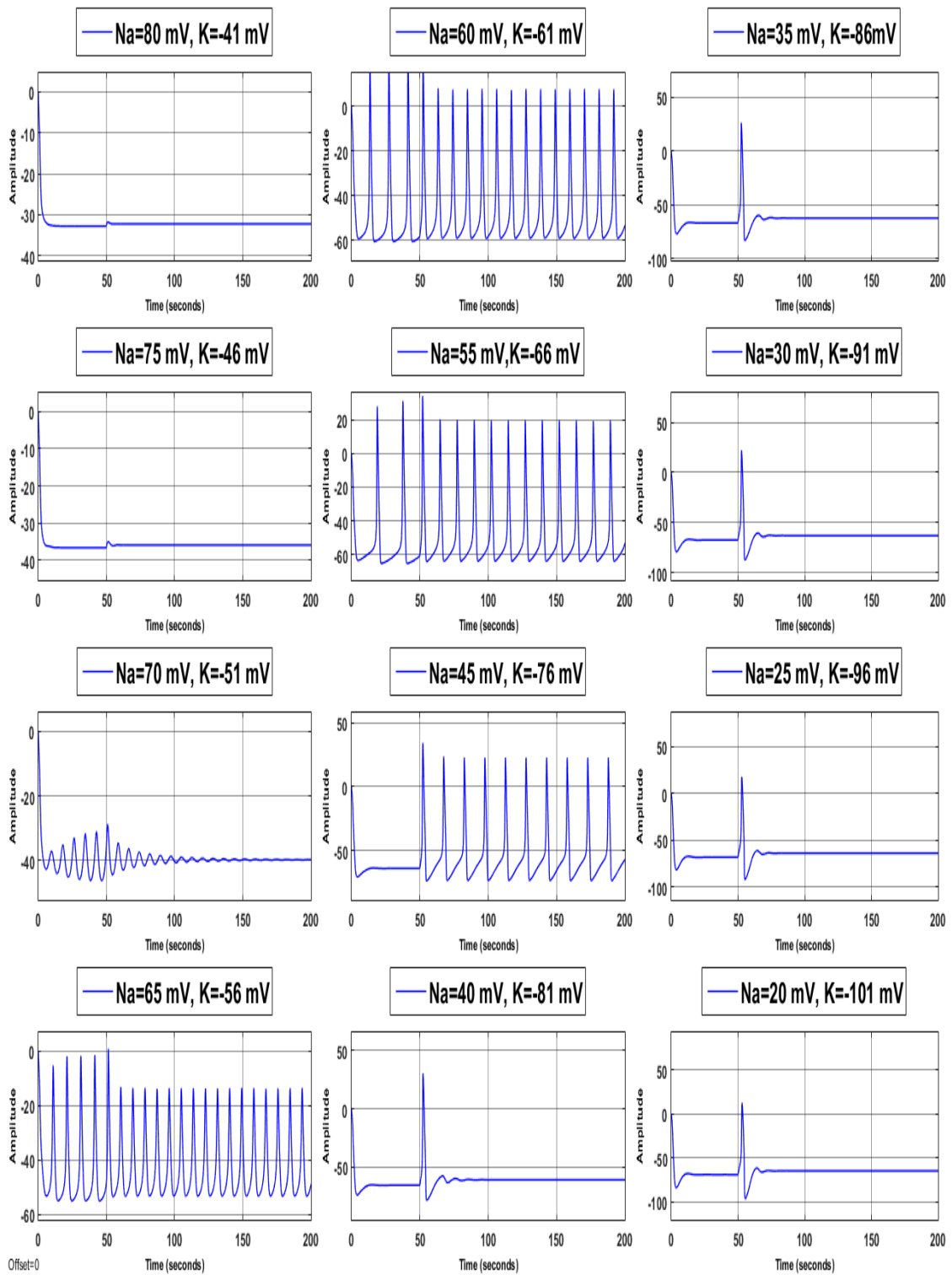
Figure 3.4 – Sodium and potassium changes and the responses of neurones in the course of hypernatremia-hyperkalaemia and hyponatremia- hypokalaemia.
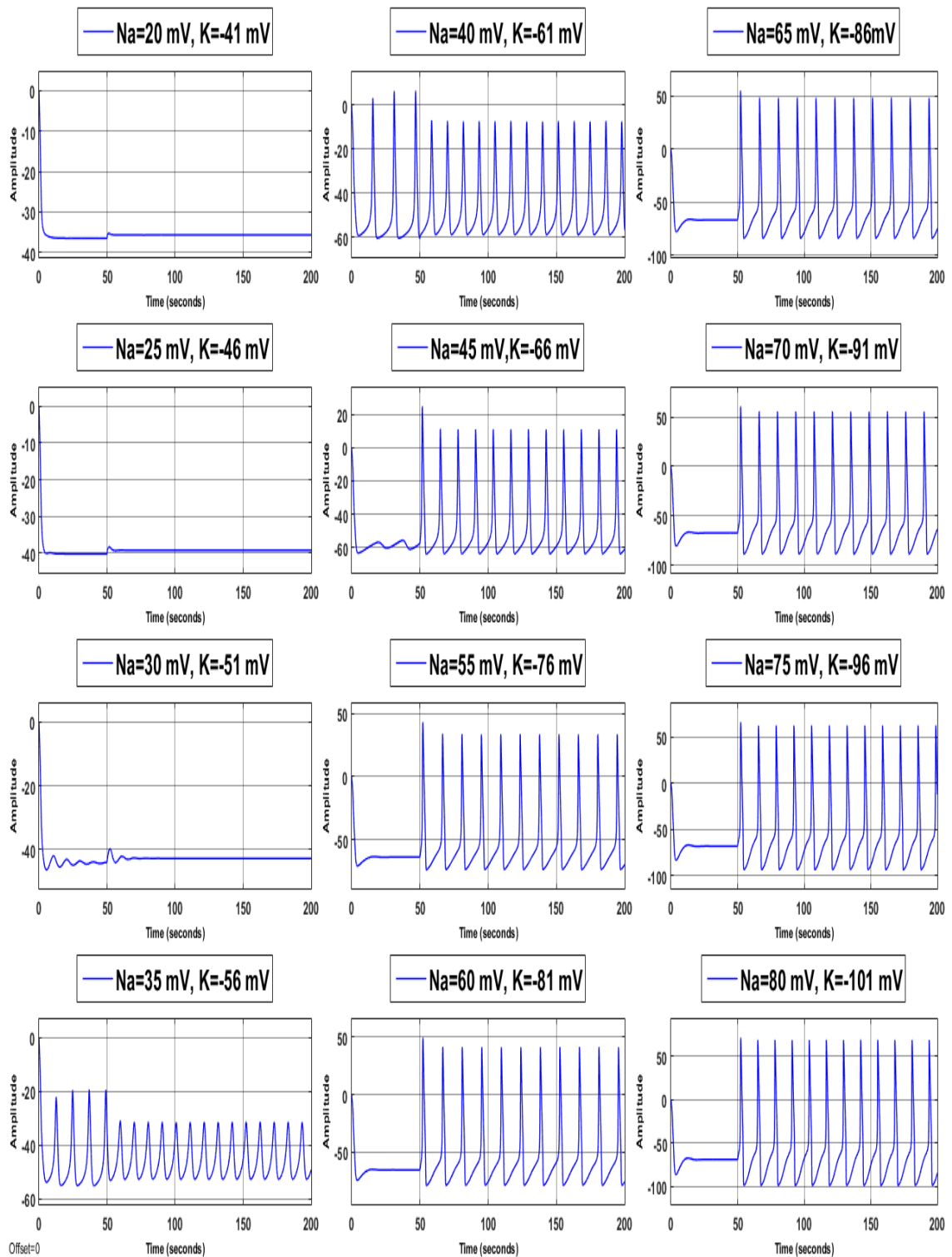
Figure 3.5 – Sodium and potassium changes and the responses of neurones in the course of hyponatremia-hyperkalaemia hypernatremia-hypokalaemia.

3.7 Analysis of the responses

The results of these experiments show that there is a significant relationship between sodium and potassium changes and the level of the action potential and resting potential. As mentioned earlier the concentrations of both potassium and sodium ions determine the characteristic of the spike train (Chappell & Payne, 2016). The results for the various values of potassium and sodium and their combinations are shown in Tables (3.1) – (3.4). These tables show both the mean interspike intervals and the average magnitudes of the spikes trains.

From these results, it can be seen that although the magnitude of the spikes increases with an increase in sodium ion concentration, there is no proportional change in the resting response of the neurone. Another feature is that the rate at which spikes are generated increases, which is the interspike interval is reduced. This is in line with the common perception that sodium increase the rates of responses of neurones, and is often reflected in the way the heart rate changes with sodium (Walkowska, 2016). On the other hand for changes in potassium, it can be seen that there is a change in the resting response of the neurone. The resting potential is reduced at the same time, the magnitude of the spikes increases and then decreases and the interspike interval increases with an increase in potassium ion concentration. Again this is in line with a feature seen in neurones, where potassium causes weak responses in muscles as its concentration changes (Gijsbersa, et al., 2016). These results are summarised in Table 3.2.

The impressive set of results occurs when both sodium and potassium are changing. These can be seen in Tables 3.3 and 3.4. What can be seen is that potassium ion concentrations dominate the responses, even when sodium concentrations change. Indeed, when sodium is low, it would be natural to expect a result which would reflect low sodium. However, the potassium ion dominates the nature of the response across all

the ranges. Even an increase in sodium is not reflected in the resting response of the neurone. At the same time, higher levels of both sodium and potassium indicate that the interspike interval is smaller than at the opposite end.

3.8   Discussion

The results in the previous sections can be summarised in the following figures (See Figure 3.6 - Figure 3.8). The interesting feature of the results is to see the combined effect of the concentrations of the two ions in the neurone. The results of the project, show the responses of a neurone when imbalances in both sodium and potassium occur. This should help, in the understanding of neuronal disorders e.g. tremors, motor neurone disease, amongst others. The reason for this is that intracellular and extracellular potassium and sodium concentrations play a vital role in the electrophysiological function of the body and neurones that control it. These ions are essential in maintaining cellular homoeostasis, and most metabolic processes are dependent on or affected by these electrolytes (Chappell & Payne, 2016).

The results show that the resting membrane potential of a neurone is dominated by the concentration of the potassium ion, and thus the potassium concentration gradient across the membrane (see equations (3.1), (3.2)). The results also show that when both the sodium potential and the potassium potential change simultaneously, the membrane experiences slightly stronger changes in resting potential (see Table 3.4). The results obtained from the hypernatremia and hyponatremia in Table 1 shows slight changes in resting potential with hypernatremia and hyponatremia. Therefore, changes in sodium ion concentration have a relatively minor effect on the resting potential. As the membrane of the resting neurone is more permeable to potassium than to any of the other ions present, and on the other hand, there is more potassium inside the neurone than outside,

so this results can be acceptable. It is worth mentioning that the selective permeability to potassium is caused by potassium permeable membrane channels that are open in resting neurones. The results can be summarised as shown in Figure 3.6. Both the peak magnitude and the interspike intervals are dependent on polarisation and depolarising characteristics of the action potential and ion concentrations. These are now summarised in Figure 3.6 - Figure 3.8.

The chapter presented results which indicate that responses to changes in the ion concentrations can be simulated. These results and the ability to represent changes in ion concentrations and the gradients across membranes will help in developing models for more complex networks of neurones. Such simulations would be of help in studying the physiological effect of ion concentration changes (which could be a reflection of diets). Such studies will assist in the development of an artificial human brain, and also increase our insight into various neuronal disorders, without the need of physical specimens.

Ideally, these type of models would present an alternative to studying on some diseases process and increasing therapeutic efficiency or reducing the risk of side effects of drugs without any aggressive action on the human. In the future, it would be crucial to developing computational models to study diseases like Alzheimer's disease (AD).
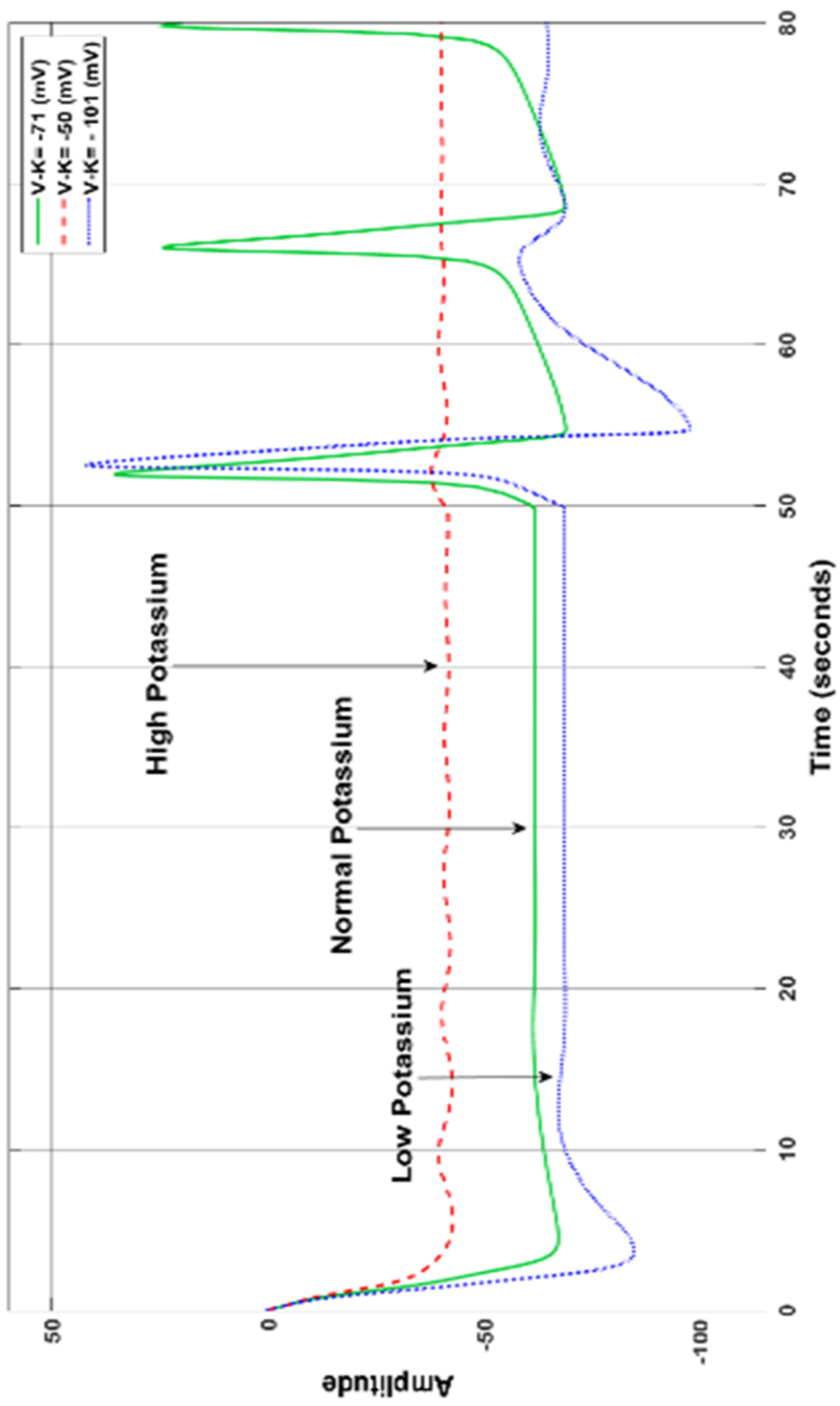
Figure 3.6 – Increasing the extracellular level of potassium means more K+ enters the cell and it goes resting potential up. In comparison, decreasing the extracellular level of potassium means more net K+ leaves the cell, and it goes resting potential down.
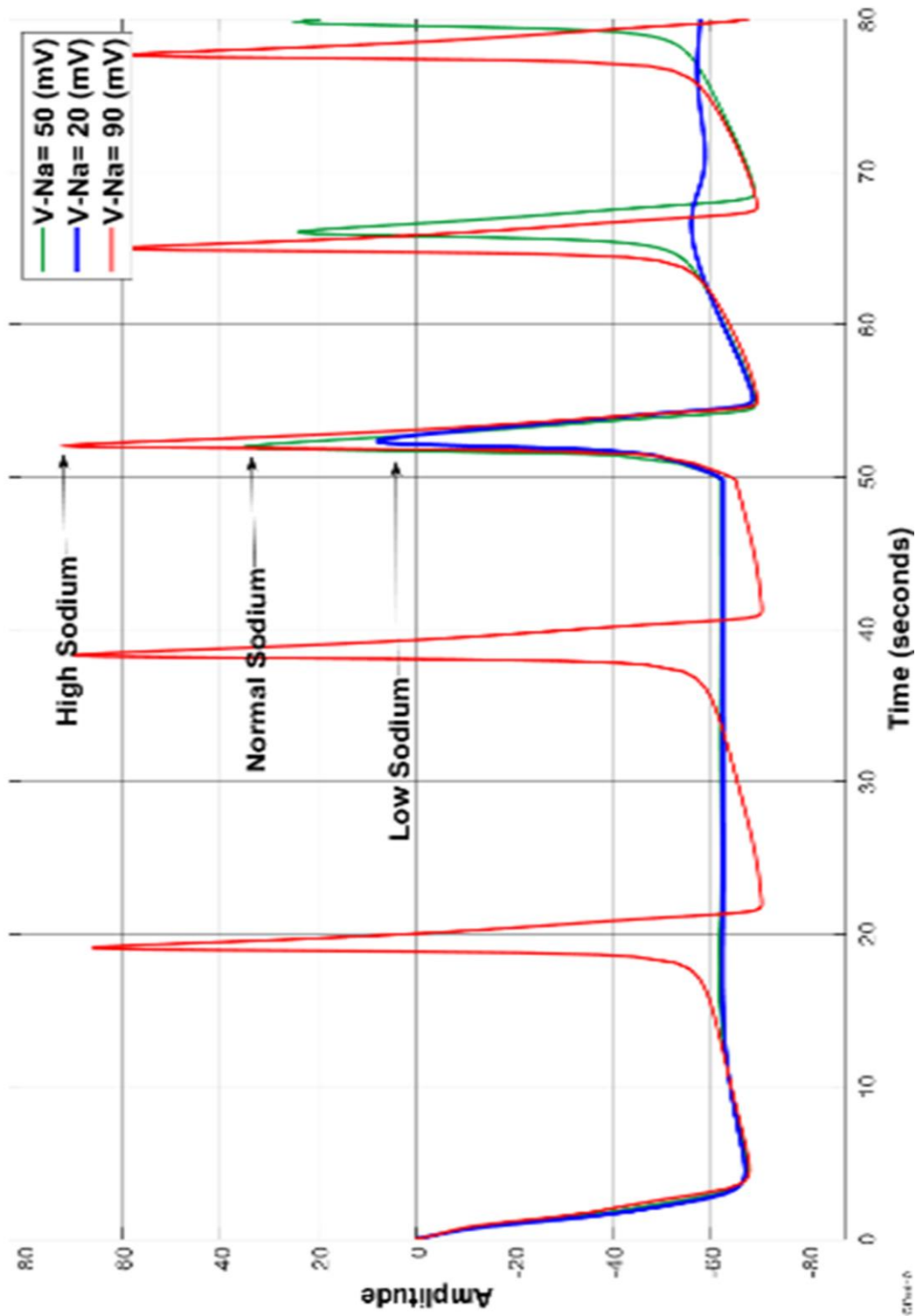
Figure 3.7 – The effects of changes in plasma Na+ concentration on the action potential.

89
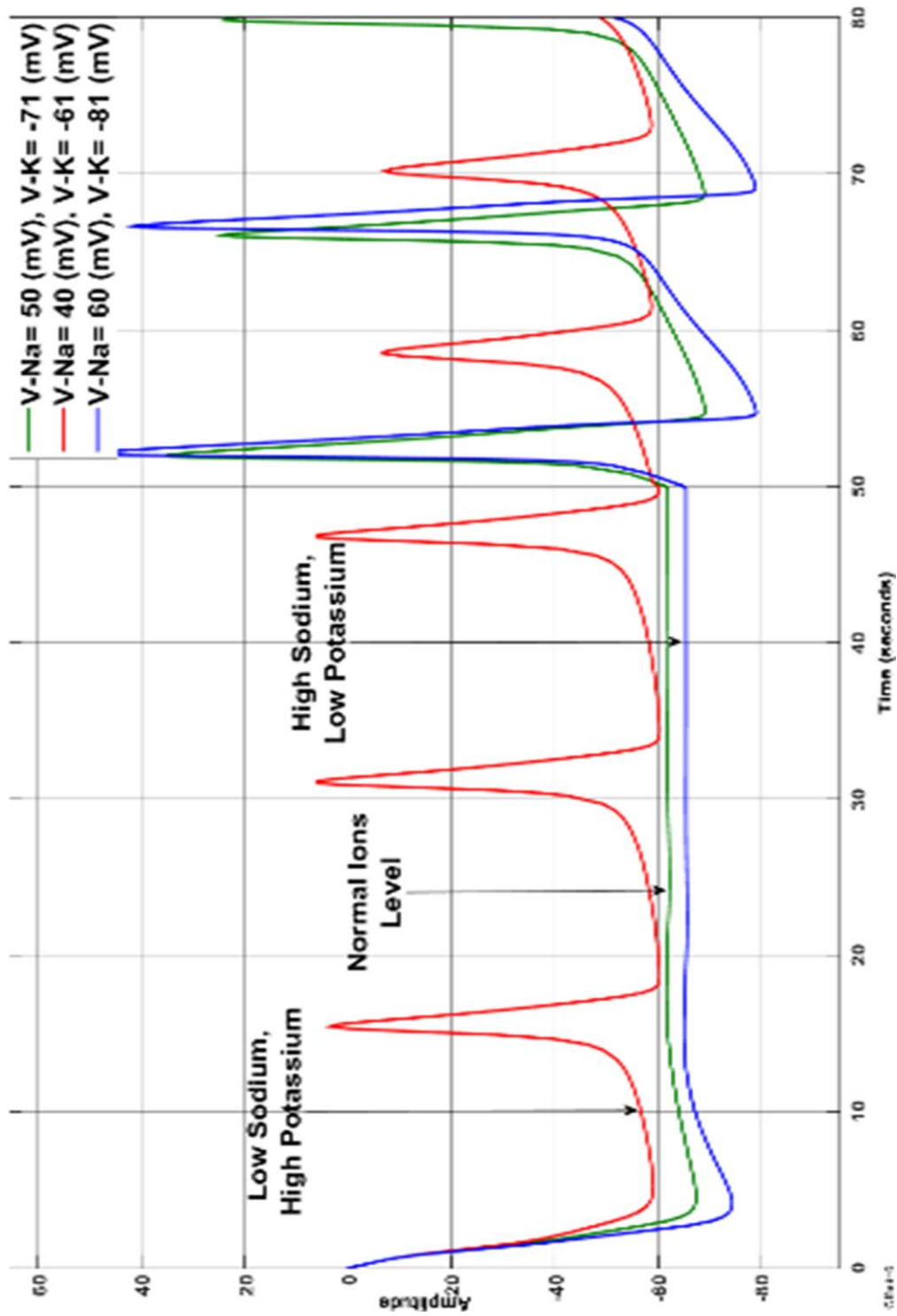
Figure 3.8 – The effects of combination change in plasma Na+ and K+ concentration on the action potential

V_{Na}	V_K	Average of interspike intervals	Average of spike amplitude	Average of resting potential
37	-71	14.8758	10.5017	-63.147
39	-71	14.6256	12.7988	-63.0698
41	-71	14.419	14.9694	-62.9902
43	-71	14.2437	17.0482	-62.9082
45	-71	14.0917	19.0959	-62.8236
47	-71	13.9576	21.0912	-62.7366
49	-71	13.8381	23.0628	-62.647
51	-71	13.7303	24.9737	-62.5314
53	-71	13.6328	26.9014	-62.4066
55	-71	13.5434	28.7872	-62.2764
57	-71	13.4618	30.6524	-62.1405
59	-71	13.386	32.5133	-61.9995
61	-71	13.316	34.3568	-61.8532
63	-71	13.2507	36.2006	-61.7031
65	-71	13.1902	38.0149	-61.5476
67	-71	13.1332	39.8285	-61.3425

Table 3.1 – The average of interspike intervals, spike amplitude and resting potential for sodium changes

V_K	V_{Na}	average of interspike intervals	Average of spike amplitude	Average of resting potential
-54	51	8.9409	-29.4676	-43.4319
-56	51	9.429	-20.1778	-45.7897
-58	51	10.0725	-10.8664	-48.2264
-60	51	10.7669	-2.0199	-50.6534
-62	51	11.4796	5.4973	-53.0263
-64	51	12.1655	11.8297	-55.3149
-66	51	12.7091	16.7945	-57.5069
-68	51	13.1191	20.5768	-59.5972
-71	51	13.7303	24.9737	-62.5314
-73	51	14.0605	27.1349	-64.3668
-75	51	14.3446	28.8061	-66.1146
-77	51	14.6	30.101	-67.7798
-79	51	14.8463	31.0643	-69.3698
-81	51	15.1144	31.6804	-70.8918
-83	51	15.4791	31.8291	-72.3523
-85	51	16.3436	17.8592	-73.7592
-87	51	15.2674	-6.6938	-74.967

Table 3.2 – The average of interspike intervals, spike amplitude and resting potential for potassium changes

V_{Na}	V_K	average of interspike intervals	Average of spike amplitude	Average of resting potential
61	-61	10.7507	9.15	-50.6863
59	-63	11.5193	15.0944	-53.3364
57	-65	12.2319	19.5401	-55.8509
55	-67	12.7956	22.3954	-58.2245
53	-69	13.2503	24.0747	-60.4547
51	-71	13.7303	24.9737	-62.5314
49	-73	14.1821	25.1313	-64.4641
47	-75	14.655	24.6221	-66.2517
45	-77	15.2735	23.2745	-67.9267
43	-79	17.1933	22.2911	-69.5016
41	-81	18.5022	12.8711	-70.9864

Table 3.3 – The average of interspike intervals, spike amplitude and resting potential for comparing hypernatremia with hyperkalaemia and hyponatremia with hypokalaemia

V_{Na}	V_K	average of interspike intervals	Average of spike amplitude	Average of resting potential
61	-81	14.2604	42.6119	-70.574
59	-79	14.2584	39.5384	-69.0874
57	-77	14.2096	36.2934	-67.5346
55	-75	14.109	32.8513	-65.9258
53	-73	13.9515	29.1059	-64.2593
51	-71	13.7303	24.9737	-62.5314
49	-69	13.4389	20.3621	-60.7339
47	-67	13.0706	15.0905	-58.852
45	-65	12.7161	9.244	-56.8996
43	-63	12.2359	2.2251	-54.8835
41	-61	11.6431	-5.9305	-52.8135

Table 3.4 – The average of inter-spike intervals, spike amplitude and resting potential for comparing hypernatremia with hypokalaemia and hyponatremia with hyperkalaemia.

4 Ionic imbalances and coupling in synchronisation of responses in neurons

4.1 Introduction

In the nervous system, neuronal cells (neurons) communicate with each other via electrical events. These neurophysiological electrical events called action potentials. Action potentials within a neuron are generated because of both an external stimulus, and chemical diffusion of ions. This has been extensively studied, e.g. Squid Axons (Hodgkin & Huxley, 1952a), frog (Dodge, 1967), dog (Matsuda, et al., 1958), rabbit (Amthor, et al., 1984), cat (Ahmed, 1997), and the Purkinje cell (Raman & Bean, 1999). The common feature in all these studies is the close relationship between the ions within a neuron and the external stimulus. Neurones have three essential components: the soma, axon, and dendrites (see Figure 2.2).

The external stimulus, when applied to a neuron, results in changes within the neuron which generate an action potential. This action potential, which is transmitted from one neuron to another, is characterised by the magnitude of the spikes and the interval between the spikes. These characters following a principle in neurophysiology called All-or-None. All-or-none is a principle whereby the strength by which an excitable cell response to any stimulus is not dependent on the strength of that stimulus, given that the stimulus is of an adequate strength. More details about all-or-none principle are provided in section 2.1.8 and the work by Sadegh-Zadeh & Kambhampati (Sadegh-Zadeh &

Kambhampati, 2017). Although the effect of chemical imbalances on neuronal signals has been studied (Trenor, et al., 2017), (Cleeremans, 2014), these have not included the effect of chemical imbalances over a network of neurons. In coupled neurons, it is important to understand the manner in which the neurons work synchronously and the nature of the resultant spike train as an output. A chemical imbalance in one neuron changes the dynamics of other neurons connected to it; as a result, there are two kinds of effects in a chain of neurons, one is the loss of synchronicity, and the other is a change in an inter-spike interval and the magnitude of the spikes. A change in the chemical balance results in a change to the action potential.

Synchronisation is the mechanism that maintains vital rhythms like that of respiration. The firing of many neurons, if they are synchronised, gives rise to measurable fluctuations of the electroencephalographical (EEG) signal. Synchronisation is also responsible for the generation of pathological tremors (Freund, 1983) and plays a significant role in several neurological diseases like epilepsy (Engel, et al., 2008). Spectral analysis of EEG shows that neurons can oscillate synchronously in various frequency bands from less than 2 Hz to greater than 60 Hz (Singer, 1999). Numerical experiments suggest that when two sets of equations, like the Hodgkin-Huxley model, are coupled, their solutions seem to synchronise. Experimental findings of synchronisation in excitable tissue provide these results. However, mathematical models for these systems are typically very complicated. For couplings between oscillators, two types of couplings can be found in the real nervous system:

     1) The chemical synapse

     2) The electrical synapse

Chemical synapses contain nonlinear couplings; whereas electrical synapses have linear membrane potentials (see Figure 4.1) (Labouriau & Rodrigues, 2003).

In the recent years, several studies have been performed on investigating the various effects of coupling and synchronisation in neuronal systems. These studies range from effects of the spike plasticity on the synchronisation (Borgesa, et al., 2016), synchronisation in clustered networks (T. de L., et al., 2014), synchronisation in the different type of networks (Vladimir N., et al., 2008), (Hansel, et al., 1995), and dynamics of coupled neurons (Batistaa, et al., 2010), (HAN, et al., 2011). Studies have been carried out investigating responses to different classes of stimuli, e.g. visual (Gray, et al., 1989) odorous (Stopfe, et al., 1997), tactile (Steinmetz, et al., 2000) or synchronisation of neurons, as reported by Stern et al. (Stern, et al., 1998). However, the majority of these studies often concentrate on either the theoretical or practical concepts of synchrony and most of them separate computational applications from the clinical point in their investigations.

4.2 Neuronal dynamics

A number of different types of neurons have been studied and modelled (Hodgkin & Huxley, 1952a), (Dodge, 1967), (Matsuda, et al., 1958), (Amthor, et al., 1984), (Ahmed, 1997), and (Raman & Bean, 1999). The common feature of these neurons is that they are based on membrane potentials of the cells and the ion channel dynamics. These dynamics were formulated by Hodgkin and Huxley. Thus the membrane potential based model takes the form

$$\frac{dV}{dt} = I_{inj} + \sum_{i=1}^{N} g_i \, \psi_i(y_i)(V - V_i) \tag{4.1}$$

where ψ are given by *n, m, h* and it has a value in [0,1] interval. The variable g_i is a function of the probabilities of the opening and closing of channels and the conductance

of that particular channel. I_{inj} is the current, V is the membrane in mV. V_i the potential

of specific ion. y_i presents the channel status. This model describes the time behaviour

of the intracellular membrane potential and the currents through the channels. It is

possible to explain observed phenomena accurately, and the change of voltages and

currents on the nerve cell membrane can be analysed quantitatively (Perez, et al., 2016).

For the channels under consideration, the parameters as given in equations (2.4) to (2.6)

are defined as equations (2.8) to (2.13).

4.3   Generalized form of neurons

In this section, a generalized form of a neuron is presented for N channels and m gates.

The reason is rewriting a mathematically pure form. First, consider the equations (2.3).

In this equation the part $g_i(V - V_i)$ is common for all channels. When $i = 0$ there is a

leakage current. For ion currents the activation and deactivation gates can be rewritten as

follow:

$$m^3 h = u_{Na}(m, h) = \gamma_m^3(v)\gamma_h(v) = \psi_{Na}(y) \tag{4.2}$$

$$n^4 = u_K(n) = \gamma_n^4(v) = \psi_K(y) \tag{4.3}$$

These equations calculate the probability of the opening/closing channel for sodium and

potassium, respectively. Using this information the generalized form of a neuron with N

channels and m ionic gates is of the form:

$$\frac{dV}{dt} = I + g_0(V - V_0) + \sum_{i=1}^{N} g_i\psi_i(y)(V - V_i) \tag{4.4}$$

Where each part $g_i \psi_i(y)(V - V_i)$ models specific ion channel. The channel status is denoted by variable y. In the original Hodgkin-Huxley model with two channels and three gates the variable y= (y_1, y_2, y_3) and the functions ψ are the $\psi_1 = y_2^3 y_3$ and the $\psi_2 = y_1^4$. These functions are defined as probabilities and are in the range of [0, 1]. Therefore, for this model $y_1 = n, y_2 = m,$ and $y_3 = h$.

From the equation in (2.4) get:

$$\frac{dn}{dt} = \alpha_n(v)(1 - n) - \beta_n(v)n = \alpha_n(v) - n\big(\alpha_n(v) + \beta_n(v)\big) \tag{4.5}$$

By dividing and multiplication the right side of (4.5) with $\alpha_n(v) + \beta_n(v)$:

$$\left(\frac{\alpha_n(v)}{\alpha_n(v) + \beta_n(v)} - n\right)\big(\alpha_n(v) + \beta_n(v)\big) \tag{4.6}$$

If $y_i = n$, $\sigma_i(v) = \frac{\alpha_n(v)}{\alpha_n(v) + \beta_n(v)}$ and $\delta_i(v) = \alpha_n(v) + \beta_n(v)$ the equation (4.5) is rewritten as follows:

$$\frac{dy_i}{dt} = (\sigma_i(v) - y_i)\delta_i(v) \tag{4.7}$$

Finally, the generalized form of neuron model with N channels and m gates can be rewritten as follows:

$$\begin{cases} \dfrac{dV}{dt} = I + g_0(V - V_0) + \displaystyle\sum_{i=1}^{N} g_i \, \psi_i(y_i)(V - V_i) = L(v, y, p), & \psi_i: \mathfrak{R}^m \to \mathfrak{R} \\[2em] \dfrac{dy_j}{dt} = (\sigma_j(v) - y_j)\delta_j(v) = K_j(v, y_j), & \begin{aligned} & \delta_j, \sigma_j: \mathfrak{R} \to \mathfrak{R} \\ & \delta_j, \sigma_j(v) \neq 0 \end{aligned} \end{cases} \tag{4.8}$$

Where parameters $p = (g_0, \dots, g_N, V_0, \dots, V_N, I)$. The dynamics of each gate variable y_j depends only on itself and the voltage V by smooth function σ_i and diagonal matrix $\delta_i(v)$ with for all values of V. Each of the terms $g_i \, \psi_i(y_j)(V - V_i)$ in (4.8) with constant g_i refers to an ionic channel. It adjust the voltage V across the nerve cell's membrane and makes the dynamics of the ith channel. Therefore, the generalized form of neuron model in (4.8) represents N channels and m gates where N and m are not necessarily equal. The model in (4.8) is suitable for shaping a single neuron behaviour. However, when two or more than neurons in a network work together, they are coupled by synapse spaces which are not referred to in equation (4.8). The missing link here is coupling phenomenon which is discussed in the next section.

4.4   Coupled type equations

Coupling in the neurons is done via synapses. An alive neuron as an oscillator can be coupled to the chain of neurons (see Figure 4.1). A synapse can be explained as a site where a neuron makes a communicating connection with the next neuron. On the one side of the synapse is a neuron that transmits the signal via axon terminal which is called the presynaptic cell and on the other hand is another neuron or a surface of an effector that receives the signal which is called the postsynaptic cell. In nervous systems, there are three general types of synaptic connections among neurons (College, 2015).
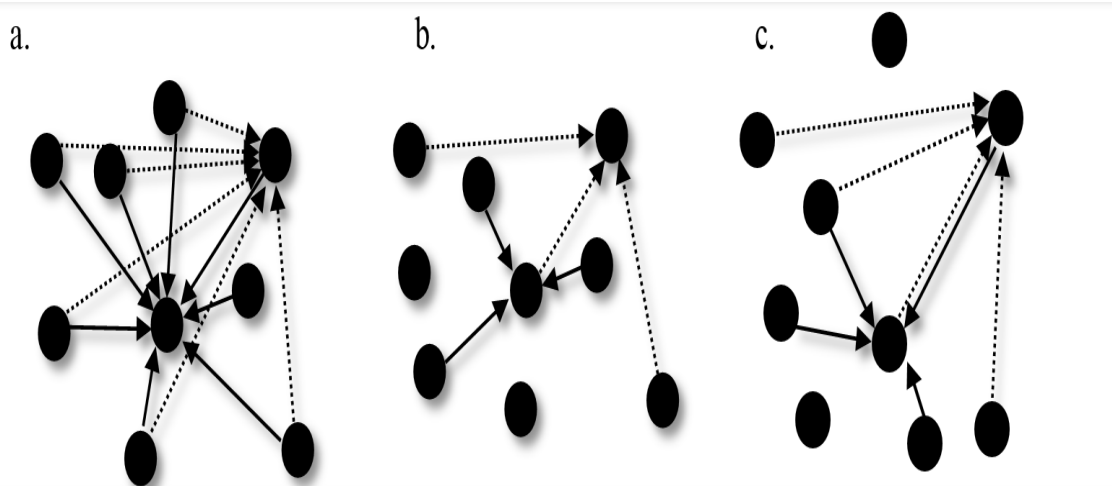
Figure 4.1 – The schemes of coupling in neural networks. a. Full connectivity: a network of 9 neurons with all-to-all coupling. The input links are shown for two representative neurons. Self-couplings are not indicated b. Random coupling with fixed connection probability. The input links are larger than in a network with the population of 9. c. Random coupling with a fixed number of inputs. The number of connections from input links to two representative neurons does not change when the size of the network is increased.

All kind of synapses is shown in Figure 4.1. Electrical connections are also known as gap junctions. Other forms of synapses are two types of chemical connections, excitatory and inhibitory. This study constructs neuron pair models by electrical synapse. The electrical connections are usually axon-to-axon, or dendrite-to-dendrite and are shaped by channel proteins that span the membranes of both connected neurons. Electrical coupling is ubiquitous in the brain, in particular among the dendritic trees of inhibitory interneurons. This kind of direct non-synaptic interaction allows for electrical communication between neurons. All models with electrical coupling necessarily involve a single neuron model that can represent the shape of an action potential.
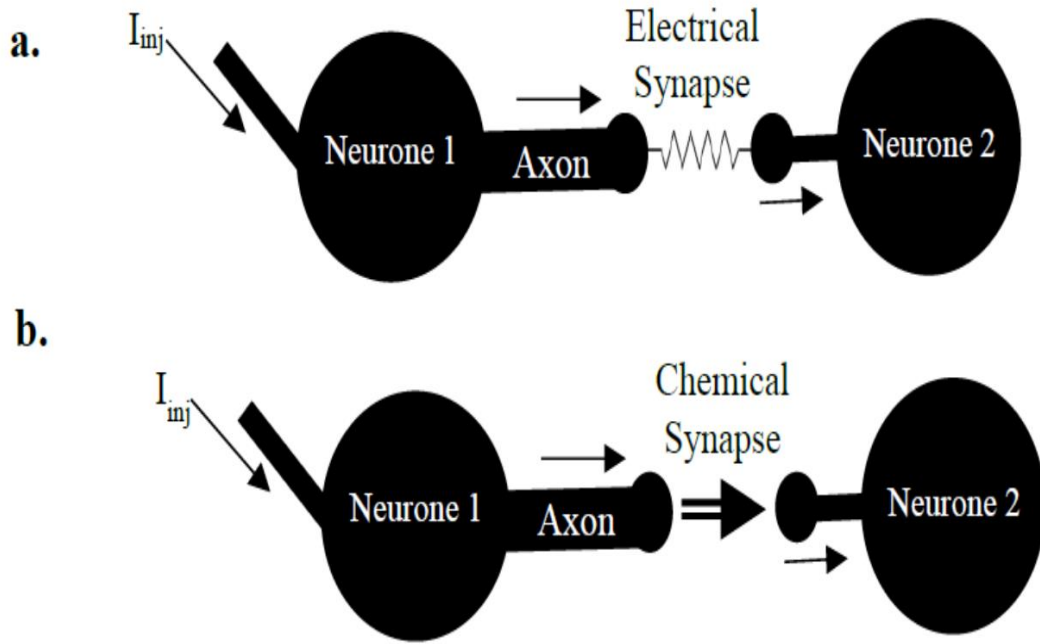
Figure 4.2 – Neuronal circuitry with electrical and chemical synapses. a. A model of electrically coupled neurons b. A model of chemically connected neurons.

The experiments in this study show that when two equations of neuron model are coupled, their solutions seem to synchronise. This project investigates two same action potential equations, coupled only with the electrical potential of each neuron. Choosing a large enough coupling strength forces the neuron to have the same behaviour regardless of the initial condition. Mathematical models for such systems are frequently very complicated. Consider a pair of equations for a neuron model with partial coupling and coupling constants p_1, $p_2 \geq 0$, using the equation (4.8) (Labouriau & Rodrigues, 2003):

$$(HHC) \begin{cases} \dfrac{dv}{dt} = -p_1(v - u) + L(v, y, p) & \dfrac{du}{dt} = -p_2(u - v) + L(v, y, p) \\ \dfrac{dy_j}{dt} = K_j(v, y_j) & \dfrac{dz_j}{dt} = K_j(v, y_j) \end{cases} \qquad (4.9)$$

Later it will be shown that for sufficiently large p_1 and p_2 the solutions of above equation always synchronise. Synchronicity is tackled in the next section.

4.5 Synchronization in coupled neurones

In this section, the mathematical background for synchronisation of coupled neurons is presented. Synchronisation is a phenomenon that can be seen in two or even more coupled neurons. It is achieved by an adjustment of rhythms of their oscillations. Synchronisation is one of the important features of nonlinear systems. Nonlinear systems can show behaviours that are impossible in linear systems (Pikovsky, et al., 2003). Synchronisation analysis is a principle to discover interactions between nonlinear oscillators (Pikovsky, et al., 2003). In synchronisation between two neurones, their action potentials have relatively equal frequencies. This closeness relies on the strength of the coupling. Therefore, spike synchronisation depends crucially on the interspike frequency. The general case of two coupled neuron can be characterised as follow:

$$\dot{v}_1 = L\left(v_1, v_2, \lambda_1\right) \qquad \dot{v}_2 = L\left(v_2, v_1, \lambda_2\right), \qquad v_1, v_2 \in R^n \qquad (4.10)$$

which are dependent on parameter λ, where $\lambda_i = (g_0,...,g_N , V_0,...,V_N , I)$. Perfect synchronization happens when $v_1(t) = v_2(t)$ for all times t (Labouriau & Rodrigues, 2003). This coupled system is called symmetric if $\lambda_1 = \lambda_2$ and asymmetric if $\lambda_1 \neq \lambda_2$. Perfect synchrony usually does not happen in asymmetric systems. Consider the equation (4.9). In this equation when $p_1 = p_2$ the coupled system is symmetric (Labouriau & Rodrigues, 2003). A solution for (4.10) is synchronised if $v_1(t)$ and $v_2(t)$ remain close to each other in the next periods of action potentials. It means that, if there is a constant

$\gamma > 0$ and a continuous function like $f(t) \geq 0$ defined for $t \geq t_0$ which $\lim\limits_{t \to \infty} f(t) = 0$

in a way that for all $t \geq t_0$, the following are true (Labouriau & Rodrigues, 2003):

$$|\Delta v(t)| \leq \gamma . f(t) . |\Delta \lambda| \qquad (4.11)$$

After a short while of interaction between the two neurons the synchronicity becomes higher between them. Generally, for the symmetric case, there is an exponential decay to perfect synchronisation. (Labouriau & Rodrigues, 2003).

4.6   The region of synchronicity

Coupled neurons often possess symmetries; these behaviours are important for understanding dynamical effects in such systems. The simplest symmetric system contains two coupled neurons. Figure 4.3 presents two coupled neurons.
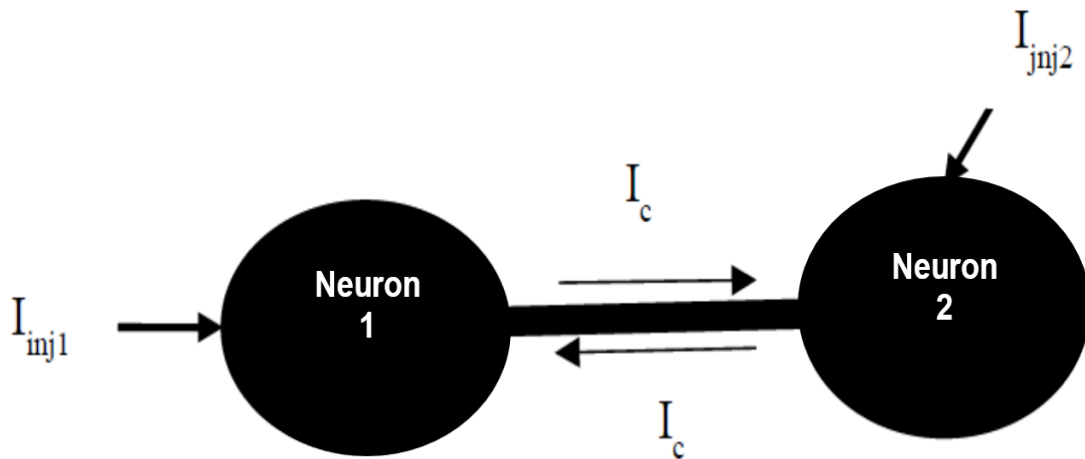
Figure 4.3 – Couplings between neurons. Schematic representation of the signalling of electrical coupling in neurons.

When the input current I_{inj1} is applied, it integrates into the axon hillock of the first neuron. These synaptic inputs cause the membrane to depolarise; that is, they cause the

membrane potential to rise. If this polarisation causes the membrane potential to rise up to the threshold, an action potential V_1 can be raised. When an action potential is triggered, it abruptly generates a dendritic current that flows through the axon I_c in the output of the first neuron. By considering equations (2.1) to (2.3) and equations (2.15) to (2.17), the output of the first neuron for original Hodgkin-Huxley model is:

$$
\begin{aligned}
\dot{V}_1 &= \frac{1}{C_m}\left[I_{inj2} - I_{Na} - I_K - I_L + I_c\right] \rightarrow C_m\dot{V}_1 \\
&= I_{inj1} - I_{Na} - I_K - I_L + I_c
\end{aligned}
\tag{4.12}
$$

similarly, for the second neuron, the output is:

$$
\begin{aligned}
\dot{V}_2 &= \frac{1}{C_m}\left[I_{inj2} - I_{Na} - I_K - I_L + I_c\right] \rightarrow C_m\dot{V}_2 \\
&= I_{inj2} - I_{Na} - I_K - I_L + I_c
\end{aligned}
\tag{4.13}
$$

In entirely normal conditions if the neuron number two is stimulated only by neuron number one and it does not get any other stimuli from other neurons, then the outputs of equations (4.12) and (4.13) should be equal. Therefore:

$$
I_c \geq \frac{I_{inj1}}{2}
\tag{4.14}
$$

It means to make synchronisation between two neurons the minimum condition in (4.14) should be respected.

4.7 Simulation and results

4.7.1 Ion imbalances in neural network

Two sets of experiments were carried out. The first set of these experiments compared the behaviour of the output of action potentials in the hyper/hyponatremia and hyper/hypokalemia conditions for a single neuron and the second set of experiments is done for coupled neurons. All the experiments are carried out at simulation time 1000.0s. The 1000-second time was obtained by using the trial and error method as the best time in the experiments. The injected current varies from 0 *nA*, between 0.0 to 50.0 seconds, and between 51.0 to 1000.0 seconds it is to 10 *nA*. The reason for considering two different injection currents was to have the behaviour of the system under both stimulation and non-stimulation. A key element of this study is to investigate the effect of changing ion concentrations. These concentrations affect both the currents and the voltages in the model. The effect of the concentration of the ions is given by the Nernst Equation (Rossetto, 2016) shown in equation (2.18) and rewritten as (3.1) and (3.2). Where $[K^+]_o$ is the extracellular concentration of potassium. $[K^+]_i$ is the intracellular concentration of potassium. $[Na^+]_i$ is the intracellular concentration of sodium. $[Na^+]_o$ is the extracellular concentration of sodium. Therefore, increasing/decreasing the *V*, has direct relation with increasing/decreasing the $[Na^+]_o$ and $[K^+]_o$. Hypernatremia (hyponatremia) and hyperkalemia (hypokalemia) are a high (low) serum sodium and potassium levels, respectively, so changing the potential of sodium and potassium means changing the $[Na^+]_o$ and $[K^+]_o$ as in equations (3.1) and (3.2), $[Na^+]_o$, $[K^+]_o$ have direct relation to V_{Na^+} and V_{K^+}. For this reason in the experiments by increasing or decreasing V_{ion} the specific ion imbalances are simulated.

Figure 4.4 shows the responses of the neuron for the nominal set of values. It can be seen that the response is a series of spikes, which have two characteristics. One is the

magnitude of the spike and the other is the time between spikes, known as an inter-spike interval. This response is taken to be the ideal response, and all comparisons are made to this response. The comparison is carried out for four different electrolyte diseases, i.e., hypernatremia, hyponatremia, hyperkaliemia, and hypokalemia and combinations thereof.
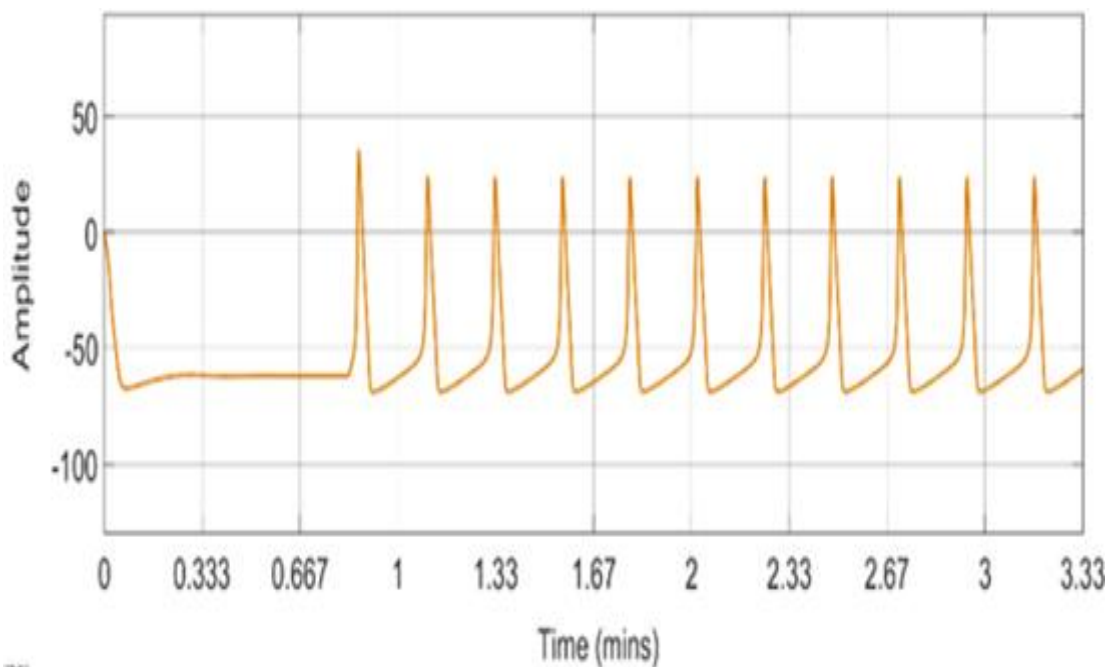
Figure 4.4 –The running of experiments for three single neurons without any changes. All three graphs have been overlapped. V_{Na}=50 mV, V_K= -71 mV.

Low levels of ions imbalances may lead to irregular heartbeat, confusion, blood pressure changes, nervous system or bone disorders. High levels of ions imbalances may lead to weakness or twitching of the muscles, numbness, fatigue, irregular heartbeat and blood pressure changes.

4.7.2   Ion imbalances in coupled neurons

Neural populations in nervous system consist of millions of individual neurons linked together through direct synaptic space. The action potential sent through the synaptic

connections instructs the connected neurons to change their behaviour so that effectively alters the phase of the connected neurons and brings them closer or further away from firing their signals (Sadegh Zadeh & Kambhampati, 2017). It should be emphasised here that to simulate large-scale networks of spiking neurons the simple models are useful. Different level of ions and the structure of how neurons are connected in a network have a large impact on the multitude of synchronized behaviours. This set of experiments describes the nature of how ion imbalances affect the electrical dynamics of the connected neurons using modelling of two conductance-based neurons. Two neurons have the same properties but, the first neuron is suffering different kinds of electrolyte imbalance in each round of experiment. The second neuron is in the healthy condition. From the experiments, it can be said that the timings between coupled neuron's firing with a high value of coupling conductance is fixed while this varies between uncoupled neurons or even between very weak coupled neurons.

In the first experiment, the first neuron has sodium imbalances. In the second round, it has potassium imbalances. In the third round, it experiences both sodium and potassium imbalances, and finally, the fourth round is same as the third round, but in the reverse order for sodium and potassium imbalances. Some of the critical characteristics of action potential like the average of time intervals, the average of peak intervals, and the average of resting potential were investigated. For this reason, a train of action potentials for each round in the 1000 seconds was run on the model. The results for the various values of potassium and sodium and their combinations are shown in Table 4.1 to Table 4.4 and Figure 4.6 to Figure 4.9. The tables consist of three sections. The first part represents the results for changes in the single neuron. The second section lists the results of the first neuron in the coupling condition. Finally, the third part of the table reveals the functions of the second neuron and the outputs of the system in the coupling state.
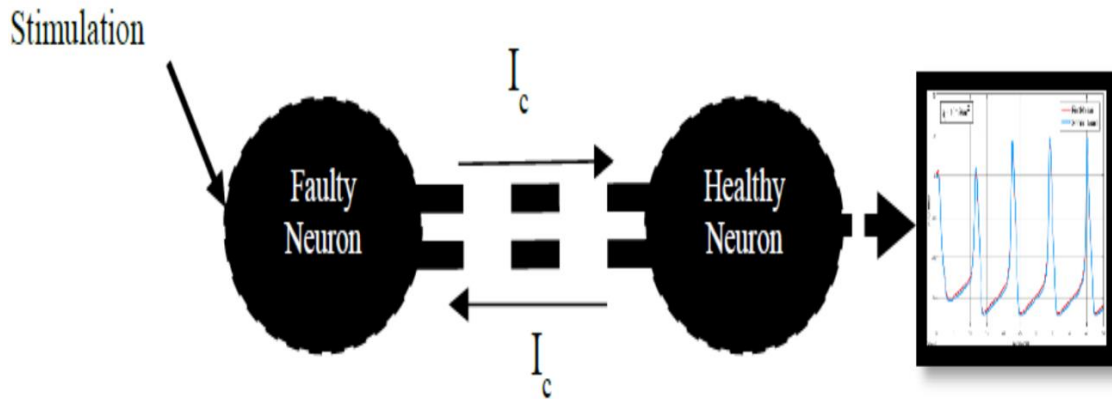
Figure 4.5 – In some diseases (like ALS, Multiple Sclerosis, Parkinson, and so on) the neuron(s) entire the neural networks in the brain or spinal cord do not work properly. The affected nerve cells have the problem to transmit signals from one area of the brain to another or even they can no longer do it. The model of this problem here is simulated on a very small scale. The first neuron works as a faulty neuron and the second one works as healthy neurons entire the neural network.

The results for the coupled model for both Hyper and Hyponatremia are presented in Table 4.1 and Figure 4.6. The results for both Hyper and Hypokalemia are presented in Table 4.2, Figure 4.7. Finally the results for Hyper and Hyponatremia plus Hyper and Hypokalemia at the same time represented in Table 4.3 and Table 4.4.

4.7.3 The Effect of Coupling Conductance on Synchronization

How big should a coupling conductance be? Previously, in the section 4.6, the minimum current for synchronisation has been suggested. As is shown in the equation (4.14) the minimum current I_c for the second neuron has to be at least $\frac{I_{inj1}}{2}$. As $I_c = \Delta V * g_c$ so the value of g_c is crucial for the synchronisation. The experiments shown by increasing the g_c the synchronicity in coupling becomes more. Figure 4.10 shows the results. As results show, further increasing the coupling parameter or coupling conductance leads to a globally synchronous regime.
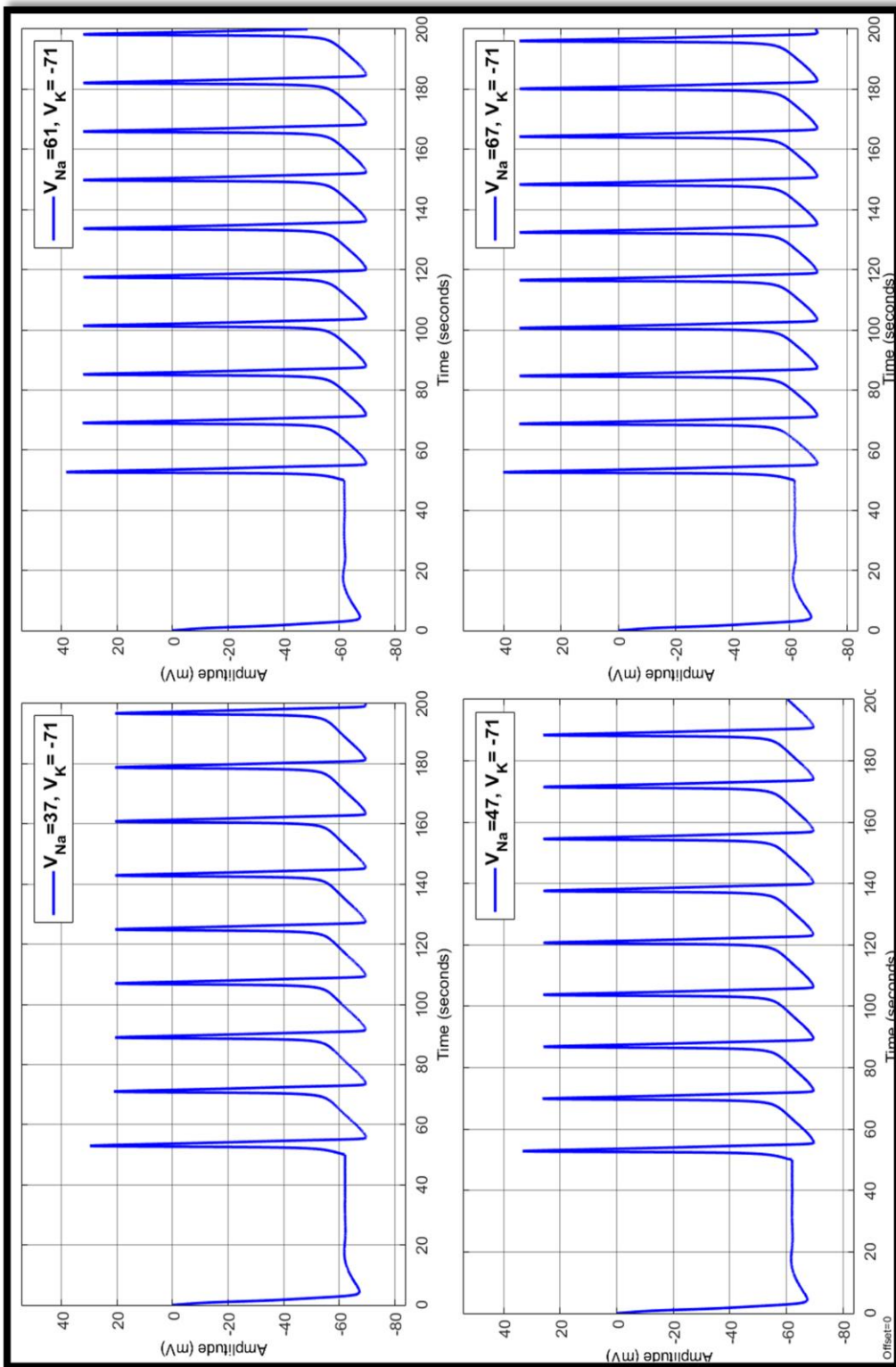
Figure 4.6 – Sodium changes and the responses of coupled neurons in the course of hypernatremia and hyponatremia. The potassium value for all of these experiments remained as normal, $V_K = -71$

Ions		Single Faulty Neuron			Faulty Neuron in the Chain			Output of the Coupled Neuron		
V_{Na}	V_K	Ave. of Inter-Spike Intervals	Ave. of Spike Amplitude	Ave. of Resting Potential	Ave. of Inter-Spike Intervals	Ave. of Spike Amplitude	Ave. of Resting Potential	Ave. of Inter-Spike Intervals	Ave. of Spike Amplitude	Ave. of Resting Potential
37	-71	14.8758	10.5017	-63.147	17.9775	19.8064	-60.4662	17.9775	21.6552	-60.4557
47	-71	13.9576	21.0912	-62.7366	16.9507	26.3103	-59.9166	16.9468	26.7907	-59.9224
50	-71	13.7303	24.9737	-62.5314	16.7455	28.1351	-55.0608	16.7455	28.1554	-55.0897
61	-71	13.316	34.3568	-61.8532	16.1699	34.5527	-59.3163	16.1699	32.7097	-59.3666
67	-71	13.1332	39.8285	-61.3425	15.9336	38.0282	-59.0507	15.9336	35.1541	-59.1272

Table 4.1 – The average of interspike intervals, spike amplitude and resting potential for sodium changes
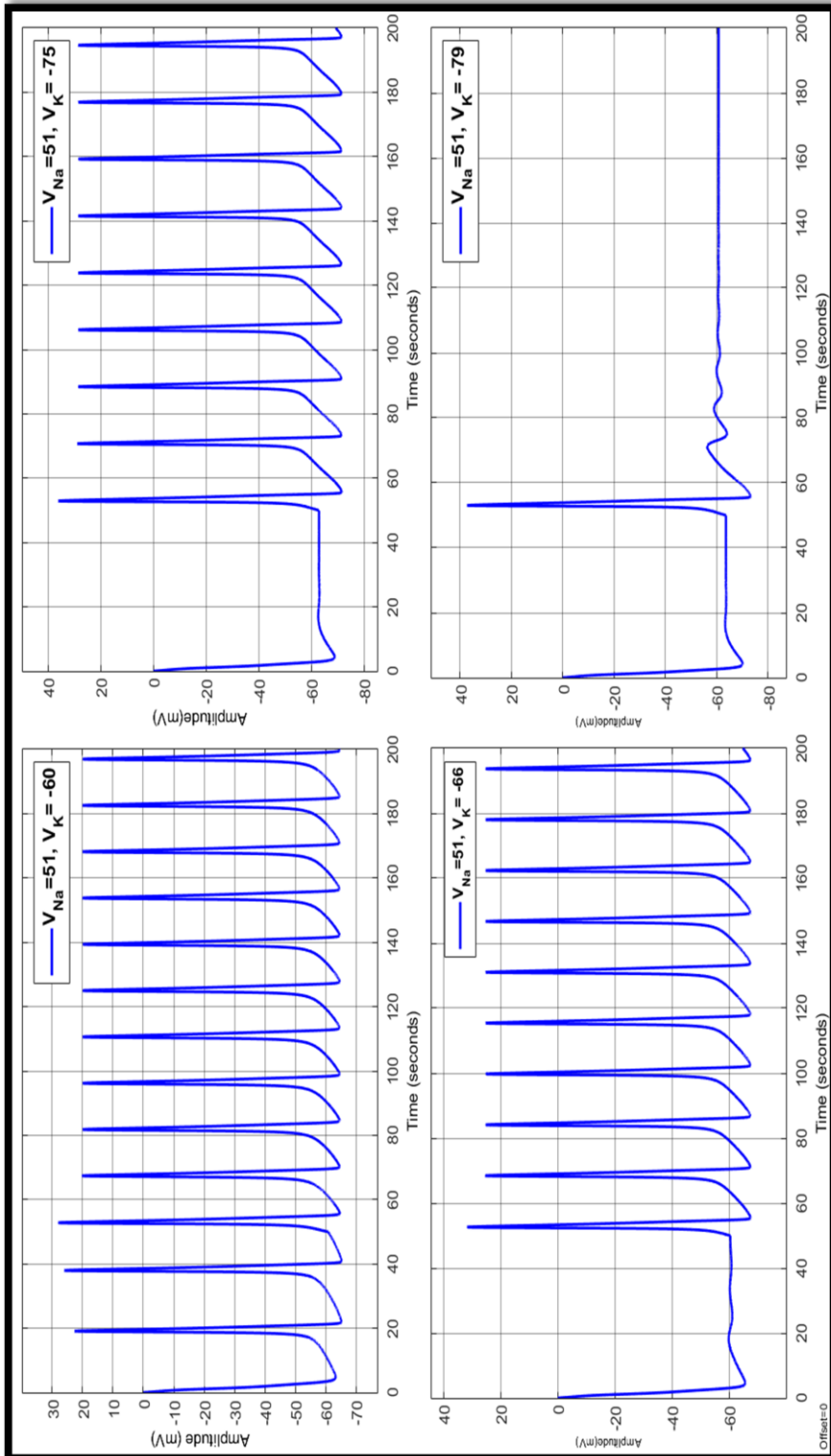
Figure 4.7 – Potassium changes and the responses of coupled neurons in the course of hyperkalemia and hypokalemia. The sodium value for all of these experiments remained as normal, V_{Na} =50.

Ions		Single Faulty Neuron			Faulty Neuron in the Chain			Output of the Coupled Neuron		
V_{Na}	V_K	Ave. of Inter-Spike Intervals	Ave. of Spike Amplitude	Ave. of Resting Potential	Ave. of Inter-Spike Intervals	Average of Spike Amplitude	Ave. of Resting Potential	Ave. of Inter-Spike Intervals	Ave. of Spike Amplitude	Ave. of Resting Potential
51	-60	10.7669	-2.0199	-50.6534	14.8411	21.2079	-52.9945	14.8411	20.8429	-53.3918
51	-66	12.7091	16.7945	-57.5069	15.7142	25.6603	-58.0945	15.7142	25.4610	-58.2092
50	-71	13.7303	24.9737	-62.5314	16.7455	28.1351	-55.0608	16.7455	28.1554	-55.0897
51	-75	14.3446	28.8061	-66.1146	17.8316	28.8506	-61.0727	17.8316	28.9676	-61.0148
51	-79	14.8463	31.0643	-69.3698	20.0183	31.2381	-61.9963	20.0183	31.4256	-61.9135

Table 4.2 – The average of interspike intervals, spike amplitude and resting potential for potassium changes
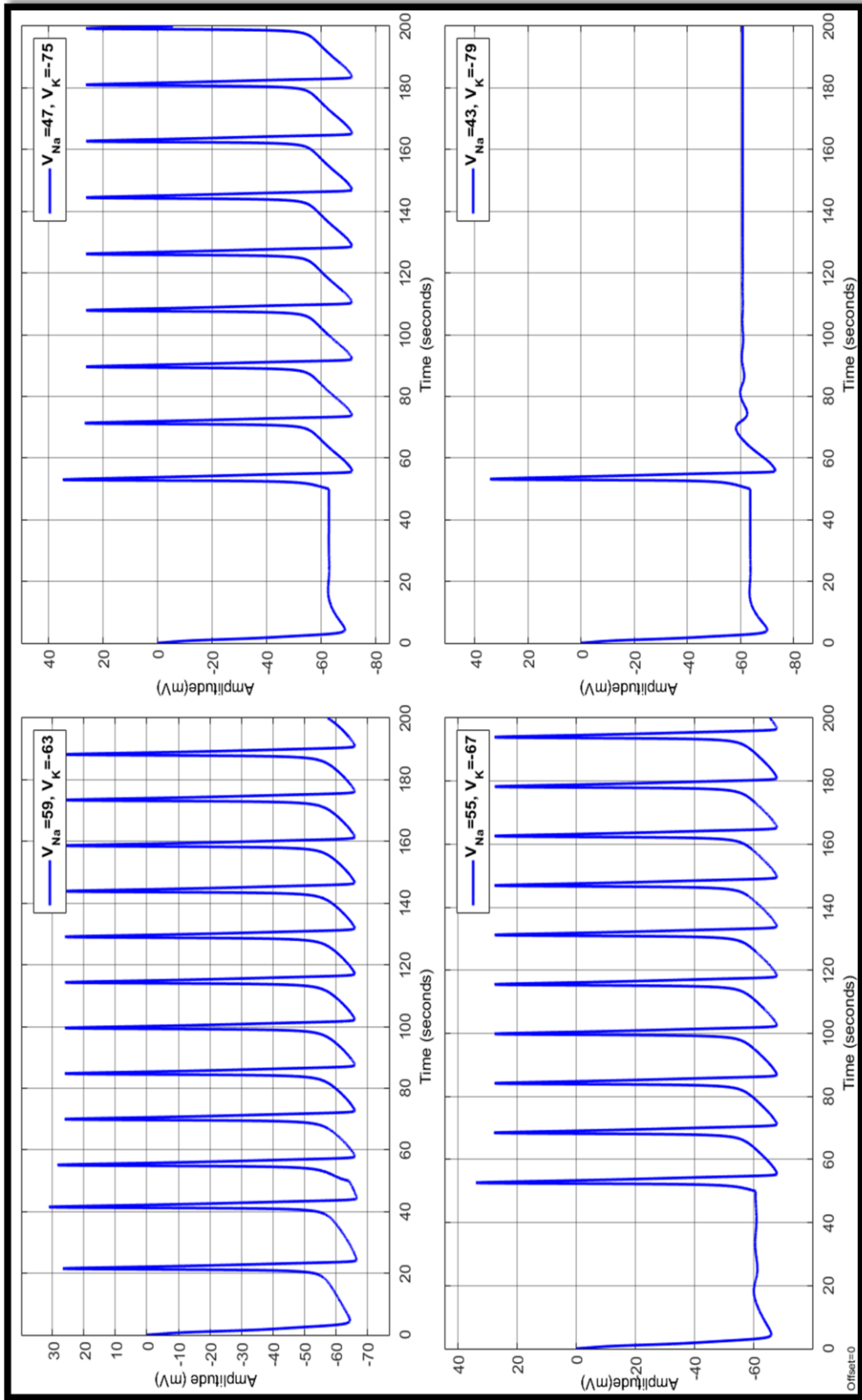
Figure 4.8 – Sodium and potassium changes and the responses of coupled neurons in the course of hypernatremia-hyperkalaemia and hyponatremia- hypokalaemia.

114

Ions		Single Faulty Neuron			Faulty Neuron in the Chain			Output of the Coupled Neuron		
V_{Na}	V_K	Ave. of Inter-Spike Intervals	Ave. of Spike Amplitude	Ave. of Resting Potential	Ave. of Inter-Spike Intervals	Average of Spike Amplitude	Ave. of Resting Potential	Ave. of Inter-Spike Intervals	Ave. of Spike Amplitude	Ave. of Resting Potential
59	-63	11.5193	15.0944	-53.3364	15.1529	28.2043	-53.3745	15.1529	26.7059	-53.7817
55	-67	12.7956	22.3954	-58.2245	15.7045	29.0433	-58.2096	15.7045	29.0433	-58.2096
50	-71	13.7303	24.9737	-62.5314	16.7455	28.1351	-55.0608	16.7455	28.1554	-55.0897
47	-75	14.655	24.6221	-66.2517	18.2881	26.6333	-61.1840	18.2881	27.1293	-61.1367
43	-79	17.1933	22.2911	-69.5016	-	32.8146	-62.5148	-	34.3358	-62.4243

Table 4.3 – The average of interspike intervals, spike amplitude and resting potential for comparing hypernatremia with hyperkalemia and hyponatremia with hypokalaemia
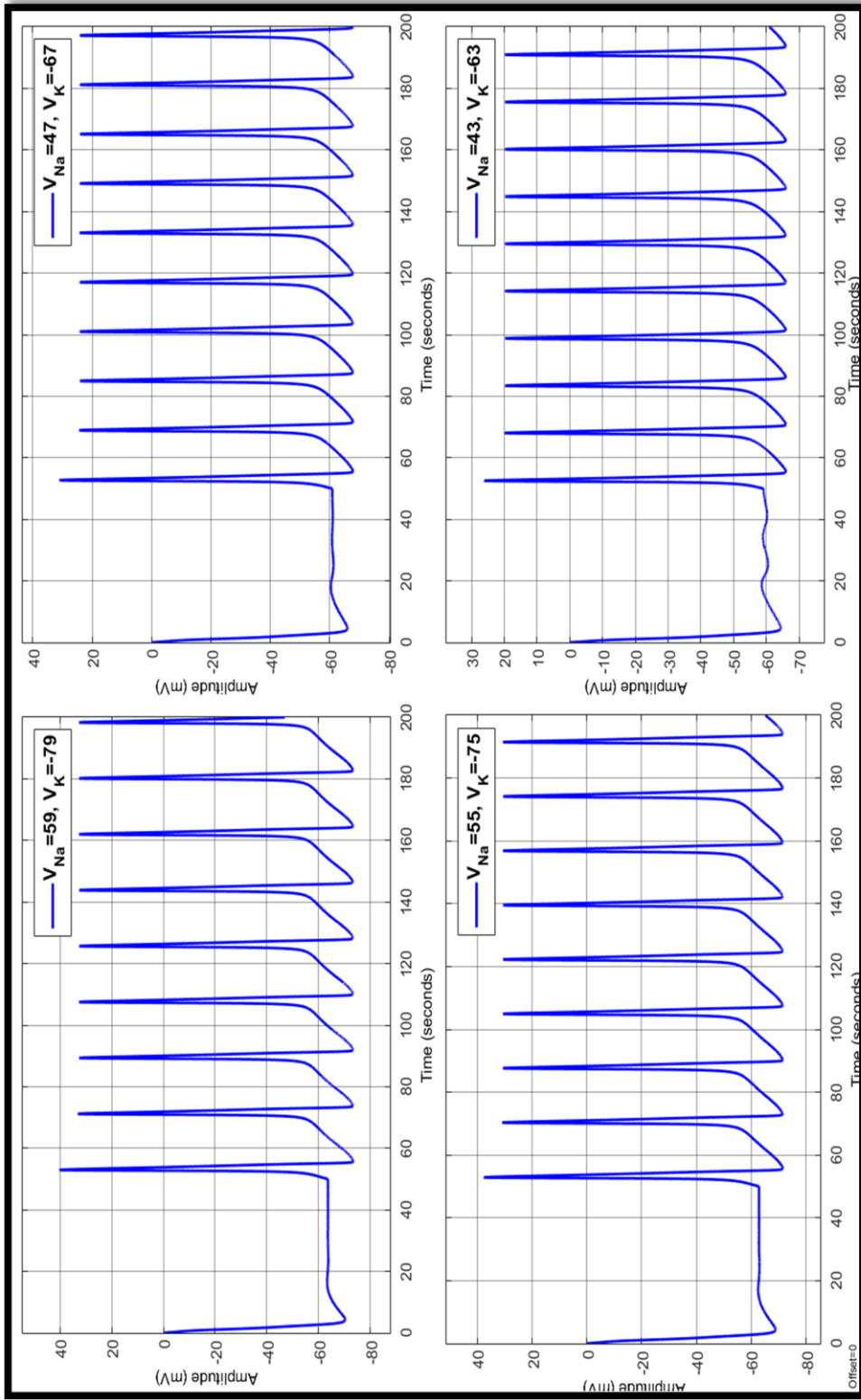
Figure 4.9 – Sodium and potassium changes and the responses of coupled neurons in the course of hyponatremia-hyperkalaemia and hypernatremia-hypokalaemia.

Ions		Single Faulty Neuron			Faulty Neuron in the Chain			Output of the Coupled Neuron		
V_{Na}	V_K	Ave. of Inter-Spike Intervals	Ave. of Spike Amplitude	Ave. of Resting Potential	Ave. of Inter-Spike Intervals	Average of Spike Amplitude	Ave. of Resting Potential	Ave. of Inter-Spike Intervals	Ave. of Spike Amplitude	Ave. of Resting Potential
59	-79	14.2584	39.5384	-69.0874	18.1669	34.9578	-61.8693	18.1669	33.5213	-61.8110
55	-75	14.109	32.8513	-65.9258	17.3166	32.2044	-60.6708	17.3166	31.4881	-60.6250
50	-71	13.7303	24.9737	-62.5314	16.7455	28.1351	-55.0608	16.7455	28.1554	-55.0897
47	-67	13.0706	15.0905	-58.852	16.0560	24.5569	-58.7456	16.0560	24.8891	-58.8273
43	-63	12.2359	2.2251	-54.8835	15.3754	19.6940	-57.1269	15.3791	20.3892	-57.2454

Table 4.4 –The average of inter-spike intervals, spike amplitude and resting potential for comparing hypernatremia with hypokalemia and hyponatremia with hyperkalemia
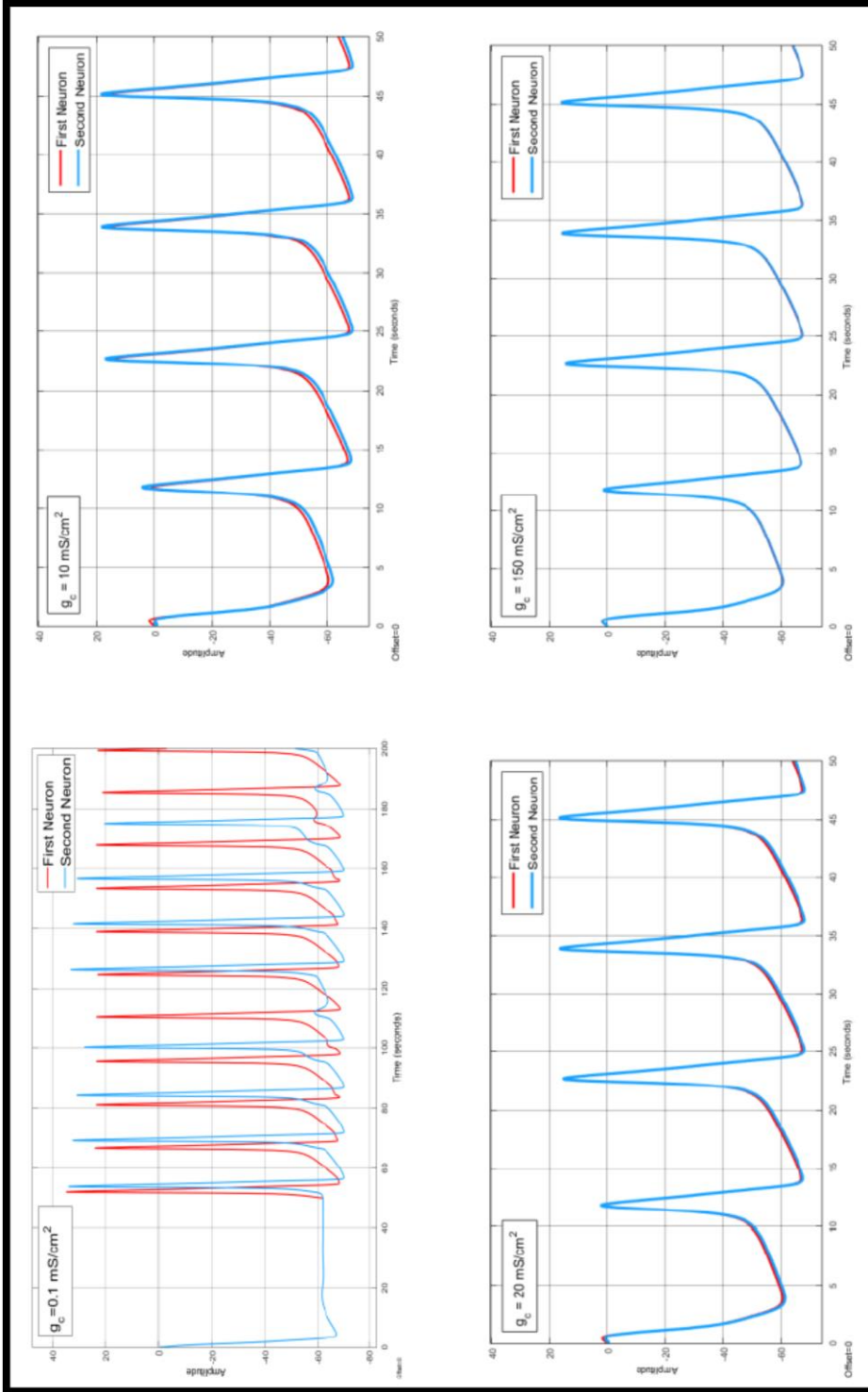
Figure 4.10 – Increasing coupling conductance. The results obtained from coupled Hodgkin-Huxley neural model which the coupling conductance is progressively increased in the steps. The current injection for this experiment was 20 mA.

As coupling conductance is increased, the synchronisation is more triggered (see Figure 4.10). After further coupling conductance increasing both action potentials coincide with each other's, except for slight defects. As results show by picking sufficiently large coupling conductance, cell synchronisation occurred. The reason behind increasing the synchronicity of coupled neurons, by increasing the coupling conductance g_c relates back to the nature of g_c. By considering the relation of g_c with resistance which is $g_c = \frac{1}{R}$ someone can conclude that increasing the coupling conductance causes to decreases resistance between two neurons, and by decreasing resistance between two neurons; the neurons become more synchronized.

4.8 Discussion

The computational models applied in this chapter are simple circuits which integrate differential equations representing abnormalities in the different levels of electrolyte potential for coupled neurons. The model can easily set into a regime that reproduces the same action potential as the firing patterns observed in biological neurons. The preliminary results show that the fast and slow action potential are related to the properties of internal settings of the neuron. The range of observations for single neuron which shows the response and complexity of configurations presented in the last chapter. However, coupled neurons show more complex behaviour (See Figure 4.6 - Figure 4.10). Responses to the combined effect of the concentrations of the sodium and potassium ions in the neuron for coupled neurons are presented in Figure 4.8 and Figure 4.9. This understanding can help, in the understanding of neurodegenerative diseases, e.g. tremors, motor neuron disease, Parkinson, Alzheimer's disease amongst others. The reason for this is that intracellular and extracellular potassium and sodium concentrations play a vital role in the electrophysiological function of the body and neurons that control it.

These two ions are essential in maintaining cellular homeostasis, and most metabolic processes are dependent on or affected by these electrolytes (Chappell & Payne, 2016). There is a significant relationship between sodium and potassium changes and the level of the action potential and resting potential. As the results of earlier experiments carried out on the model, it can be seen that increasing the concentration of potassium raises resting potential toward threshold and in contrast, decreasing the concentration of potassium lowers resting potential away from threshold. In the same way, increasing the concentration of sodium raises the level of action potential more positive. Inversely, decreasing the concentration of sodium reduces the level of action potential more negative.

During the combination of sodium and potassium imbalances the conditions have led to the properties of potassium concentration (see Table 4.3 and Table 4.4). It means important features of an action potential like the rates of rising of the action potential, its peak amplitude, and duration are more dependent on properties of potassium. By pointing to the biological fact, a possible explanation for these observations could be related to the amount of concentration of sodium and potassium. The normal concentration of sodium in the blood serum is 136 -146 mMol /L and the normal potassium level is 3.5 - 5 mMol/L (Kashyap, et al., 2016). Therefore, It can be interpreted that as the amount of sodium is much more than the amount of potassium (around 39 times) so changing only a small amount of potassium can have a significant impact on the volume of its total amount, while the reduction of small volumes of sodium does not have a large impact on the total volume. For this reason, it can be seen that during the combination of sodium and potassium imbalances the impact of potassium on neuronal functions is much stronger than sodium.

Another characteristic which is interesting is the impact of coupling conductance on the synchronicity of coupled neurons. The results indicate how any changes in the coupling conductance can drive the neurons into different degrees of synchronisation. These results are displayed in Figure 4.10. In general, the experiments with the coupling conductance contribute directly to our understanding of the origin of synchronisation in a network of neurons through regularisation of the conductance.

Some characteristics of action potential have displayed considerable changes during the experiments for coupled neurons in compare to firing the single neuron. This model study has shown that electrical coupling can either increase or decrease the frequency of action potential. Results in Figure 4.10 demonstrates that coupling conductance, g_c, and properties of the postsynaptic signal of membranes can greatly influence the frequency changes in the coupled neurons. The coupling between two neurons is variable; it increases any time that the two neurons are simultaneously active. From a computational point of view, this can be interpreted through equation (4.9). Two neurons are simultaneously active when in this equation, $p_1 = p_2$. Results demonstrated that coupling has effects on the average of spike amplitudes and the average of resting potential, as well. Table 4.1 to Table 4.4 show that after applying coupling parameters on the model the average of spike amplitudes and the average of resting potential became greater than the same condition in the single neuron. On the other hand, comparing the experiments of the single neuron presented in last chapter with coupled neurons in the Table 4.1 – Table 4.4 reveals that coupled neurons can shape the frequency and waveform of the action potential, as well. The experiments also reveal coupling maxima between neurons when both neurons have the same settings (i.e. same level of sodium and potassium ions).

5 A computational investigation of the role of Amyloid peptide channels

5.1 Introduction

Neurodegenerative diseases are a kind of progressive disease in which the structure or function of the neurons is gradually destroyed and ultimately leads to the death of neurons. The neurons cannot be replaced by the biological body system if they become damaged or even die. That's why such diseases are incurable (Andreas & Bowser, 2017). Alzheimer's disease is an example of a neurodegenerative disease that causes dementia with no known cure (Gallaway, et al., 2017). Following the Office for National Statistics, Dementia, including Alzheimer's disease, has overtaken heart disease and became the leading cause of mortality in the United Kingdom (Patel, 2017). This deadly neurodegenerative disease causes problems with mental functioning like cognitive, memory, and behavioural impairments. The most important Alzheimer's disease symptoms can be *intracellular* neurofibrillary tangles and the *extracellular* deposition of beta-amyloid (Aβ) plaques (Suh, 2017), (Mattson, 2004). Therefore, it can be said the driving force for Alzheimer's disease pathogenesis on outside the cell is the accumulation of Aβ oligomers or plaques and as a result the formation of Aβ channels (Montoliu-Gaya & Villegas, 2018). This accumulation usually happens because of some imbalances between synthesis and clearance as a result of abnormal processing of amyloid precursor protein (Hardy & Selkoe, 2002). Extensive research shows the Aβ accumulation as an

important factor in the development of early cognitive impairment can be seen in the very early stages of Alzheimer's disease (Takahashi, et al., 2017). It has been discovered that Aβ peptide forms large permeable channels under physiologic conditions (Lee, et al., 2017). However, the exact mechanism is not fully understood (Perez, et al., 2017). The channels made by Aβ are selective for cations over anions and can be inserted into the cell membrane from aqueous solution. These channels are voltage-independent, and they can be very large. Different types of these channels are heterogeneous and allow the flow of physiologically relevant ions such as Na+, K+, Ca2+, Cs+, and Li+ across the cell membrane (Lee, et al., 2017). The discovery of Aβ channels hypothesis led to a wide range of research. The focus of most studies has been centred on the effects of these channels. So far, more than a dozen channels have been known to create these kinds of channels, and all have the same properties (Canale, et al., 2018). Investigation of Aβ channels has shown that approximately all of the properties of these channels are preserved in all Aβ channels forms. These properties explain the cause of the toxicity of amyloid peptides, and this can distinguish these kinds of channels from the regular voltage-gated ion channels in excitable neurons. According to the Aβ channels hypothesis, these channels create an unregulated ionic leakage pathway in the cell membrane. They lead to cell depolarisation and irregular flow of ions such as Na^+, K^+. Therefore, this procedure damages the cellular processes, specifically inhibitory neurons, and causes vital energy stores to drop since the cellular pumps try to leak.

Various studies on the dysfunction of inhibitory neurons and Aβ channels have been published. Busche et al., (Busche, et al., 2008) suggest that an impaired inhibitory neuron near amyloid plaques rather than the firing of an excitatory neuron underlies the hyperactivity in the neuronal network activity. Verret et al. (Verret, et al., 2012), evaluated inhibitory neurons and found that the disruption in the inhibitory neurons

causes spontaneous epileptiform activity and hypersynchrony in human Alzheimer's disease patients. In line with these studies, Hazra et al. (Hazra, et al., 2013), have recently shown the failure of inhibitory neurons leading to disruptions in Hippocratic circuit activity to fire action potentials in the aged mouse model of Alzheimer's disease. In their study, Perez et al. (Perez, et al., 2017) applied Hodgkin-Huxley model to use dynamic sodium conductance in the inhibitory neuron to find the pathways leading to impaired inhibitory neuronal activity in the hippocampus of aged mice model of Alzheimer's disease. Their observations indicate that inhibitory neurons in confronting with Aβ channels causing leakage of sodium cannot reliably fire action potentials and have higher resting membrane potentials. For this reason, they elevated the conductance of sodium leak channels to create conditions similar to Aβ channels in a single inhibitory neuron. As Aβ channels are permeable to all cations, this study considered both sodium and potassium as two significant cations in the neuronal process in a single inhibitory neuron. Therefore, the conductance of potassium leak channels in addition to the sodium leak channels elevated. This chapter organized as follows. Section 2 describes the pathological background. Section 3 introduces computational method. Sections 4 presents the computational results, and finally, section 5 discusses the results of this study.

5.2 Pathological background of Alzheimer's disease

Neurons during their processes, in addition to releasing neurotransmitters in synapse space, they release very tiny peptides which are called amyloid beta. Neurotransmitters or chemical messengers are released in the synaptic space in order to communication between neurons. In the very early stage of the disease, these spaces are targeted by Alzheimer's. These peptides typically clean microglia and are also metabolize by them.

124

For many decades, the action of microglia was completely unclear (Arcuri, et al., 2017). However, these days it is known that cellar debris from nervous tissue is cleared by the microglia. Young et al (2014) showed that Alzheimer's disease is predicated on the presence of amyloid beta protein and the channels it creates (Young, et al., 2014). These additional channels allow for more NA+ and K+ to cross over, thereby creating a synaptic disorder. In general it takes about 15-20 years before Alzheimer's disease becomes apparent. The reason for is that amyloid peptide forms a sticky aggregate called amyloid plaques which then leads to a molecular cascade (Cristina, et al., 2011). At this stage, the microglia cells become hyper-activated and release chemicals causing inflammations and neuronal damage. After the onset of the inflammation, an important protein which is called Tau becomes hyper-phosphorylated and twists itself into tangles (see chapter 2 – the membranes are formed by Phosphates). Tangles choke off the neuron from the inside and the neuronal apoptosis begins. Therefore, in order to detect the disease at an early stage, the focus on Aβ peptide is very important.

Aβ peptide is a small fragment of a more abundant protein called amyloid precursor protein. However, researchers have not yet distinguished the normal function of the amyloid precursor protein, but they know how it appears to work (Andreas & Bowser, 2017). The amyloid precursor protein through the passage of the membrane around the nerve cell develops from the inner environment of the nerve cell to the outside. Then amyloid precursor protein is cut by other proteins into separate, smaller sections. It stays inside and outside the nerve cells. Under some circumstances, there are different methods for cutting amyloid precursor proteins. One of these produced cut-off pieces is called Aβ peptides.

AS mentioned above, Aβ channels are permeable to cations including sodium and potassium (Perez, et al., 2017), (MA, et al., 2008). In healthy neurons, there is a balance

in the inflow of NA$^+$ and the out flow of K$^+$, however with these additional channeles this balance is perturbed such that there is a reversal in the potential of the ionic currents which results in change of permeability for cation i.e. $P_K > P_{Na}$. Aβ oligomers increase the area per molecule of the membrane-forming lipids, accordingly thinning the membrane, and as a result, it lowers the dielectric barrier and increases the conductance of neuron (Arispe, et al., 2007). Therefore in general, it can be said that Aβ can assume a conformation that enables the molecule to enter the lipid bilayer plasma membranes and form cation-selective channels.

Recent studies, (Vitvitsky, et al., 2012), (Perez, et al., 2017) have shown that abnormal levels of ions like sodium and potassium in neurons cause an ionic imbalance that is linked to Alzheimer's disease pathogenesis. To test their hypothesis, they analysed sodium and potassium in post-mortem brain samples of 12 normal and 16 Alzheimer's disease individuals. They found ion imbalances in the cortical (sodium) and cerebellar (potassium) brain part of people with Alzheimer's disease. They suggested that the changes seen in tissue samples reflect the changes in the intracellular pool. Using the mathematical modelling of experimental data from ion concentrations between normal and Alzheimer's disease brain tissues they showed that the intracellular sodium increases by a 2-fold and the intracellular potassium increases 8–15% in cortical and cerebellar of Alzheimer's disease brain, respectively.

5.3 Computational model for amyloid channels

This section presents a computational model of a single neuron with Aβ plaques.The membrane potential, *V*, of a single neuron is modelled by:

$$V = \frac{1}{C_m} \int_0^T \sum_j G_j(V_j - V) + I_{inj} \, dt, \qquad (5.1)$$

Where, V_j is the reversal potential for current j which obtain from Nernst equation. $(V_j -$ $V)$ is driving force for current j. I_{inj} is external current. For original conductance-based model this equation is as follows:

$$V = \frac{1}{C_m} \int_0^T (I_{inj} + \sum_j I_j) \mathrm{dt},$$

(5.2)

where $j = Na^+, K^+, L, and\ etc$ and

$$G_j = \overline{G}_j p_j^x q_j^y,$$

(5.3)

where

$$\frac{dp}{dt} = \alpha_p(1-p) - \beta_p p \quad \text{and} \quad \frac{dq}{dt} = \alpha_q(1-q) - \beta_q q,$$

(5.4)

where p, q are gating variables. For instance, $m^3 h$ and n^4 (See chapter 4) are gating variables for sodium and for potassium. Therefore, for sodium and potassium the equation (5.3) is $G_{Na} = \overline{G}_{Na} m^3 h$ and $G_K = \overline{G}_K n^4$. The following will show that amyloid aggregation will result in disruption of the sodium and potassium gate variables. The parameters α and β are opening and closing rates of the ion channel state transitions that are dependent on V. For sodium and potassium these parameters are as equations (2.8) to (2.13). For sodium, potassium, and leakage the currents are as equations (2.15) to (2.17). Where G_{Na}, G_K, and G_L are obtained from equation (5.3) and Nernst potential for sodium current (V_{Na}) is gained using Nernst equation in equation (3.1). Where $[Na^+]_{out}$ represents extracellular sodium concentration and $[Na^+]_{in}$ represents intracellular sodium concentration. In normal conditions $[Na^+]_{out} \gg [Na^+]_{in}$. The extra channels produced by the Aβ deposits provides conditions for the amount of intercellular Na^+ to increase. It can be seen from Equation 3.1, that V_{Na} has direct relation with $ln\left(\frac{[Na^+]_{out}}{[Na^+]_{in}}\right)$. Therfore by increasing the $[Na^+]_{in}$ the amount of V_{Na} decreases. Vitvitsky et al.

(Vitvitsky, et al., 2012) have shown that the amount of intracellular sodium in the competed Alzheimer's brains changes by 2-fold. Based on (2.15) by decreasing V_{Na} the current flow of Na^+ increases. Nernst potential for potassium current is gained by equation (3.2). Where $[K^+]_{out}$ represents extracellular potassium concentration and $[K^+]_{in}$ represents intracellular potassium concentration. Vitvitsky et al. (Vitvitsky, et al., 2012) also have proven that the amount of intracellular potassium in the competed Alzheimer's brains changes up to 15% of normal brain. Following the above equation and by considering the truth that the $[K^+]_{out} \ll [K^+]_{in}$ in confrontation with Aβ channels the amount of $[K^+]_{in}$ decreases. Therefore, unlike the sodium the value of $ln\left(\frac{[K^+]_{out}}{[K^+]_{in}}\right)$ increases.

The Nernst potential for leakage current is:

$$V_{Cl} = 26.6 \ln\left(\frac{[Cl^-]_{out}}{[Cl^-]_{in}}\right), \tag{5.5}$$

$$V_L = 26.6 \ln\left(\frac{0.085[Na^+]_{out} + [K^+]_{out} + 0.1[Cl^-]_{out}}{0.085[Na^+]_{in} + [K^+]_{in} + 0.1[Cl^-]_{in}}\right), \tag{5.6}$$

as can be seen, these equations are related to intercellular and extracellular ion concentrations. The Aβ peptides damage the membrane of neurons and it affects the total tissue sodium and potassium concentrations. The total tissue concentrations of sodium and potassium are described by below equations:

$$[Na]_{tot} = \frac{[Na^+]_{in}[Vol]_{in} + [Na^+]_{out}[Vol]_{out}}{[Vol]_{in} + [Vol]_{out}} \tag{5.7}$$

$$[K]_{tot} = \frac{[K^+]_{in}[Vol]_{in} + [K^+]_{out}[Vol]_{out}}{[Vol]_{in} + [Vol]_{out}} \tag{5.8}$$

where $[Na]_{tot}$ and $[K]_{tot}$ are total sodium and potassium concentration in tissue. $[Na]_{in}$, $[Na]_{out}$, $[K]_{in}$, and $[K]_{out}$ are intracellular and extracellular sodium and potassium concentrations respectively. $[Vol]_{in}$ and $[Vol]_{out}$ show intercellular and extracellular volume in the tissue. The volume is total volume occupied by all neurons in the tissue sample. By considering the unit volume $[Vol]_{in} + [Vol]_{out} = 1$, the equations transform to:

$$[Na^+]_{tot} = \big([Na^+]_{in}[Vol]_{in} + [Na^+]_{out}(1 - [Vol]_{in})\big) \qquad (5.9)$$
$$= [Na^+]_{out} + ([Na^+]_{in} - [Na^+]_{out})[Vol]_{in}$$

$$[K]_{tot} = \big([K^+]_{in}[Vol]_{in} + [K^+]_{out}(1 - [Vol]_{in})\big) \qquad (5.10)$$
$$= [K^+]_{out} + ([K^+]_{in} - [K^+]_{out})[Vol]_{in}$$

these equations show that the total tissue concentrations of sodium and potassium are linear functions of the relative cell volume. It means that an increase in the cell volume makes a decrease in total sodium concentration and increase in total potassium concentration. These happen because

$$[Na^+]_{in} - [Na^+]_{out} < 0 \qquad (5.11)$$

$$[K^+]_{in} - [K^+]_{out} > 0, \qquad (5.12)$$

The relations (5.11) and (5.12) in the healthy neuron is always established. However, by increasing Aβ channels this relation changes to $[Na^+]_{in} - [Na^+]_{out} \to 0$ and $[K^+]_{in} - [K^+]_{out} \to 0$ then following the Nernst equations in equations (3.1) and (3.2) for sodium and potassium ions $V_{Na^+} \to 0$ and $V_{K^+} \to 0$ that cause neural deterioration.

The sodium and potassium ion concentrations inside and outside of the neuron can obtained as follow:

$$\frac{d[K^+]_{out}}{dt} = \frac{1}{\tau} \left(\gamma \beta I_K - 2\beta I_{pump} - I_{glia} - I_{diff} \right) \qquad (5.13)$$

$$\frac{d[Na^+]_{in}}{dt} = \frac{1}{\tau} \left(-\gamma I_{Na} - 3\gamma I_{pump} \right) \qquad (5.14)$$

Where concentrations are calculated in millimolar (mM). I_{pump} is the current of the neuronal Na+/K+ pump. I_{glia} is the current associated with the glial buffering. I_{diff} is the K+ diffusion current. $\gamma = 4.45 \times 10^{-2}$ is a unit conversion factor. This factor converts the membrane currents into mM/sec. $\beta = 7$ is the ratio of the interacellular to extracellular volume. $\tau = 10^3$ is the molar currents (mM/sec) and balances the time units. The pump, glia, and diffusion molar currents are as follow:

$$I_{pump} = \rho (1 + \exp\left(\frac{25 - [Na^+]_{in}}{3}\right))^{-1} \left(\frac{1}{1 + \exp(5.5 - [K^+]_{out})}\right) \qquad (5.15)$$

$$I_{glia} = G \left(1 + \exp\left(\frac{18 - [K^+]_{out}}{2.5}\right)\right)^{-1} \qquad (5.16)$$

$$I_{diff} = \varepsilon([K^+]_{out} - K^+_{bath}) \qquad (5.17)$$

Where $\rho = 1.25 \frac{mM}{sec}, G = 66.666 \frac{mM}{sec}$, and $\varepsilon = 1.333\ Hz$. K_{bath} is the potassium concentration in the reservoir and is $K_{bath} = 4\ mM$ for normal physiological conditions. To simplify the model and reduce complexity, this study decided to neglect pump, glia and diffusion currents in our experiment. The intracellular potassium and extracellular sodium concentrations are as follow:

$$[K^+]_{in} = 140 + (18 - [Na^+]_{in}) \tag{5.18}$$

$$[Na^+]_{out} = 144 - \beta\ ([Na^+]_{in} - 18) \tag{5.19}$$

An ion channel transmits ions with a given conductance or in other words, resistance. By understanding the physical properties of Aβ channels someone can estimate the exact function of this channels and its deleterious effects on the neuron. It can be approached by getting the ion flux across the membrane. Following Arispe's study (Arispe, et al., 1993) the ion flux φ inside the membrane can be obtained using the following equations:

$$\varphi_i = (\rho_i I_i)/F \tag{5.20}$$

where φ_i is the ion flux, ρ_i is the fractional open time, I_i is the ion current through the open Aβ channel, and F is the Faraday constant which is equal to 96.480 C/mole. Therefore, if a single *4 nS* channel became active in a neuron of 25 μm diameter, the sodium influx could be calculated as 0.6 fmol/sec, and the intracellular sodium concentration change would be *10$\mu M/sec$*. By the equation (5.18) someone can say Alzheimer concentrates on the improper cation ions fluxes inside the nervous cells. The reason which are addressing this is as following computational reasons.

Following equation (5.3) the conductance of sodium (G_{Na}) can represents as:

$$G_{Na} = \overline{G}_{Na} m^3 h \tag{5.21}$$

As it is shown in the equations (5.3), (5.4), (5.7), (5.8), (5.9), and (5.10) the conductance of sodium is depended on the other variables i.e. m, n, V then it can be rewritten as:

$$G_{Na} = \overline{G}_{Na} f(m, n, V) \tag{5.22}$$

On the other hand, the current of sodium in (2.15) following the equation (3.1) is depended on the $Na_{in}, Na_{out},$ and V. Therefore, the equation (2.15) can be written as:

$$I_{Na} = \overline{G}_{Na} f(m, n, V). \overline{\varphi}(Na_{in}, Na_{out}, V) \tag{5.23}$$

Where $\overline{\varphi}$ is a function which represents $(V - V_{Na})$ using Nernst equation in (3.1). Following these changes the sodium flux across the membrane which obtain from equation (5.20) is converted to

$$\varphi_{Na} = \rho_{Na}(\overline{G}_{Na} f(m, n, V). \overline{\varphi}(Na_{in}, Na_{out}, V))/F \tag{5.24}$$

If Na_{in} increases and Na_{out} remains stable (like the condition which occurred in accumulation of Aβ deposition) then one or more variables like ρ_{Na}, m and h are changed. ρ_{Na} is the fractional open time and it is representing the fraction of the time that channel is open. It's modulated by the Na_{in} concentration. Its function is somewhat like the functions of m and h in activation and deactivation of sodium channel. The ρ_{Na} makes sever interruptions in exact configuration of m and h and somehow these gates lose their real performance. With this description and from the above computational relations, it can be concluded that secretion of Aβ in Alzheimer's disease causes a disease like channels dysfunction in the nervous system. The same condition can be defined for potassium flux in neuron, as well.

Therefore, in order to computationally simulate amyloid peptide channels at plasma membrane in the Alzheimer's disease condition, this study needs to increase the amount of cations inside the cell. As noted above and shown in equation (5.24) for given ion like sodium, the maximum conductance of sodium has a direct relation with the ion flux inside the membrane. Therefore, for any changes of intercellular ions, the maximum

conductance should be changed. In support of this, this study can refer to the work of Perez, et al. (Perez, et al., 2017). In their work for intercellular ion changes which are increased by created Aβ channels, Perez, et al (Perez, et al., 2017) changed the maximum conductance of related ion. But how much is needed for changing the concentration of sodium and potassium? In order to find out these values the study get benefit from the model introduced by Vitvitsky et al. (Vitvitsky, et al., 2012). For this reason, the intracellular sodium increased by a 2-fold and the intracellular potassium increased 8–15%. The nominal channel conductivity for sodium is 120 ms/cm^2 for potassium is 36 ms/cm^2. The equilibrium potential applied for sodium is 50 mV, for potassium is -71 mV and for leakage is -51 mV. The injected current is 10 nano-Amps. These equations are solved using the Ode45 method which is based on an explicit Runge-Kutta method, with a time step of 0.01 ms.

5.4   Computational Results

In the following, the responses of a neuron with Aβ channels is compared to the standard neuron. It can be seen that the presence of Aβ channels increase in the amplitude of membrane potential and the increased number of spikes (see Figure 5.1.D). Further study was carried out to investigate this further. The first experiment is performed with all conductances having nominal values. The second and third experiments are done by a 2-fold intracellular sodium increases and 15% intracellular potassium increases, respectively. The final experiment performed by 2-fold intracellular sodium and 15% intracellular potassium increases, simultaneously. This reflects the increase in channels due to the AB deposits as speculated by Vitvitsky (2012). All the experiments are carried out at simulation time 150.0s. The injected current varies from 0 nA, between 0.0 to 50.0 seconds, to 10 nA, between 51.0 to 1000.0 seconds. The reason for considering two

different injection currents was to have the behaviour of the system under both stimulation and non-stimulation conditions.
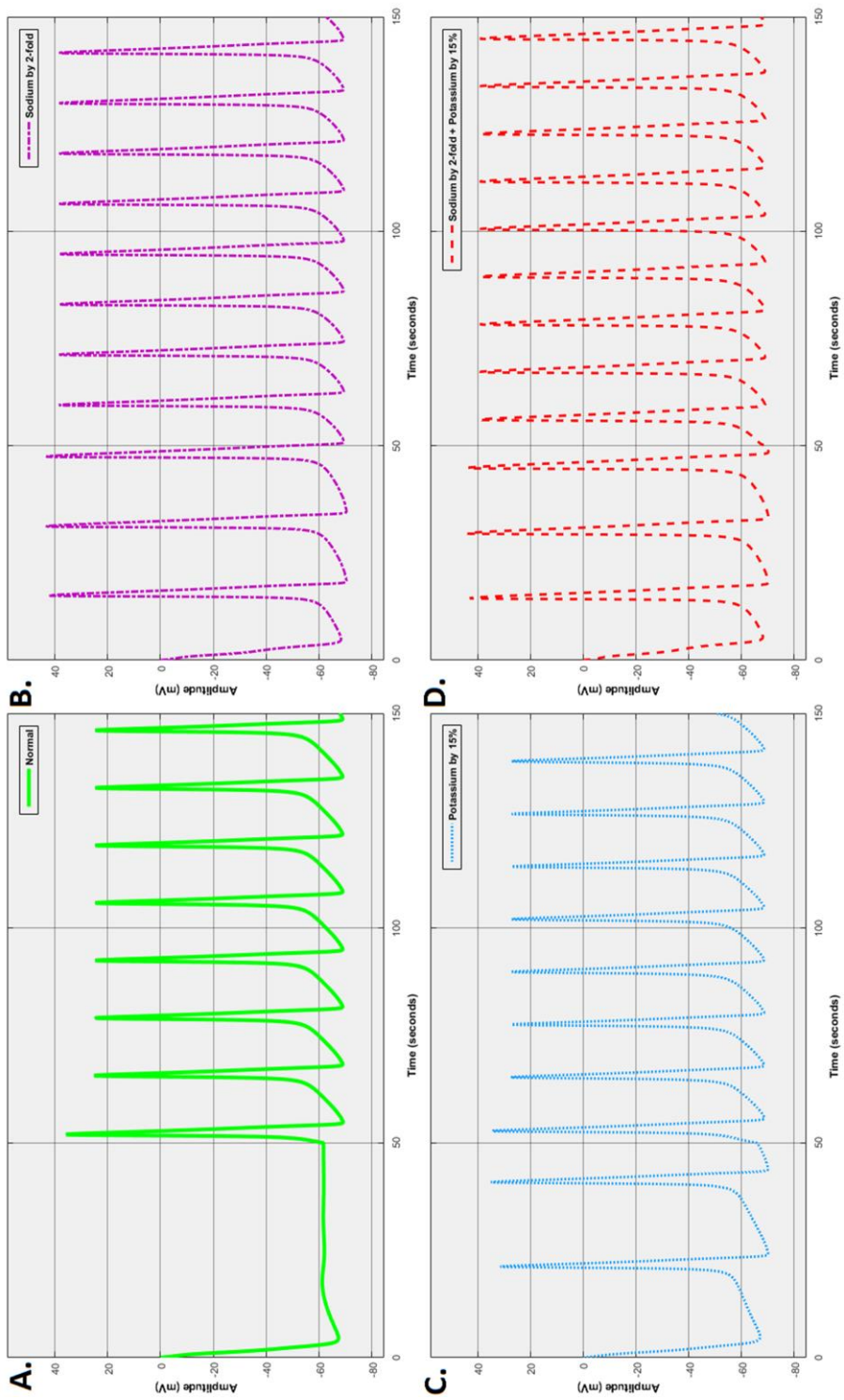
Figure 5.1 – The output of experiments. A. The output with nominal values; B. The output of increasing sodium conductance by 2-fold; C. The output of increasing potassium conductance by 15%; D. The output of increasing both sodium and potassium conductance, simultaneously.

Figure 5.1.A shows the responses of the neuron for the nominal set of values. This spike is taken to the ideal response, and all comparisons are made to this response. As it is shown, the reactions are series of spikes. These spikes have two main characteristics. The first characteristic is the magnitude of the spike and the second is the inter-spike intervals. The analyses of these two characteristics for all changes are shown in Figure 5.3 and Figure 5.4. The Figure 5.1.B presents the reaction of the neuron to the change of sodium conductance. 2-fold increasing changes the sodium ion conductance. It can be seen that as the sodium ion conductance is increased from its nominal value, the magnitudes and the inter-spike interval are both increased. In other words, neuron responds with more massive spikes at a more rapid rate.

In the same way, results obtained for the conductance of potassium ion. The reaction is shown in Figure 5.1.C. In this experiment, the effect of potassium conductance is more pronounced. 15% increasing changes the potassium conductance. It can be seen that as the potassium ion conductance is increased from its nominal value, the time of inter-spike intervals is decreased (see Figure 5.3). As the outcome indicates, the nerve cell is more sensitive to any potassium changes inside the cell than to sodium ion changes.
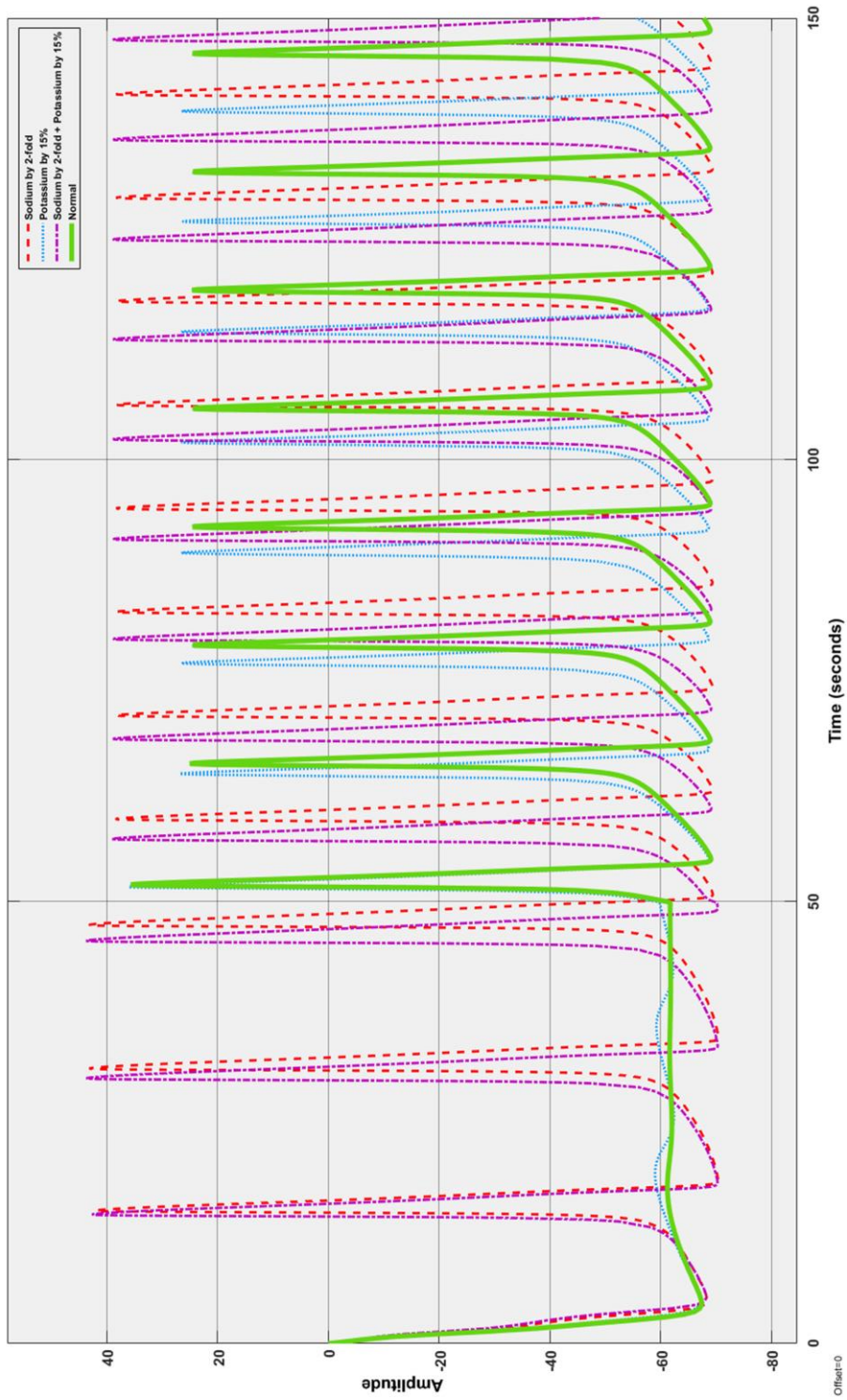
Figure 5.2 – Overlapped graphs

137

The next set of the experiment meant to changes combination of sodium and potassium conductance in a single neuron, simultaneously. This result is shown in Figure 5.1.D. From the results, it is evident that both sodium and potassium conductance changes at the same time affected almost every element of the output, i.e. inter-spike interval and magnitude of the spikes. Results from this figure can be compared with results in Figure 5.1.B which show when combined conductance changes occur in the cell the effects are more severe than (but are consistent with) those reported in the individual sodium or potassium conductance changes. Overlap graphs to acquire a better comprehension of these changes is presented in Figure 5.2.

Increasing G_{Na} leads to increase the amplitudes of action potential of neuron (see Figure 5.3.B). On the other hand, increasing G_K as compared to the value applied for normal neuron increases the amplitudes of spikes (see Figure 5.3.C). As shown in Figure 5.2.A combining both changes on a single neuron leads to increasing the amplitude of action potentials even more than the both previous single changes. In case of G_K on the other hand, a much higher change in G_K is required to reproduce the observed behavior in case of increasing G_{Na}. In line with observations, as it can be shown depolarization linearly increased. However, increasing combined both G_K and G_{Na} does not change the slope significantly, inconsistent with increasing only G_{Na}.

As shown in the Figure 5.4.B by increasing G_{Na} the time interval of the response of neuron to stimulation is decreased. The same behavior is observed in the Figure 5.4.C for increasing G_K. The response of neuron to the combined changes is shown in the Figure 5.4.A. The changes shown an decrease in the time intervals of action potentials but the slop of changes doesn't show significant changes with single changes of G_{Na} and G_K.
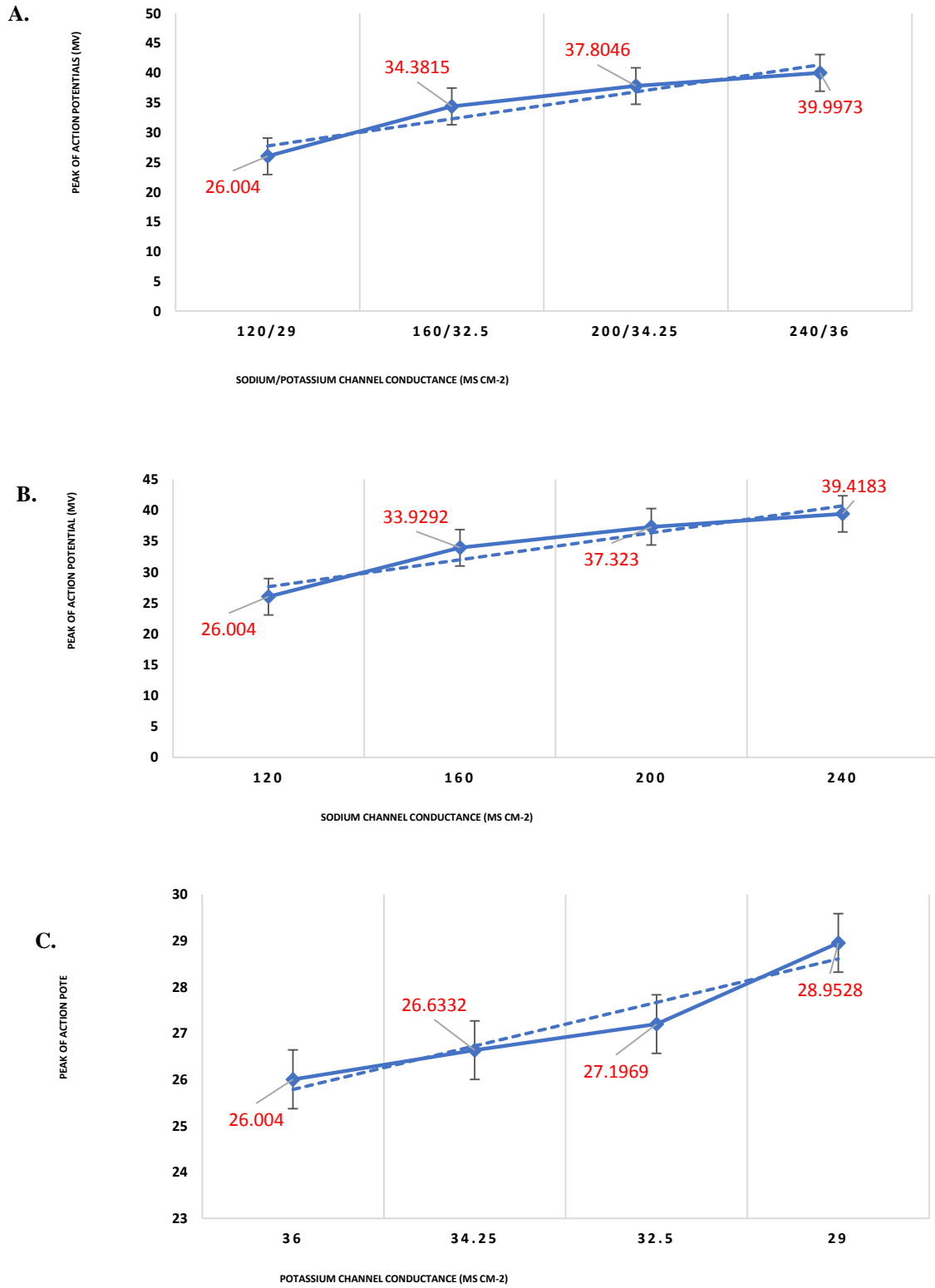
Figure 5.3 – The changes of Action potential amplitudes A. in both sodium potassium conductance B. sodium conductance C. potassium conductance
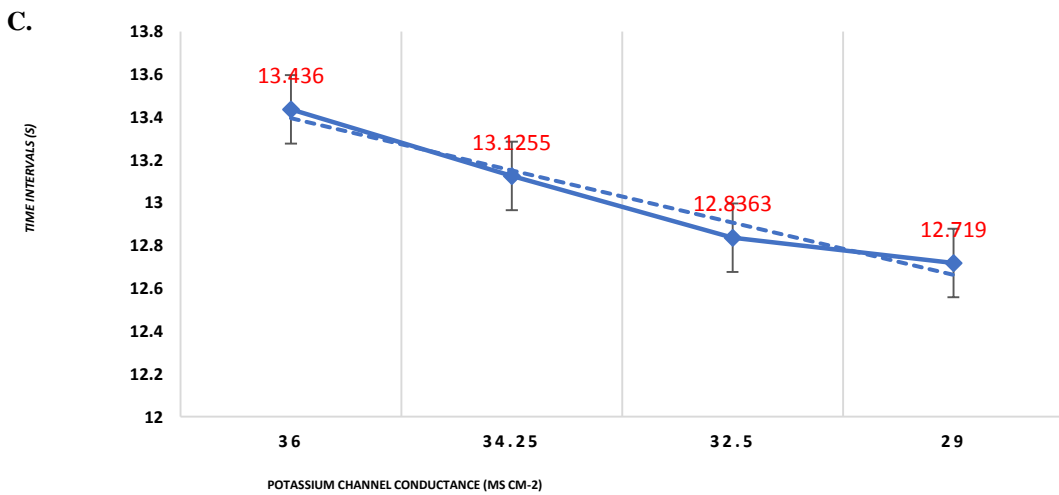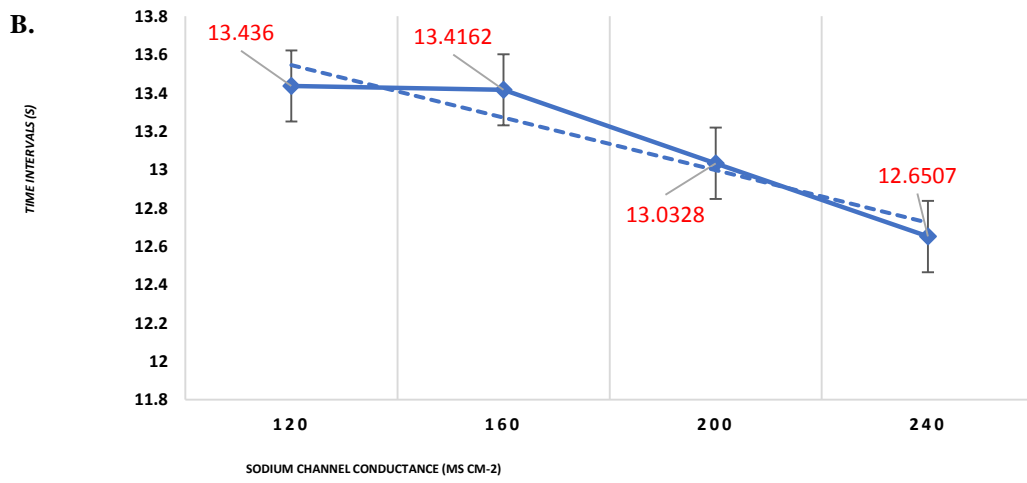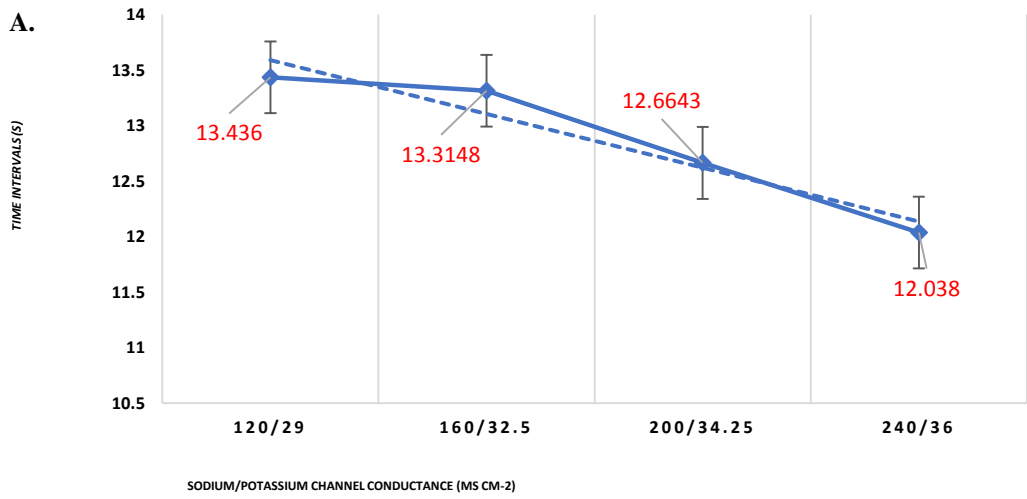
Figure 5.4 – The changes of time intervals of action potentials A. both sodium potassium conductance B. sodium conductance C. potassium conductance

The sodium and potassium fluxes across the membrane for a given neuron with single *4 nS* channel and *25 μm* diameter in the normal and affected by amyloid-β are shown in Figure 5.5 and Figure 5.6, respectively.
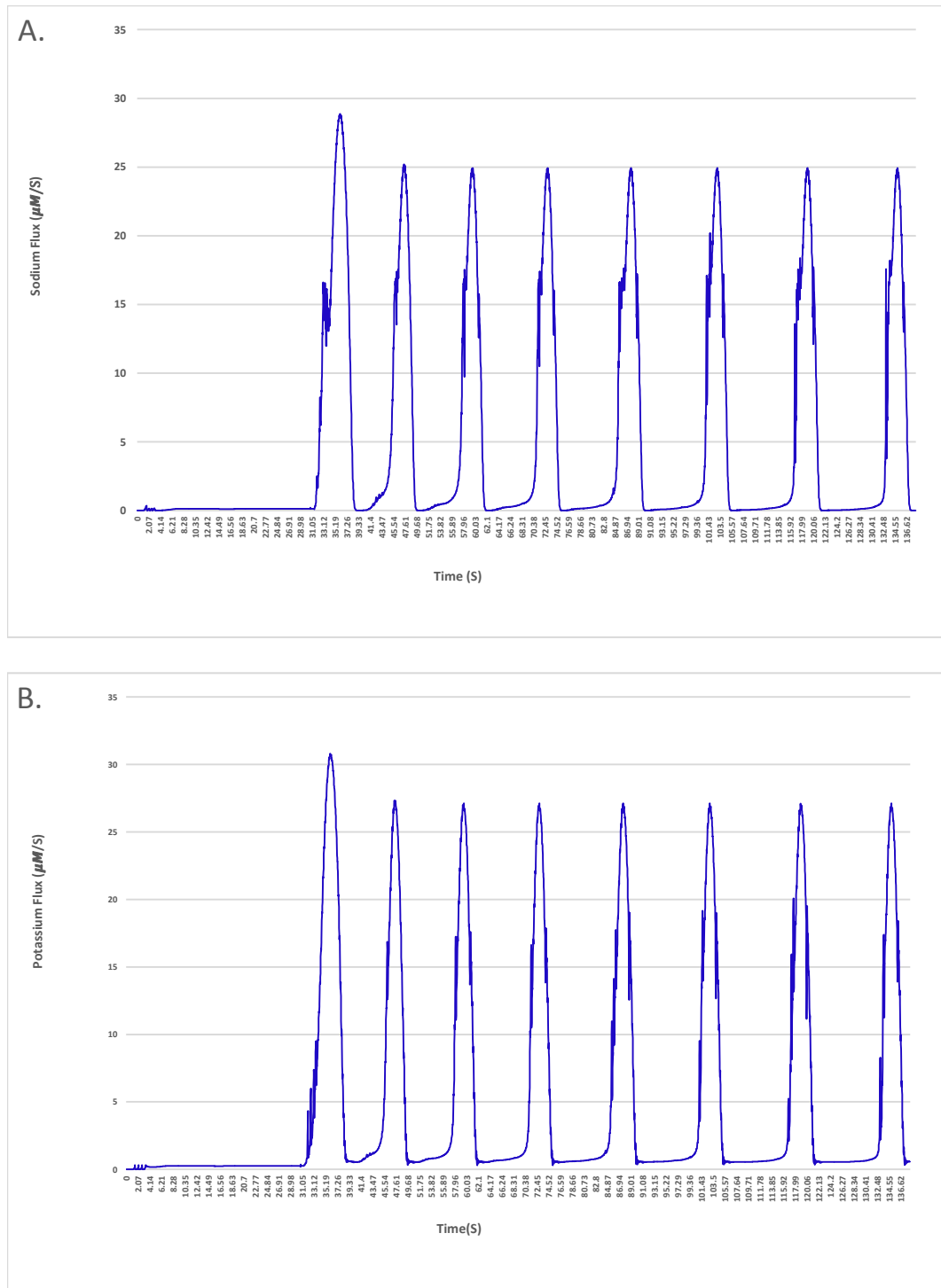
Figure 5.5 – The changes of ions flux in normal condition A. Sodium flux B. Potassium flux
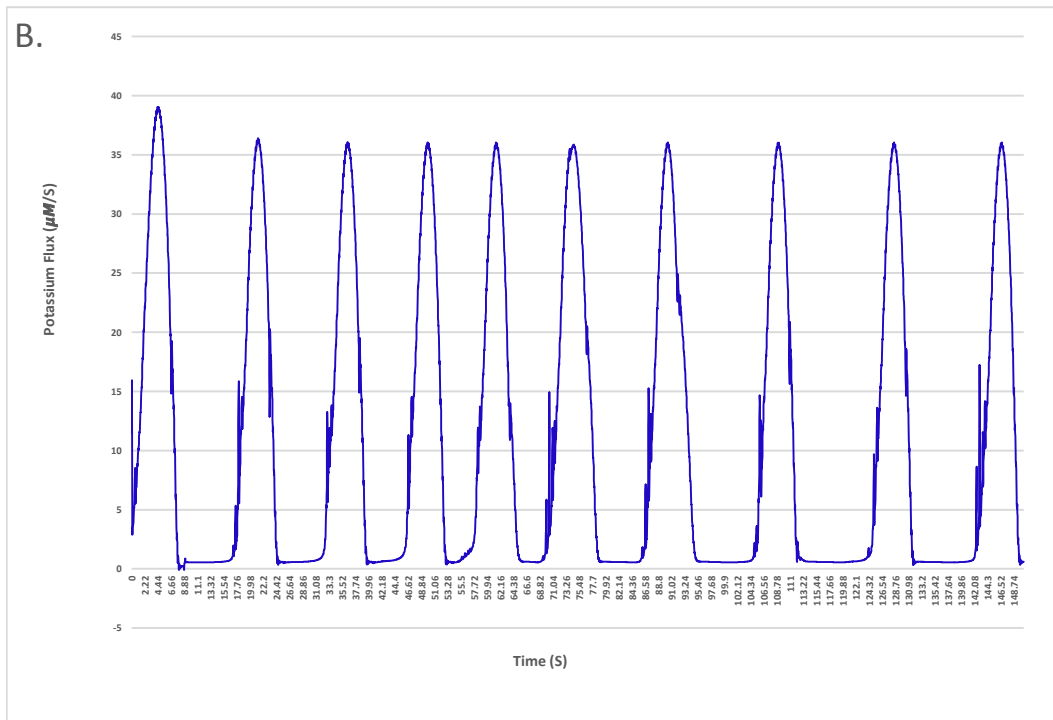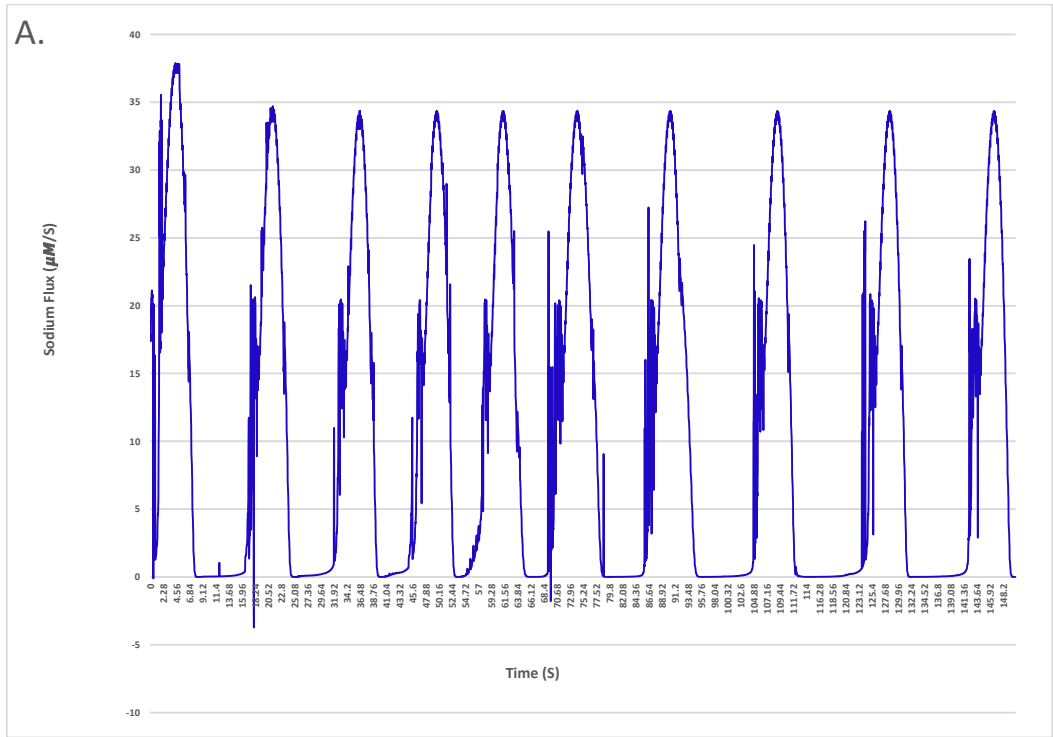
Figure 5.2 – The changes of ions flux when the intercellular concentration of sodium 2 fold and potassium 15% increased A. Sodium flux B. Potassium flux

The results indicate a deterioration of ions exchange in the vicinity of the plasma membrane with Aβ protein. As shown in Figure 5.6 in hyperpolarization step the neuron experiences huge fluctuations for sodium exchange. This delay or even fault in the turnover of ions flux across the neuronal membrane may eventuate in crucial impairments of cellular performances and it will also lead to a potential threat to nerve cell longevity. The fluctuations are driven solely by Aβ pores which are permeable to sodium and potassium. The pores make damage to membranes of nerve cell and transform its specific functions such as ion homeostasis and action potentials as shown in the results.

5.5 Discussion

There is growing evidence which indicates that neurodegenerative disorders have a an origin in the presence of dysfunctional ion channels. Many neurodegenerative disorders like Alzheimer's disease, Parkinson's disease, and age-related disorders are caused due to the transformation of functionality in ion channels (Kumar, et al., 2016).

The results in this chapter show that the presence of Aβ channels on the membranes cause hyperactivity in the function of the neuron. The results summarised in Figures 5.1.B to 5.1.C illustrate the complexity and the response of these channels for separated sodium and potassium ions. Figures 5.1.B shows the output of increasing sodium conductance by 2-fold and Figures 5.1.C shows the output of increasing potassium conductance by 15%. In comparison to Figures 5.1.C, the hyperactivity has been exacerbated in Figures 5.1.B more. The reduction in the magnitude of the spikes is a result of lowering of the dielectric barrier due to the inoic changes. Since the output due to changes in sodium (see Figure 5.1.B) and the output of combined changes in sodium

and potassium (see Figure 5.1.D) are very similar. Thus it can be seen that Aβ disrupts sodium homeostasis in neuron, and it can be inferred that Aβ peptides function similar to sodium channels. In the studies of real brain tissue, Vitvitsky et al. (Vitvitsky, et al., 2012) have shown that abnormal levels of ions like sodium and potassium in neurons cause the ionic imbalance that is linked to Alzheimer's disease pathogenesis. They found remarkable ion imbalances in the cortical (sodium) and cerebellar (potassium) of Alzheimer's disease brain. Based on other research (Migliaccio, et al., 2015), (Stage, et al., 2017), (Mendez, 2017), (Ballarini, et al., 2016) which were done on the early- and late-onset stages of Alzheimer's disease, in the early stages of Alzheimer's the cortical areas are most involved. After considering these studies and taking into account the results of our experiments it may be concluded that changes of sodium ions in the intracellular neurons of the cortical regions can be considered as a hallmark of early detection of Alzheimer's disease.

These results indicate the conditions for neuronal hyperactivity (see Figures 5.1.D) and when considered together with the studies of (Migliaccio, et al., 2015); (Stage, et al., 2017); (Mendez, 2017); (Ballarini, et al., 2016) show the possibility of developing test in Alzheimer's disease. But this raises another issue that, despite the fact that there is an increased excitability in hyperactive neurons, how can the neurodegeneration seen in Alzheimer's disease be associated with a reduction in the overall activity in neurons. This question was answered by another study done by Busche et al. (Busche, et al., 2008) and the role of inhibitory neurons in the general structure of the nervous system. Busche et al. mapped the distribution types of neurons. In their studies, they showed that there are three types of neurons about the nearest three-dimensionally Aβ accumulations. These three types are included as *hyperactive*, *silent*, and *normal* neurons. Hyperactive neurons are found only in very close proximity (usually less than 60 μm) to the borders of Aβ

plaques. After this border and at increasing distances, the proportion of silent neurons significantly increased. Thus, a possible explanation for the two types of hyperactivity and silent neurons may be an impairment on inhibitory neurons. As it turns out from the results and studies done by Perez et al. (Perez, et al., 2017) and Busche et al. (Busche, et al., 2008) the hyperactivity which is caused by Aβ channels, exacerbates the activity of inhibitory neurons. For this reason, one can assume that the activities of the neurons surrounding the hyperactive neurons are looked as silence and in general, someone can see the lowering of neuronal activities in the central nervous system.

The results of the function of an individual neuron in the direct vicinity of Aβ plaques show the epileptiform activity in Figure 5.1.B, 5.1.C, and 5.1.D. As it is shown, the neuron experiences several action potentials even when there are not any stimuli for the neuron. These results confirm the studies done by (Busche, et al., 2008) (Minkeviciene, et al., 2009) (Palop & Mucke, 2009) (Roh, et al., 2012) (Berridge, 2014). They revealed that in addition to the increased neuronal activity in the direct vicinity of Aβ plaques the risk of epileptic seizures is high in Alzheimer's disease. In answer to our key question, the study should point to this novel idea that Aβ is toxic to cortical and cerebral neurons as this kind of protein forms the aberrant ion channel in the plasma membrane of the neuron. As a result, it disrupts neuronal homeostasis, partially or completely. Aβ interact with different types of membranes which leads to the formation of Aβ ionic channels and it could support the idea that Aβ is cytotoxic largely, due to the action of Aβ channels in the plasma membrane of the neuron. As Aβ gets more deposited the channels for sodium exchange increases and therefore it can be seen that Na_{in} increases and eventually, the relation 5.11 leads to $[Na^+]_{in} - [Na^+]_{out} \rightarrow 0$ that is a deterioration in the neuron. It is clear that there is a deterioration in the signals. The rate at which this change occurs is important from the point of view of detecting the problem at an early stage.

Aβ accumulation has been discovered to form large, relatively cation-permeable channels under physiologic conditions. These channel formation in membranes of a neuron could cause cell depolarisation, sodium and potassium dysregulation, depletion of neural energy stores, and other types of cellular dysfunction. As shown in Figure 5.6 the build-up of Aβ depositions during the onset of Alzheimer's disease has profound effects on the activity of the local community of neurons in the central nervous system. For instance, in hyperpolarization step of action potential the neuron experiences huge fluctuations in sodium exchange. These effects can include enhanced neural activities (Busche, et al., 2008), spontaneous epileptiform activities (Minkeviciene, et al., 2009), (Palop & Mucke, 2009), and incidences of epileptic seizures (Roh, et al., 2012), (Berridge, 2014). According to the results of the experiments, it can be well understood that the neurodegeneration observed in Alzheimer's disease has been associated with the increase of toxicity of Aβ depositions. Concertedly, this study reveals that accumulation of Aβ during Alzheimer's disease causes neuronal hyperexcitability in inhibitory neurons as well as, makes neural networks susceptible to epileptiform activities.

6 Fault investigation for dysfunction of neurons

6.1 Introduction

A mathematical model of a biologic system provides a perception of that system. Models of diseases have been increasingly used in research (Andreas & Bowser, 2017), e.g. mathematical model of the nervous system can be applied to study and explain neurological diseases (Awasthi, et al., 2017).The nervous system has a very complex structure, with highly interconnected cells. In this chapter a set of neurons modelled using four-dimensional differential equations are studied to understand the dysfunction in neurons, and the effect this has on the action potential of nerve cells in the nervous system (Baravalleab, et al., 2017).

However, despite the existence of a nervous system model for understanding neural activities, these models are often inaccurate, in that the neurons often don't follow the laws precisely. A reason for this is that noise or extraneous signals can get amplified resulting in errors. Thus estimating the state of the neuron or neurons becomes an important problem.

This chapter applies linear (Kalman) and nonlinear (Extended Kalman) observers to detect faults i.e. to detect dysfunction of inhibitory neurons in Alzheimer's disease. In order to further verify the efficiency of the detection scheme, another nonlinear observer

by coordinate transformation proposed by Delgado, et al. (Delgado, et al., 2005) was applied.

Over recent years, several studies have been used to apply the Kalman filter on the Hodgkin-Huxley model as a model observer system. A work by Kawai et al (Kawai, et al., 2008) has applied the Kalman filter as an observer on a locally linearized model of the Hodgkin-Huxley in order to estimate current state from the input and parameters of the model. In another work (Lankarany, et al., 2014) the Kalman filter method was extended for the Hodgkin-Huxley model to estimate the unknown parameters as well as the intrinsic dynamics of the model. However, such studies often concentrate only on the observer itself. This study designs a linear observer based on the Kalman filter in order to be able to detect faults in neurons, especially to detect the dysfunction of inhibitory neurons in Alzheimer's disease.

6.2 Kalman Filter

System states describe the behaviour of internal variables of systems of which, in most of systems, only a few can be measured. In other words not all system states are achievable through measurement and furthermore only some of them appear explicitly in the measurement equations. To obtain system states for different purposes such as control, fault detection, etc. they should be estimated through observers. The Kalman filter as a minimum mean square error estimator is a well-known stochastic observer employed to estimate system states (Grewal & Andrews., 2015) . It uses a system model as well as a series of measurements over time for state estimation. It contains statistical noise and other inaccuracies and finally, it turns out estimates of unknown variables. This experiment shows that a Kalman filter framework can adapt neuronal data from only single voltage measurements and after that reconstruct the required ionic dynamics.

Kalman filters are designed for linear dynamical systems and perturbed by additive Gaussian noises in system and measurement models. In many cases, the number of outputs that are measured not the same as the number of states, thus the observers are a way of recreating these extra states. This is done in the presence of noise and disturbances. In these cases, it is necessary to think of a way of finding an optimal estimation of all the states of the system. The optimal means the optimal in terms of minimum variance or least squares. Generally, it can be done by constructing a mathematical model of the system dynamics in order to track the states. The results of the state noise are obtained by spreading the state noise through a completely similar mathematical model and filtering it from the estimation of states with a weight based on the measurement noise. Given that no analytical solution is actually needed, the differential equations of the state and noise will be solved recursively in order to find the estimations of state. One of the most commonly used mathematical models for noise suppression is the Kalman filter.

In this section, Kalman filtering is applied to be employed for estimation of system states and then the estimated states are employed for fault detection. The details of the implementation are omitted here and can be found in (Grewal & Andrews., 2015).

6.2.1 Proposed observer for the neuron model

This experiment uses the neuron model to demonstrate dynamical behaviours of neural cells. For more about the neural model refer to section 2.3.

6.2.2 Detection of faults using a linear observer

For fault detection, an analysis of the difference between the sensor and expected values derived from the model, called the residual is required. If the residual goes above a certain threshold, a fault is detected. It is worth mentioning that the concept of threshold in this chapter is totally different from previous chapters. In this chapter the term of threshold

used as the threshold of fault, however in other chapters it used as threshold of an action potential. The residual signal is normally zero when our system is fault free, while it is not zero when a specific fault is present in the system. There are several residual generation methods, which are listed in section 2.18.1. Among them, for fault detection the study chooses observer based residual generation as it has wide applications in the framework of control theory. In addition, this study can also estimate the internal states of the system (Yang & Tang, 2007); (Edwards, et al., 2000); (Yang & Saif, 1998); (Li, et al., 2010); (Q Cheng, et al., 2005); (Sadeghzadeh-Nokhodberiz & Poshtan, 2014).

As mentioned above there are several residual generation methods and this study uses observer based residual generation in which Kalman filter is employed as a linear observer. In order to detect faults by residual generation, the following residual is employed:

$$r(t) = y(t) - C\hat{x}(t) \tag{6.1}$$

Where C is the measurement matrix that determines the relation between state and output of the model, $\hat{x}(t)$ is the output of the observed and $y(t)$ is the real outputs. Then, this study computes the Euclidean norm as $\|r(t)\|$ and compare it with a predefined threshold, say μ, which is determined through trial and error to specify a binary decision if a fault is occurred or not.

6.2.3 Simulation results

In this experiment, a neural model with the same characteristics as in the previous experiments is applied to produce the response of a neuron to a stimulation. The neural model properties are presented in Table 6.1.

Symbol	Specification	Description
V_L	-51 mV	Leakage potential
V_{Na}	50 mV	Sodium potential
V_K	-71 mV	Potassium potential

g_L	0.3 mS/cm2	Leakage conductance
g_{Na}	120mS/cm2	Sodium conductance
g_K	38 mS/cm2	Potassium conductance
C_M	1.0 μF/cm2	Membrane capacitance

Table 6.1 – Model specifications

The stimulus, I_{stim}= 10 μA/cm2, 50ms ≤ t ≤ 200ms, is considered as the injected current. The states *n, m* and *h* are random number distributed uniformly over the interval [0, 1]. As shown in Figure 6.1, the output of intracellular voltage (v) and the output of estimated membrane voltage are shown with good accuracy. This figure presents the performance of the Kalman Filter in estimating the parameters of the neural model.
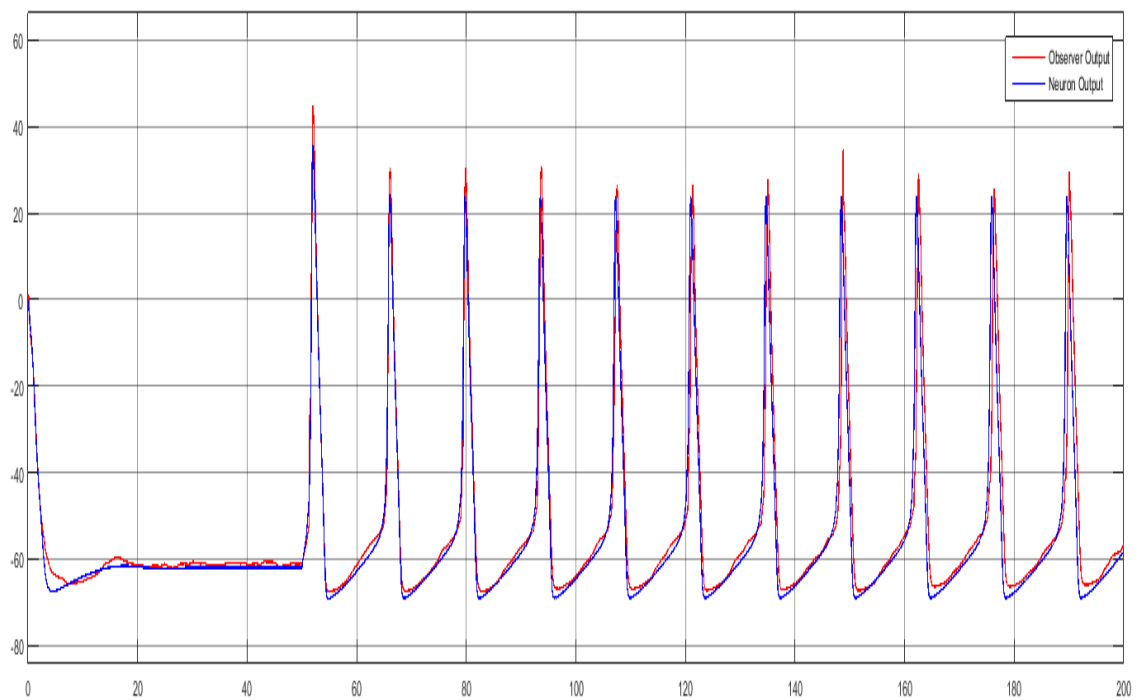
Figure 6.1 – Observed membrane vs. normal membrane
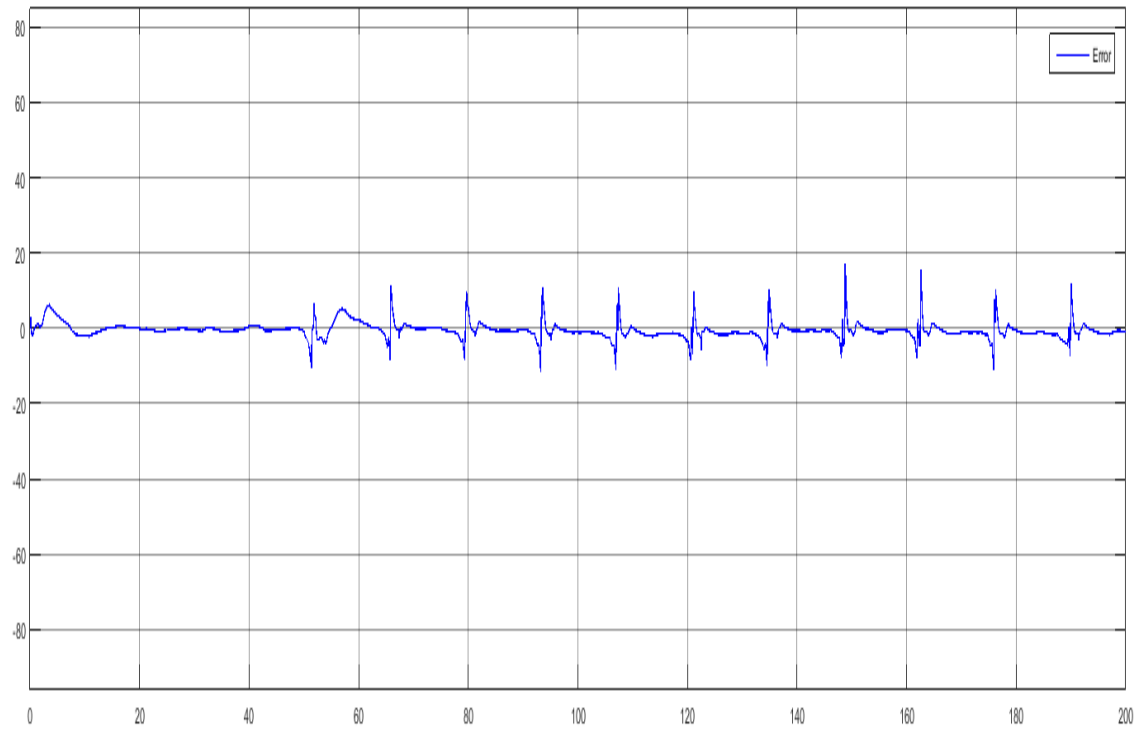
Figure 6.2 – Error of model when G_{Na} = 120. The nominal value of GNa = 120
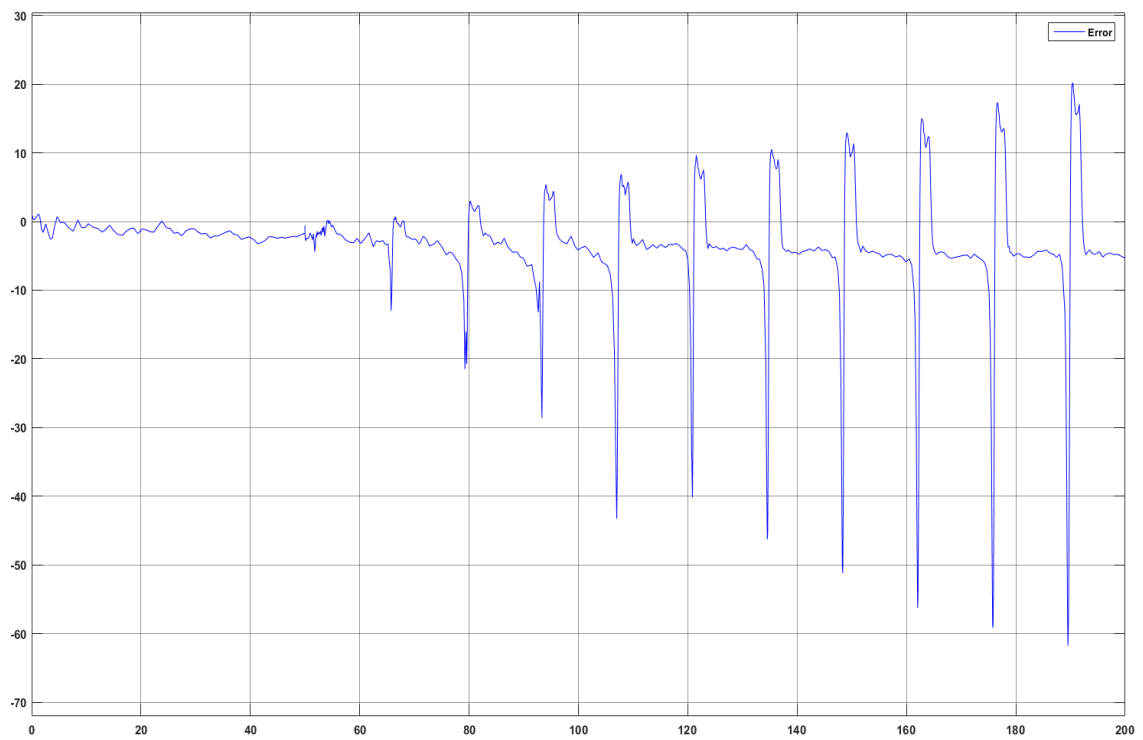
Figure 6.3 – The output estimation error of model when G_{Na} = 121. The nominal value of G_{Na} = 120

The output estimation error is shown in Figure 6.2 for normal condition and in Figure 6.3 for a condition which G_{Na} = 121 (faulty condition). A fault is detected if the value of the residual exceeds the predefined threshold. The residual *r (t)* is given by (6.1). A fault occurs when *r(t)* exceeds the threshold μ and the fault f(t) is given by

$$f(t) = \begin{cases} 1 \ if \ r(t) \geq \mu \\ 0 \ if \ r(t) < \mu \end{cases}$$

In this case the threshold is set at$\pm 20mV$. Figure 6.3 shows the responses when hypernatremia occurs, in case G_{Na} was set to 121. The error or the residual exceeds the threshold. And as it is exceeded the fault flag in now set to 1.
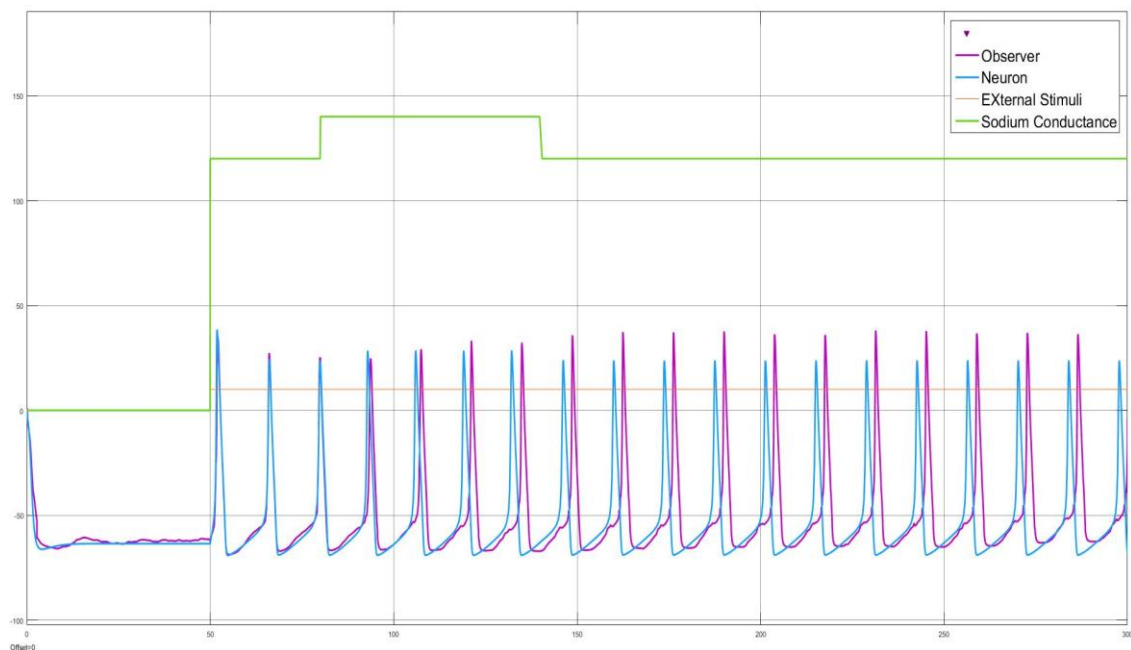
Figure 6.4 – The output of faults applied between the time 80 and 140 seconds for Kalman filter

From figure 6.3 it is seen that the residual increase with time, a reason for this is that the fault is accumulating, and at the same time in the neuron there has been a time shift. The inter-spike interval in the neuron has changed (see chapter 3) while that of the observer has remained the same. When the fault is removed, although the spike train returns to its original, there is an apparent time shift in the neuronal response, which causes the error

153

to remain. If the time element was rest as fault is removed, the two trains would be as before (see Tables 6.2, 6.3 and 6.4). In order to test the strategy further, a sequence of events were generated,

$$G_{Na} = \begin{cases} 120 \; for \; t = [50 - 80]S \\ 141 \; for \; t = [81 - 140]S \\ 120 \; for \; t \geq 141 \; S \end{cases}$$

The properties of action potential before applying fault, during applying fault and after applying fault are presented in Table 6.2 to Table 6.4.

	Before Fault		During Fault		After Fault	
	Av. of Inter-spike Intervals (S)	Av. of Spike Amplitude (mV)	Av. of Inter-spike Intervals (S)	Av. of Spike Amplitude (mV)	Av. of Inter-spike Intervals (S)	Av. of Spike Amplitude (mV)
KF	13.92	24.24	13.73	29.087	13.8	41.43
Neuron	13.75	24.09	13.03	28.32	13.76	23.98
$\|r\|$	0.17	0.15	0.7	0.767	0.04	17.45

Table 6.2 –The properties of action potential for Kalman filter G_Na=141

The same scenario is done for lower range of errors (i.e. $G_{Na} = 121 \; and \; G_{Na} = 130$) and the results are presented in Table 6.3 and Table 6.4. The reason to perform more experiments was to find out the behaviour of observe against the different ranges of faults. The properties of Table 6.3 is as follows:

$$G_{Na} = \begin{cases} 120 \; for \; t = [50 - 80]S \\ 121 \; for \; t = [81 - 140]S \\ 120 \; for \; t \geq 141 \; S \end{cases}$$

	Before Fault		During Fault		After Fault	
	Av. of Inter-spike Intervals (S)	Av. of Spike Amplitude (mV)	Av. of Inter-spike Intervals (S)	Av. of Spike Amplitude (mV)	Av. of Inter-spike Intervals (S)	Av. of Spike Amplitude (mV)
KF	13.87	24.3	13.84	24.42	13.88	24.02
Neuron	13.81	24.1	13.50	25.31	13.75	24.13
$\|r\|$	0.06	0.2	0.34	0.89	0.13	0.11

Table 6.3 –The properties of action potential for Kalman filter for G_Na=121

The properties of Table 6.4 is as follows:

$$G_{Na} = \begin{cases} 120 \ for \ t = [50 - 80]S \\ 130 \ for \ t = [81 - 140]S \\ 120 \ for \ t \geq 141 \ S \end{cases}$$

	Before Fault		During Fault		After Fault	
	Av. of Inter-spike Intervals (S)	Av. of Spike Amplitude (mV)	Av. of Inter-spike Intervals (S)	Av. of Spike Amplitude (mV)	Av. of Inter-spike Intervals (S)	Av. of Spike Amplitude (mV)
KF	13.89	24.27	13.79	26.77	13.85	33.1
Neuron	13.78	24.12	13.26	27.815	13.74	24.15
$\|r\|$	0.11	0.15	0.53	1.04	0.11	8.95

Table 6.4 –The properties of action potential for Kalman filter for G_Na=130

It can be seen that the magnitude of the fault was increased. In both case the residual signal should the same trends. These results are discussed in more detail in later section (section 6.5).

6.3   Extended Kalman Filter

The Kalman filter is based on linear transformations, but more sophisticated systems can be nonlinear. The issue of non-linearity can be found in observations, modelling, or both. The extended Kalman filter is a nonlinear version of the Kalman filter. The extended Kalman filter has been considered as a standard in the theory of nonlinear state estimation.

To formulate the continuous time Extended Kalman filter (EKF), firstly consider the following continuous time nonlinear model:

$$\dot{x}(t) = f(x(t), u(t)) + \omega(t) \tag{6.2}$$

where $x(t)$ is system state vector, $u(t)$ is system input vector, f is system nonlinear function, and $\omega(t)$ is white Gaussian noise, $\omega(t) \sim N(0, Q)$.

Now consider the following measurement model:

$$y(t) = h\big(x(t)\big) + v(t) \tag{6.3}$$

where $y(t)$ is system measurement, h is measurement function and $v(t)$ is white Gaussian measurement noise with $v(t) \sim N(0, R)$.

Now, in the following extended Kalman filter is presented:

-Initialization

$$P(0) = P_0, \qquad x(0) = x_0 \tag{6.4}$$

-Error covariance update

$$\dot{P} = AP + PA^T + Q - PC^T R^{-1} CP \tag{6.5}$$

-Kalman gain

$$K = PC^T R^{-1} \tag{6.6}$$

-The estimation update and prediction

$$\dot{\hat{x}}(t) = f(\hat{x}(t), u(t)) + K(y(t) - C\hat{x}(t)) \tag{6.7}$$

Where

$$A = \frac{\partial f}{\partial x}\Big|_{x(t) = \hat{x}(t), u(t)} \tag{6.8}$$

$$C = \frac{\partial h}{\partial x}\Big|_{x(t)=\hat{x}(t)} \tag{6.9}$$

6.3.1 Proposed extended Kalman Filter observer for the neuron model

The difference between Kalman and Extended Kalman is that for Kalman someone use a linearized model around the operation point, while in Extended Kalman someone use the nonlinear model in the prediction phase, and then it can linearize the system around the estimation point. In order to apply the extended Kalman Filter to the model, the linearized model is as follows:

$$\frac{\partial f}{\partial x}\Big|\hat{x}_{(t)} = \tag{6.10}$$

$$\frac{\partial f}{\partial x} = \begin{bmatrix} \frac{\partial f_1}{\partial V} & \frac{\partial f_1}{\partial h} & \frac{\partial f_1}{\partial m} & \frac{\partial f_1}{\partial n} \\ \frac{\partial f_2}{\partial V} & \frac{\partial f_2}{\partial h} & \frac{\partial f_2}{\partial m} & \frac{\partial f_2}{\partial n} \\ \frac{\partial f_3}{\partial V} & \frac{\partial f_3}{\partial h} & \frac{\partial f_3}{\partial m} & \frac{\partial f_3}{\partial n} \\ \frac{\partial f_4}{\partial V} & \frac{\partial f_4}{\partial h} & \frac{\partial f_4}{\partial m} & \frac{\partial f_4}{\partial n} \end{bmatrix} \Big| \hat{x}_{(t)} = A(t)$$

$$B = \frac{\partial f}{\partial u}\Big|\hat{x}_{(t)} = \begin{bmatrix} \frac{1}{C_m} \\ 0 \\ 0 \\ 0 \end{bmatrix} \tag{6.11}$$

where $\hat{x}(t) = \begin{bmatrix} \hat{V}(t) & \hat{h}(t) & \hat{m}(t) & \hat{n}(t) \end{bmatrix}^T$. Now, in the following the derivatives of equation (6.10) are computed:

$$\frac{\partial f_1}{\partial V}\Big|_{\hat{x}(t)} = \frac{1}{C_m}[-g_{Na}\hat{m}^3\hat{h} - g_K\hat{n}^4 - g_L] \tag{6.12}$$

$$\frac{\partial f_1}{\partial h}\Big|_{\hat{x}(t)} = \frac{1}{C_m}[-g_{Na}\hat{m}^3\hat{h}_.(\hat{V}_. - V_{Na})] \qquad (6.13)$$

$$\frac{\partial f_1}{\partial m}\Big|_{\hat{x}(t)} = \frac{1}{C_m}[-3g_{Na}\hat{m}^2\hat{h}_.(\hat{V}_. - V_{Na})] \qquad (6.14)$$

$$\frac{\partial f_1}{\partial n}\Big|_{\hat{x}(t)} = \frac{1}{C_m}[-4g_.\hat{n}^3(\hat{V}_. - V_.)] \qquad (6.15)$$

The f_2 derivatives are

$$\frac{\partial f_2}{\partial V}\Big|_{\hat{x}(t)} = \frac{0.01\left(1 - \exp\left[-\frac{\hat{V}_. + 55}{10}\right]\right) - \frac{1}{10}\exp\left[-\frac{\hat{V}_. + 55}{10}\right]0.01(\hat{V}_{k.} + 55)}{(1 - \exp\left[-\frac{\hat{V}_. + 55}{10}\right])^2}(1 \qquad (6.16)$$

$$- \hat{n}_.) + \frac{1.125}{80}\exp\left[-\frac{\hat{V}_. + 65}{80}\right](\hat{n}_.)$$

$$\frac{\partial f_2}{\partial h}\Big|_{\hat{x}(t)} = 0 \qquad (6.17)$$

$$\frac{\partial f_2}{\partial m}\Big|_{\hat{x}(t)} = 0 \qquad (6.18)$$

$$\frac{\partial f_2}{\partial n}\Big|_{\hat{x}(t)} = \frac{0.01\left(\hat{V}_. + 55\right)}{1 - \exp\left[-\frac{\hat{V}_. + 55}{10}\right]} - 1.125\exp\left[-\frac{\hat{V}_. + 65}{80}\right] \qquad (6.19)$$

The f_3 derivatives are

$$\frac{\partial f_3}{\partial V}\Big|_{\hat{x}(t)} \tag{6.20}$$

$$= \frac{0.01\left(1 - \exp\left[-\frac{\hat{V} + 40}{10}\right](\hat{V} + 40)\right) - 0.1\left(-\exp\left[-\frac{\hat{V} + 40}{10}\right]\right) * 0.01(V + 40)}{(1 - \exp\left[-\frac{\hat{V} + 40}{10}\right])^2} (1$$

$$-\widehat{m}) + \frac{4}{18}\exp\left[-\frac{\hat{V} + 65}{18}\right](\widehat{m})$$

$$\frac{\partial f_3}{\partial h}\Big|_{\hat{x}(t)} = 0 \tag{6.21}$$

$$\frac{\partial f_3}{\partial m}\Big|_{\hat{x}(t)} = \frac{-0.01(\hat{V} + 40)}{1 - exp\left[-\frac{\hat{V} + 40}{10}\right]} - 4\,exp\left[-\frac{\hat{V} + 65}{18}\right] \tag{6.22}$$

$$\frac{\partial f_3}{\partial n}\Big|_{\hat{x}(t)} = 0 \tag{6.23}$$

The f_4 derivatives are

$$\frac{\partial f_4}{\partial V}\Big|_{\hat{x}(t)} = -\frac{0.07}{20}\exp\left[-\frac{\hat{V} + 65}{20}\right](1 - \hat{h}) - \frac{0.1\exp\left[-\frac{\hat{V} + 35}{10}\right]}{\left(1 + \exp\left[-\frac{\hat{V} + 35}{10}\right]\right)^2}(h) \tag{6.24}$$

$$\frac{\partial f_4}{\partial h}\Big|_{\hat{x}(t)} = 0.07\exp\left[-\frac{\hat{V} + 65}{20}\right] - \frac{1}{1 + \exp\left[-\frac{\hat{V} + 35}{10}\right]} \tag{6.25}$$

$$\frac{\partial f_4}{\partial m}\Big|_{\hat{x}(t)} = 0 \tag{6.26}$$

$$\frac{\partial f_4}{\partial n}\bigg|_{\hat{x}(t)} = 0 \tag{6.27}$$

Now, the extended Kalman filter algorithm can be applied (equations (6.4) to (6.7)) to the system using the above computations.

6.3.2 Fault detection using extended Kalman filter

The residual for fault detection using extended Kalman filter is computed as follows:

$$r(t)_{.} = y(t)_{.} - h\left(\hat{x}(t)\right)_{.} \tag{6.28}$$

Now, the Euclidean norm as $\|r(t)\|$ can be computed and compare it with a predefined threshold to specify a binary decision if a fault has occurred or not.

6.3.3 Simulation results

In this experiment an observer with extended Kalman filter on the neural model is applied to produce the response of a spiking neuron to an stimulation. The stimulus, $I_{stim}= 10$ μA/cm2, 50ms $\le$ t $\le$ 200ms, is considered as the injected current. There is no response between 0 second and 50 seconds to consider the behaviour of system during the non-stimulating time. The 200 ms time was obtained by using the trial and error method as the best time in the experiments.

As shown in Figure 6.5, the output of intracellular voltage (v) and the output of observed membrane voltage are shown with excellent accuracy. This figure, however, presents the output of the extended Kalman filter by estimating the parameters of the neural model.
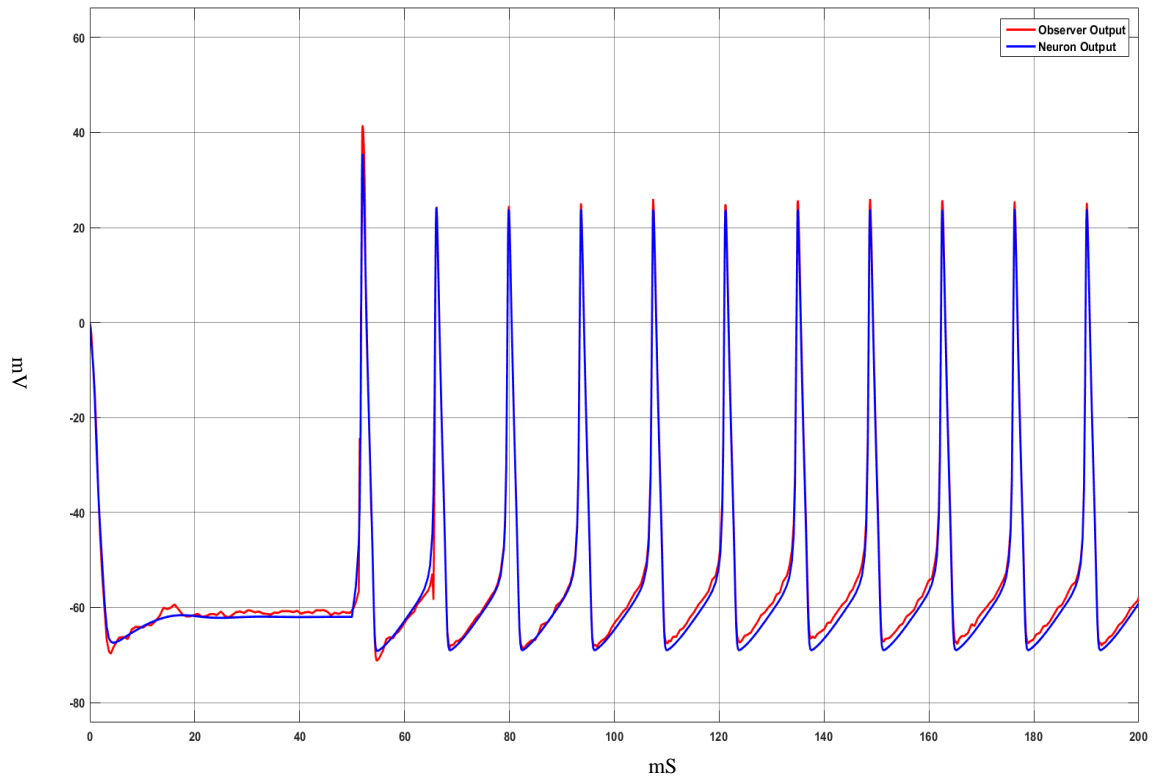
Figure 6.5 – Observed membrane vs. normal membrane
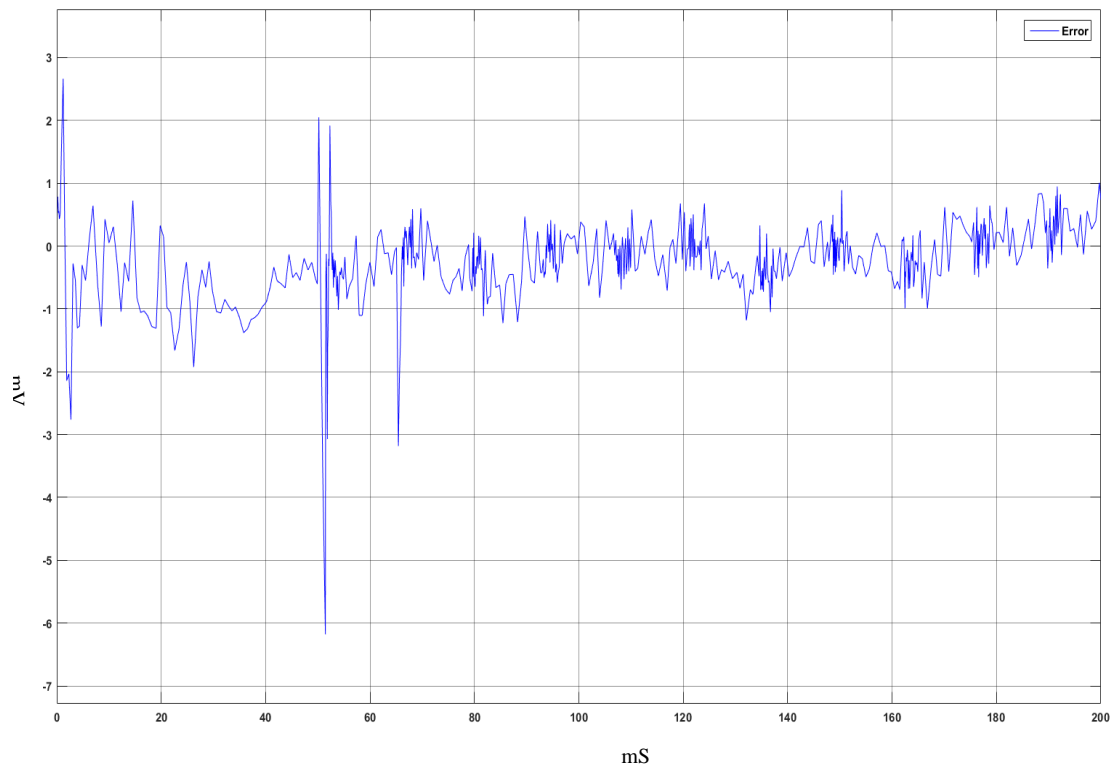
Figure 6.6 – Error of model when $G_{Na} = 120$. The nominal value of GNa = 120
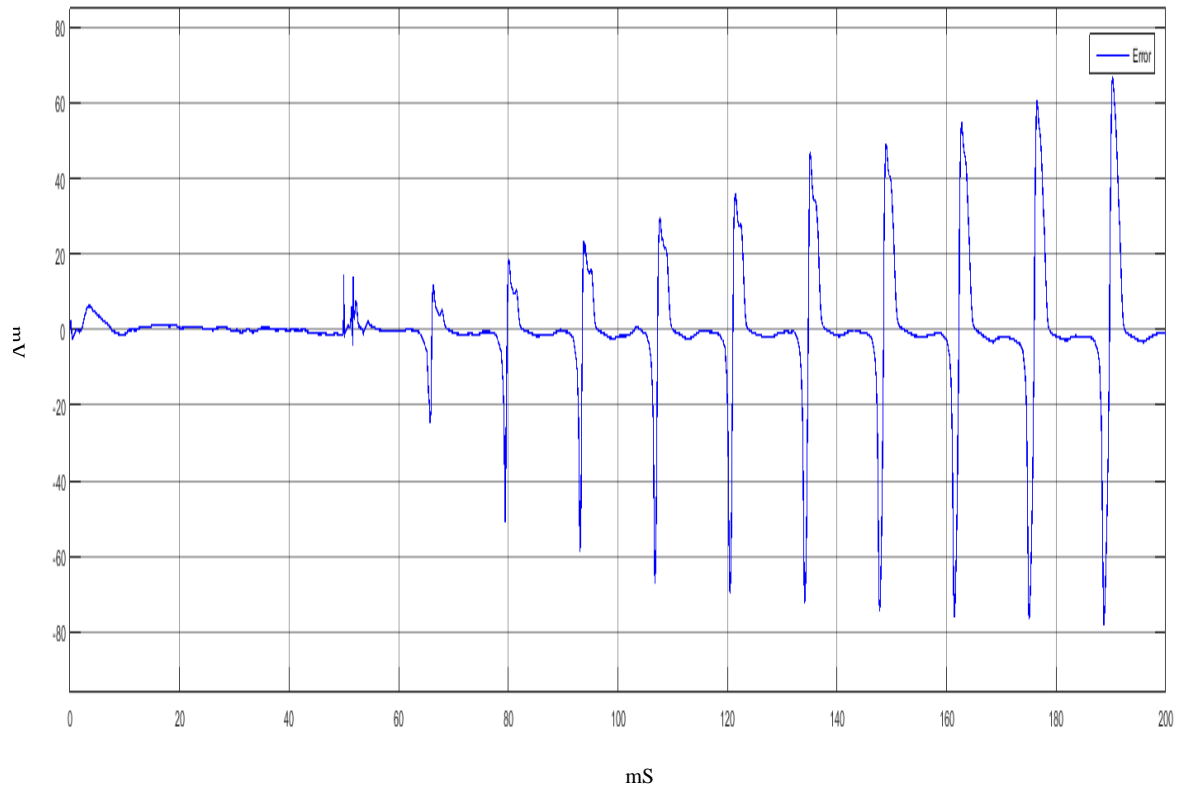
Figure 6.7 – The output estimation error of model when $G_{Na} = 121$. The nominal value of $G_{Na} = 120$

The output estimation error is shown in Figure 6.6 for the normal condition and in Figure 6.7 for a condition in which $G_{Na} = 121$. Here, this study has identified the threshold by trial and error. A fault is detected if the value of the residual exceeds the predefined threshold. The threshold was set at similar values to the previous observer. (Section 6.2). As shown in Figure 6.6 the value of error for nominal ($G_{Na} = 120$) does not exceed the specified thresholds while for the faulty condition in Figure 6.7, the error exceeds the threshold and a fault is detected.
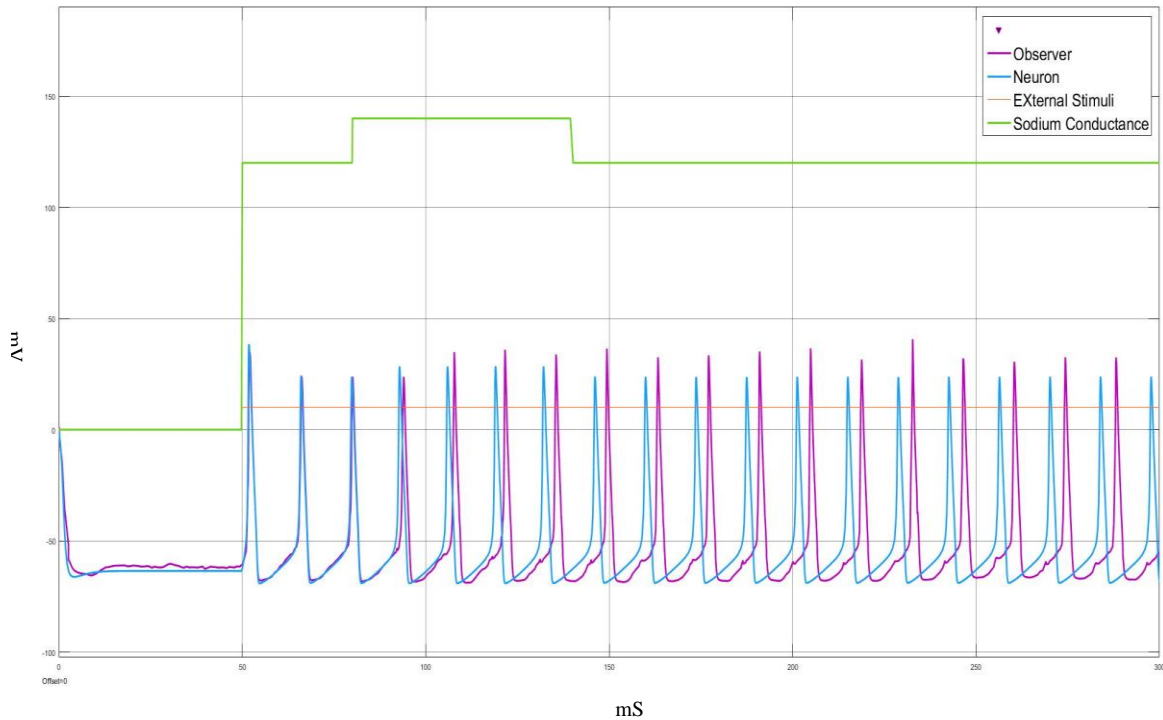
Figure 6.8 – The output of faults applied between the time 80 and 140 seconds for extended Kalman filter

A sequence of faults similar to the previous sequence was also injected here and the results are shown in figure 6.8. The properties of action potential before applying fault, during applying fault and after applying fault are presented in Table 6.5 to Table 6.7.

	Before Fault		During Fault		After Fault	
	Av. of Inter-spike Intervals (S)	Av. of Spike Amplitude (V)	Av. of Inter-spike Intervals (S)	Av. of Spike Amplitude (mV)	Av. of Inter-spike Intervals (S)	Av. of Spike Amplitude (mV)
EKF	13.58	24.58	13.77	25.575	13.73	29.38
Neuron	13.77	24.158	13.06	28.35	13.54	23.78
$\|r\|$	0.08	0.422	0.71	3.225	0.19	5.6

Table 6.5 –The properties of action potential for extended Kalman filter for G_Na=141

The same is done for $G_{Na} = 121$ and $G_{Na} = 130$ and the results are presented in Table 6.6 and Table 6.7.

163

	Before Fault		During Fault		After Fault	
	Av. of Inter-spike Intervals (S)	Av. of Spike Amplitude (mV)	Av. of Inter-spike Intervals (S)	Av. of Spike Amplitude (mV)	Av. of Inter-spike Intervals (S)	Av. of Spike Amplitude (mV)
EKF	13.80	25.08	13.36	26.7	13.78	25.0
Neuron	13.70	25.0	12.95	27.66	13.69	25.1
$\|r\|$	0.1	0.08	0.41	0.96	0.09	0.10

Table 6.6 –The properties of action potential for extended Kalman filter for G_Na=121

	Before Fault		During Fault		After Fault	
	Av. of Inter-spike Intervals (S)	Av. of Spike Amplitude (mV)	Av. of Inter-spike Intervals (S)	Av. of Spike Amplitude (mV)	Av. of Inter-spike Intervals (S)	Av. of Spike Amplitude (mV)
EKF	13.83	25.33	13.58	26.18	13.69	27.8
Neuron	13.76	24.57	12.81	27.37	13.59	24.18
$\|r\|$	0.07	0.76	0.77	1.19	0.1	3.62

Table 6.7 –The properties of action potential for extended Kalman filter for G_Na=130

6.4 Nonlinear observer by coordinate transformation

A nonlinear observer is referred to a dynamical system that receives the output or input measurements of the system to process an estimation of the nonlinear system states (Delgado, et al., 2005). Non-linear observers are more needed to identify the fault for dynamic systems. Since the majority of processes in the world around us are non-linear therefore applying linear observers reduces the efficiency of fault detection algorithms due to linearization errors. A design method for nonlinear observers was proposed in Delgado, et al. (Delgado, et al., 2005). In this work, an observer is proposed for nonlinear systems that can be transformed simply into the normal form. The method for obtaining a neural observer for non-linear systems involves two steps.

In the first stage, the input or output reaction is recognized with the dynamic neural system. In the next stage and after training dynamic neural system the observer can be designed for the neural model. At this stage, the inverse of the injective map is applied to measure the state vector of the original system from the state vector of the neural

164

observer. The inverse of the injective map transforms the nonlinear system into the neural model.

6.4.1 Proposed observer for the model of neuron

Consider the following nonlinear system:

$$\dot{x} = f(x) + g(x).u \tag{6.29}$$

$$y = h(x)$$

Where, x is the state vector, $f(x)$ and $g(x)$ are smooth vector fields. $h(x)$ is a smooth scalar field. y is the output and u is the input. A nonlinear system has a relative degree r if the input $u(t)$ emerges explicitly r times after differentiating the output $y(t)$ with respect to time. In the above system, the maximum relative degree is $r = n$ at the origin if the output and derivatives of output can be written as follow:

$$y = h(x) \tag{6.30}$$

$$\dot{y} = L_f h(x)$$

$$.$$

$$.$$

$$y^{n-1} = L_f^{n-1} h(x)$$

$$y^n = L_f^n h(x) + L_g L_f^{n-1} h(x).u$$

where at the origin $L_g L_f^{n-1} h(x) \neq 0$.

$L_f h(x) = \frac{\partial h(x)}{\partial x}.f(x) = dh(x).f(x)$ is Lie derivative of the scalar field $h(x)$ along the vector field $f(x)$. For higher order Lie derivatives someone can use $L_f^k h(x) = L_f(L_f^{k-1} h(x))$ with $L_f^0 h(x) = h(x)$.

Consider system (1) with relative degree $r = n$ around origin then the coordination bellow has a Jacobian matrix as follows:

$$\begin{bmatrix} z_1 \\ z_2 \\ . \\ . \\ z_n \end{bmatrix} = \begin{bmatrix} \varphi_1(x) \\ \varphi_2(x) \\ . \\ . \\ \varphi_n(x) \end{bmatrix} = \begin{bmatrix} h(x) \\ L_f h(x) \\ . \\ . \\ L_f^{n-1} h(x) \end{bmatrix} \qquad (6.31)$$

The above coordinate transformation can be written in compact form as $z = \varphi(x)$ and the inverse $x = \varphi^{-1}(z)$ with $\varphi(0) = 0$. By applying the above coordinate transform, system (6.29) transforms into the following form:

$$\dot{z} = A.z + F_a(z) + F_b(z).u \qquad (6.32)$$

$$y = c.z$$

where,

$$A = \begin{bmatrix} 0 & 1 & 0 & .. & 0 \\ 0 & 0 & 1 & .. & 0 \\ : & : & : & \backslash & : \\ & & & .. & 1 \\ 0 & 0 & 0 & .. & 0 \end{bmatrix},$$

$$F_b(z) = \begin{bmatrix} 0 \\ 0 \\ . \\ 0 \\ a(z_1, \ldots, z_n) \end{bmatrix},$$

$$F_b(z) = \begin{bmatrix} 0 \\ 0 \\ . \\ 0 \\ b(z_1, \ldots, z_n) \end{bmatrix},$$

the nonlinear functions are:

166

$$a(z_1, \dots, z_n) = L_f^n h(x)|_{x=\varphi^{-1}(z)} \tag{6.33}$$

$$b(z_1, \dots, z_n) = L_g L_f^{n-1} h(x)|_{x=\varphi^{-1}(z)}$$

A neural observer for system (6.32) is given by bellow:

$$\dot{\xi} = A.\xi + F_a(\xi) + k.(\hat{y} - y_0) + F_b(\xi).u \tag{6.34}$$

$$y_0 = cz$$

where $\xi \in R^n$, $y_0 \in R$

$$A = \begin{bmatrix} 0 & 1 & 0 & .. & 0 \\ 0 & 0 & 1 & .. & 0 \\ : & : & : & \backslash & . \\ & & & .. & 1 \\ 0 & 0 & 0 & .. & 0 \end{bmatrix},$$

$$F_a(\xi) = \begin{bmatrix} 0 \\ 0 \\ . \\ 0 \\ T_a(\xi_1, \dots, \xi_n) \end{bmatrix},$$

$$F_b(\xi) = \begin{bmatrix} 0 \\ 0 \\ . \\ 0 \\ T_b(\xi_1, \dots, \xi_n) \end{bmatrix},$$

$$k = \begin{bmatrix} k_1 \\ k_2 \\ . \\ . \\ k_n \end{bmatrix},$$

$$c = [1 \ 0 \ . \ . \ . \ 0]$$

To find the error $e = z - \xi$ is needed and it satisfies:

$$\dot{e} = (A - k.c).e + \{F_a(z) - F_a(\xi)\} + \{F_b(z) - F_b(\xi)\}.u \qquad (6.35)$$

6.4.2 Applying nonlinear observer by coordinate transformation on neural model

Following equation (6.29) and the Hodgkin-Huxley model:

$$\frac{dV}{dt} = \underbrace{\frac{1}{C_m} [-g_{Na}m^3h\,(V - V_{Na}) - g_k n^4\,(V - V_k) - g_l\,(V - V_l)]}_{f\,(x),\,x\,=\,V} + \underbrace{\underbrace{\frac{1}{C_m}}_{g\,(x)} \underbrace{.I_{inj}}_{u}}$$

$$y = V(t) = h(t)$$

As in this condition our related degree becomes 1 therefore:

$$n = 1 \Rightarrow r = n = 1$$

now following equation (6.31) :

$$z_1 = \varphi_1(x) = h\,(x) = V$$

following equations (6.32) and (6.33)

$$F_a(z) = a\,(z_1) = L_f^1 v = \frac{\partial h}{\partial V}\,.\,f\,(x) = \frac{\partial V}{\partial V}\,.\,f\,(x) = f\,(x)$$

and

$$F_b(z) = b\,(z_1) = L_g\,L_f^0\,h(x) = L_g.V = \frac{\partial V}{\partial V}\,g(x) = g(x) = \frac{1}{C_m}$$

and

A = 0

then following (6.32):

$$\dot{z} = 0.z_1 + F_a(z) + F_b(z).u \Rightarrow \dot{z} = f(z) + \frac{1}{C_m}.u$$

$$y = c.z \Longrightarrow y = 1.V = V$$

now someone can implement the observer for our system. Following equation (6.34)

$$\dot{\xi} = 0.\xi + f(\xi) + K(c\xi - cz) + \frac{1}{C_m}.u$$

the 'k' is not known, therefore following equation (6.35)

$$e = z - \xi$$

and then

$$\dot{e} = (A - Kc).e + \{f(z) - f(\xi)\} + \left\{\frac{1}{C_m} - \frac{1}{C_m}\right\}u$$

then the following is obtained:

$$\dot{e} = (-Kc)e + \left(-\frac{1}{C_m}(g_{Na}m^3h + g_k n^4 + g_l)z + \frac{1}{C_m}g_{Na}m^3hV_{Na} + \frac{1}{C_m}g_k n^4 V_k\right.$$

$$+ \frac{1}{C_m}g_l V_l\right) - \left(-\frac{1}{C_m}(g_{Na}m^3h + g_k n^4 + g_l)\xi + \frac{1}{C_m}g_{Na}m^3hV_{Na}\right.$$

$$+ \frac{1}{C_m}g_k n^4 V_k + + \frac{1}{C_m}g_l V_l\right)$$

$$= -kce - \underbrace{\frac{1}{C_m}(g_{Na}m^3h + g_k n^4 + g_l)}_{p}\underbrace{(z - \xi)}_{e}$$

$$= -e(kc + p)$$

then

$$\frac{de}{e} = (-kc - P)\,dt \implies \int \frac{de}{e} = \int(-kc - p)dt \implies Ln\, e = (-kc - p)t + c_1$$

then

$$e(t) = Exp((-kc - p)t + c_1) = Exp(c_1).Exp((-kc - p)t)$$

when $t \to \infty$ then $e \to 0$ and it's the stability of observer. On the other hand when $t \to \infty$

if $(-kc - p) < 0$ then $e^\infty \to 0$. If, $kc > p \implies k > \frac{p}{c} \implies k > p$, as a result for any

$k > p$ the observer is stable and it convergent to real value and it means:

$$z - \xi \to 0 \Rightarrow \xi \to z$$

hence

$$\frac{de}{e} = -(kc + p)dt$$

$$e(t) = Exp((-kc - p)t + c1)$$

6.4.3 Simulation results

In this experiment, a neural model with the same specifications as in previous experiments is applied to produce the response of a spiking neuron to a stimulation. The stimulus, $I_{stim}= 10 \ \mu A/cm2$, $50ms \le t \le 200ms$, is considered as the injected current.
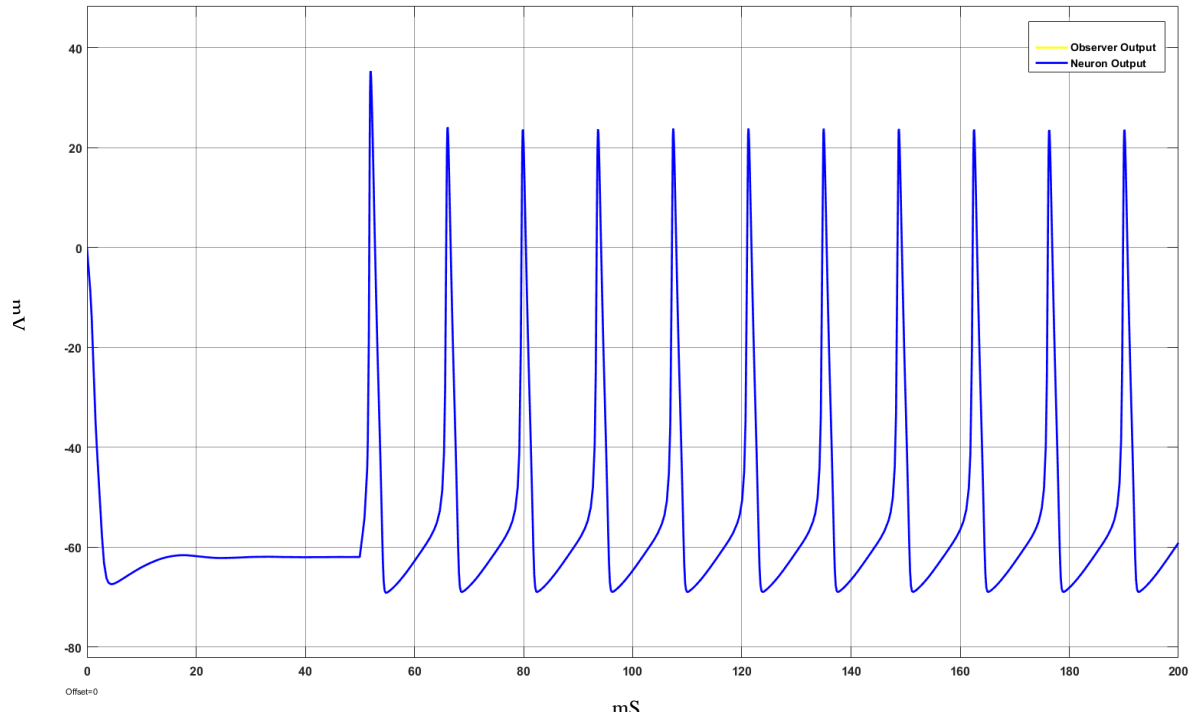
Figure 6.9 – Observed membrane vs. normal membrane

As shown in Figure 6.9, the output of intracellular voltage (v) and the output of observed membrane voltage with excellent accuracy have been shown.
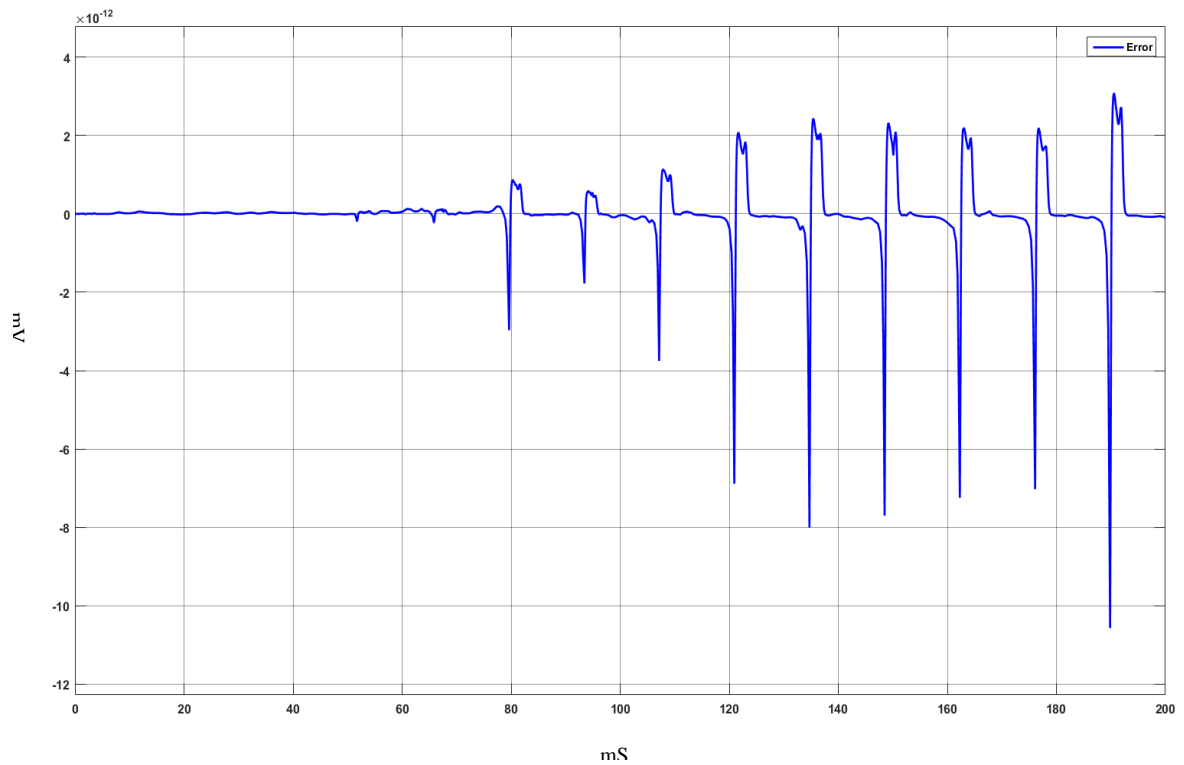
Figure 6.10 – Error of model when G_{Na} = 120. The nominal value of GNa = 120
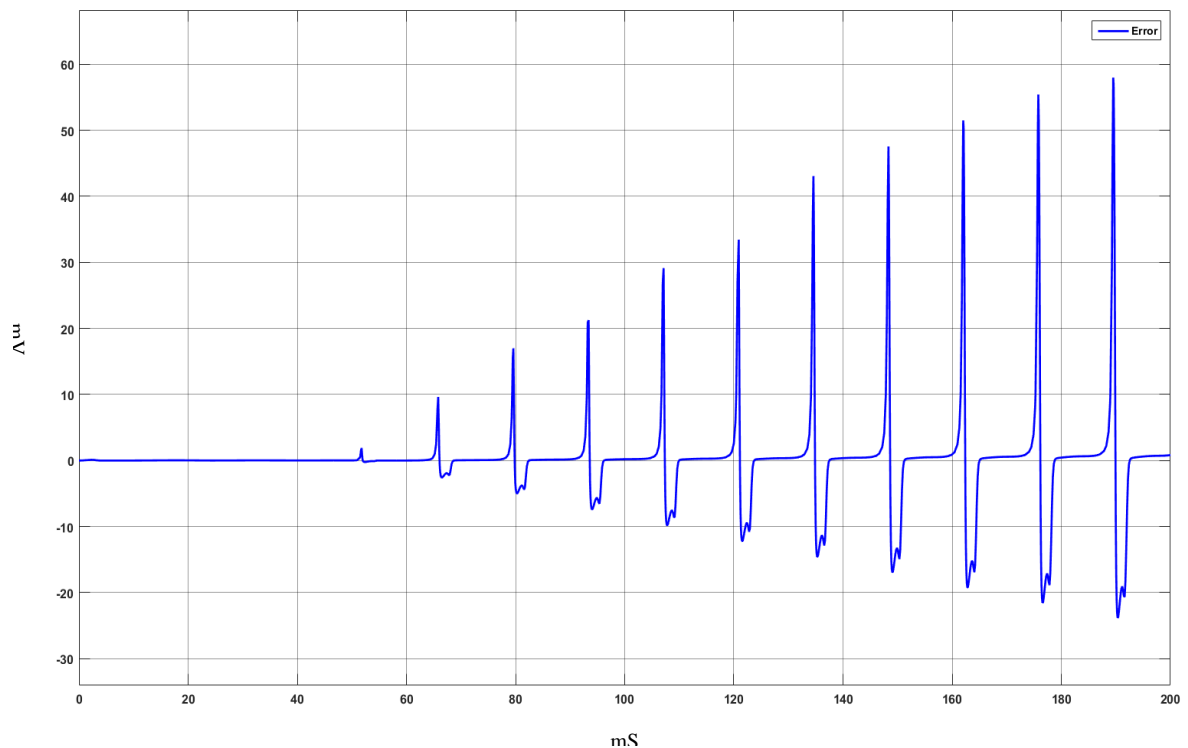
Figure 6.11 – The output estimation error of model when G_{Na} = 121. The nominal value of G_{Na} = 120

The output estimation error is shown in Figure 6.10 for normal condition and in Figure

Figure 6.11 for a condition which G_{Na} = 121. Here, this study has identified the threshold

171

with the trial and error method. A fault is detected if the value of the residual exceeds the predefined threshold. The threshold is considered as error > 20 mV or error $<- 20$ mV through trial and error method.
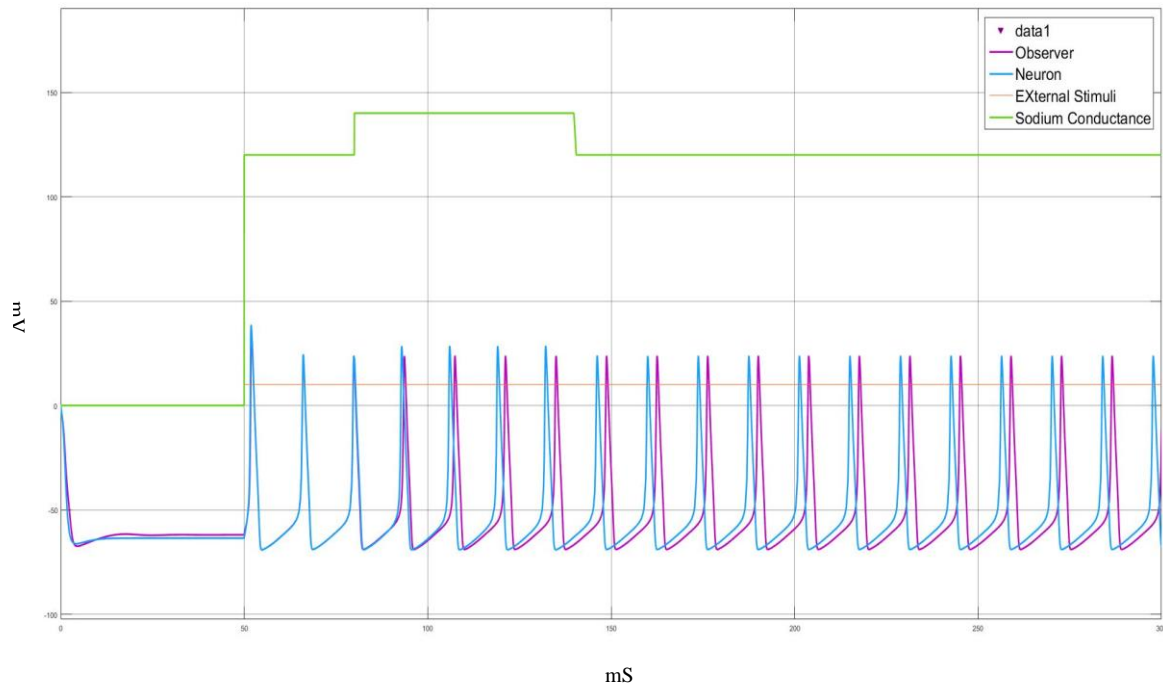
Figure 6.12 – The output of faults applied between the time 80 and 140 seconds for nonlinear observer by coordinate transformation

A sequence of faults similar to the previous sequence in section 6.2.4 and section 6.3.3 was also injected here and the results are shown in figure 6.12. The properties of action potential before applying fault, during applying fault and after applying fault are presented in Table 6.8 to Table 6.10.

	Before Fault		During Fault		After Fault	
	Av. of Inter-spike Intervals (S)	Av. of Spike Amplitude (mV)	Av. of Inter-spike Intervals (S)	Av. of Spike Amplitude (mV)	Av. of Inter-spike Intervals (S)	Av. of Spike Amplitude (mV)
Nonlinear	13.85	24.12	13.8	23.7	13.8	23.74
Neuron	13.84	24.12	13.09	28.4	13.96	23.77
$\|r\|$	0	0	0.71	4.7	0.16	0.03

Table 6.8 –The properties of action potential for nonlinear observer by coordinate transformation for G_Na=141

The same is done for $G_{Na} = 121$ and $G_{Na} = 130$ and the results are presented in Table 6.9 and Table 6.10.

	Before Fault		During Fault		After Fault	
	Av. of Inter-spike Intervals (S)	Av. of Spike Amplitude (mV)	Av. of Inter-spike Intervals (S)	Av. of Spike Amplitude (mV)	Av. of Inter-spike Intervals (S)	Av. of Spike Amplitude (mV)
Nonlinear	13.81	24.0	13.83	23.8	13.78	24.12
Neuron	13.81	24.0	13.45	24.23	13.77	24.14
$\|r\|$	0	0	0.38	0.43	0.01	0.02

Table 6.9 –The properties of action potential for nonlinear observer by coordinate transformation for G_Na=121

	Before Fault		During Fault		After Fault	
	Av. of Inter-spike Intervals (S)	Av. of Spike Amplitude (mV)	Av. of Inter-spike Intervals (S)	Av. of Spike Amplitude (mV)	Av. of Inter-spike Intervals (S)	Av. of Spike Amplitude (mV)
Nonlinear	13.79	24	13.81	23.79	13.8	24.0
Neuron	13.79	24	13.2	26.45	13.875	23.96
$\|r\|$	0	0	0.61	2.66	0.075	0.04

Table 6.10 –The properties of action potential for nonlinear observer by coordinate transformation for G_Na=130

6.5 Discussion

The application of observers is useful not only in system monitoring and regulation but also for detecting faults in any dynamical systems. Most observer designs are based on a mathematical model; therefore when designing a fault detection methodology, care must be given to distinguish between faults and the natural disturbances which occur.

This is often taken care of by using the threshold. From earlier sections it is clear, by setting the threshold at 20mV, disturbances would be excluded from the fault detection and genuine faults are detected. From Figures 6.3, 6.7 and 6.11 it can be seen that a small fault in sodium is detected.

A Kalman filter as a linear observer was first applied to our neural model. Then, extended Kalman was also applied to the model and finally nonlinear observer by coordinate transformation applied. In each case the performance of the observer is studied for different magnitudes of faults. From the results it is clear, that even after the fault has been removed the error in the observer and the neuron persist way above the threshold. The response of a neuron to a stimulus is characterised by both the inter-spike interval and the magnitude of the spikes. Thus it is reasonable to have two fault signatures when a fault occurs. This is in line with the results from Chapters 3 and Chapter 4. Thus the fault signature is simply not the differences between the magnitude of the spikes between the observer and the neuron, but must include the inter-spike interval as well. With each of the observers the sequence of changes to sodium was the same, and in each before the fault was introduced the differences in the time and the magnitude of the spikes was negligible. Once a fault has been introduced, the residual allowed the detection of the fault, however when the fault was removed the spike trains from the observer and the neuron exhibited a difference. This can be seen from the graphs and Tables 6.2 to Tables 6.11. This is as a result of the change in the spike intervals in the neuron which shifted the spike, while those in the observer remained the same. As can be seen from tables the two characteristics return to their original values when a fault in sodium levels is injected. In order to assess the method further, different levels of faults in sodium were tested. These are shown in Tables 6.2 to Tables 6.10. The faults are detected properly during the fault occurrence. Tables 6.2 and 6.4 show that as the level of faults become bigger the

behaviour of system after fault occurrence becomes more unstable (see Figure 6.4). As it can be seen in Table 6.2 to Table 6.4 the Kalman filter has an acceptable performance in counter of low range of faults but its performance for large faults is not acceptable.

The extended Kalman filter (see Table 6.5 to 6.7) exhibits a similar behaviour and can be seen in Table 6.5 to Table 6.7 and Figure 6.8. The results show that the observer based on the EKF works well for low and intermediate levels of faults. By considering the values of Table 6.7 and 6.5 it can be seen that the output of residuals in fault free conditions is much bigger than faulty conditions.

The results of nonlinear observer, which is based around a globally linearization strategy, are presented in Tables 6.8 to 6.10. The same range of faults are applied here as well. It can be seen from the results (see Tables 6.8 to 6.10 and Figure 6.12) the faults are detected, and the behaviour of the observer is such that it is able to track the neuron well.

From the results it can be seen that both the Kalman filter and extended Kalman filter performance deteriorates as the level of fault magnitudes are increased. A reason for this is that with the linear version of the filter or the extended version, both use a form of locally linearization. This therefore does not allow for large changes in the parameters of the system (neuron). These results will be similar for all levels of faults, unless the observer is an adaptive observer (Zhang, et al., 2008). However, this is computationally expensive. On the other hand the process of the nonlinear system through coordinate transformation linearizes the system globally, and is thus more effective.

7 Conclusion

7.1 Introduction

This chapter provides a summary of the thesis, with conclusions that have been drawn from the results of the project. It also highlights the novel contributions of this project from the computational neuroscience point of view including the practical implications of the project.

7.2 Research contributions and discussion

The significance and the contributions of this project can be assessed from medical and computational points of view. The results have not only prepared research on the symptoms and causes of neurodegenerative diseases like Alzheimer's disease but also highlighted those crucial moments where computational intelligence could play a remarkable role in detection of the advancement of these kinds of disease. In addition, the results have pointed to ways of deriving optimum benefits from the fields of computation, mathematics, biology, and neuroscience. In addition to all of these, the research has found significant symptoms that can be applied as biomarkers for early detection of Alzheimer's disease.

The following are the main contributions of the thesis:

- **The impact of ion gradients in exacerbating neurodegenerative diseases**

In Chapter 3, the study has highlighted the role of ion imbalances in neural activities and shown that ion imbalances can make neurodegenerative diseases worse. It has been shown that ionic imbalances in patients with neurodegenerative diseases can lead to serious disturbances in the nervous system or even death of neurons. Therefore, it was shown in a computational form that the role of ion balance in patients with neurodegenerative diseases is crucial.

- **Ion gradient and its impact on basic features of electric signalling of neuron**

The basic features of action potential, i.e. peak and resting membrane potential, have a direct relation with sodium and potassium concentrations such that increased potassium level leads to the increase of resting membrane potential and decreased potassium level has the opposite effect. Changes in sodium levels do not have significant effects on resting levels of membrane potential. However, increased sodium level leads to an increase in amplitude and decreased sodium level has the opposite effect. Chapter 3 has shown these results. The rate of these changes can help us to find a solution to stabilize changes in neuron signalling in neurodegenerative diseases.

- **The region of synchronicity**

Using mathematical relations like the generalized form of neurons and coupled type equations and the results of experiments on coupled neurons, this study obtained a relation that is essential for synchronicity in the nervous system. In entirely normal conditions if a neuron is stimulated only by presynaptic potential and it does not receive any other stimuli from other neurons to produce synchronisation between any two neurons, the minimum condition should be $I_c \geq \frac{I_{inj1}}{2}$ where I_c is coupling conductance between two neurons.

- **Increasing the coupling conductance leads to further synchronisation in the network of neurons**

Chapter 4 has shown that as coupling conductance is increased, synchronisation is more triggered. After further coupling conductance, increasing action potentials coincide with each other, except for slight defects. As the results show, by picking sufficiently large coupling conductance, cell synchronisation occurred. The results indicate how any changes in the coupling conductance can drive the neurons into different degrees of synchronisation. This is a computational proof that adjusting coupling conductance in neurodegenerative diseases like Alzheimer's by developing appropriate medications can improve the symptoms of the disease.

- **The nervous system is more sensitive to potassium changes than sodium changes.**

In Chapter 4, it was shown that, during the combination of sodium and potassium imbalances, the conditions led to the properties of potassium concentration. This means that important features of an action potential, such as the rates of rising of the action potential, its peak amplitude, and duration, are more dependent on the properties of potassium.

- **A computational model for amyloid channels**

In Chapter 5 a computational model for amyloid beta channels was presented. As was evident from the Alzheimer's pathology, amyloid accumulation in the synaptic space is a primary stage of Alzheimer's development. Therefore, focusing on the model of Aβ channels can lead us to early diagnosis or even treatment of Alzheimer's. Aβ channels are permeable to cations including sodium and potassium, as far as these channels have been identified as cation channels.

This study has shown that abnormal levels of ions like sodium and potassium in neurons cause the ionic imbalance that is linked to Alzheimer's disease pathogenesis.

- **Applying fault detection in the computational model of the neuron to detect NDDs**

    Neurodegenerative diseases like Alzheimer's disease are considered to be due to a fault in the neuron. In Chapter 6 observer-based residual generation for detection of Alzheimer's disease was considered for fault detection. In addition, the performance of Kalman filter, extended Kalman filter and neural observer by coordinate transformation in observer based residual generation was compared. It is shown that the faults in the neuron have two signatures when a fault occurs i.e. the inter-spike interval and the magnitude of the spikes.

7.3   Concluding Remarks

The main problem of neurodegenerative diseases is that these diseases are not curable (so far) and hard to detect in the very early stage of disease as these diseases do not have obvious symptoms. Moreover, these diseases are very hard to distinguish in the next stage because of similarities between different neurodegenerative diseases as well as symptoms of normal ageing. Because there are no valid methods for recognizing such diseases; scientists are extremely keen to find hidden patterns that can be useful in the early diagnosis of neurodegenerative diseases. The results of this research project have highlighted the significance of computational neuroscience and artificial intelligence in the early detection of these kinds of diseases, like Alzheimer's disease. This research has demonstrated the problems with the early detection of neurodegenerative diseases like

Alzheimer's disease and offered feasible solutions. The role of beta-amyloid in the pathogenesis of Alzheimer's disease and the abnormalities of these channels in creating the ionic imbalance that causes impairment of neuronal signalling function were presented using the computational model and simulation. Results of experiments are demonstrated and validated by other prestigious research in neurology, neuroscience and biology. In addition, this research has proposed and demonstrated a novel idea for treating neurodegenerative diseases using changes of coupling and synchronisation in the neural activities. The results of the research project have demonstrated novel and significant findings that can be applied in clinical practice for early detection and treatment of Alzheimer's disease.

7.4 Future work

In addition to the main novel contributions that have been demonstrated in previous chapters, this study hereby, demonstrates extensions and feasible solution that might support to amend and develop the shortcomings. This chapter highlights the feasible extensions of our research project using machine learning and data mining techniques to clinical applications.

- **Finding the brain waves change rates using Brain-Computer Interface (BCI)**
  The change of the neuron from a healthy state to an unhealthy state leads to gradual death of the neuron. This period of changes is typically observed in many disorders such as neurological diseases include Alzheimer's Disease (AD), Parkinson's Disease (PD), and Motor Neuron Diseases. At the onset of the disease, the neuron starts to change in neural spiking and its function. This changes can be observed in the dynamics of the neuron.

One future augmentation of this research project is designing Brain-Computer Interface (BCI) which finds the rate of changes in brain waves due to beta-amyloid secretion in order to apply on electroencephalogram machines.

- **Applying machine learning to detect NDDs using neurons signal changes**

Although there are very accurate tests for patients with NDDs but there are not good tests in order to detect diseases in very early stage or even future NDDs like Alzheimer's (Bondi, et al., 2017). Machine learning has entered into the field of diagnosis in medicine, therefore, it can have a lot of benefits in finding a comprehensive solution to this. Nowadays this branch of artificial intelligence can predict various crucial diseases like Brain Strokes or Heart Attacks even more accurately and better than any expert. But, what someone can do about NDDs? Techniques in machine learning over the past decades are significant for the prognosis and diagnosis of neurological disorders, particularly for Alzheimer's disease.

Diagnosis of the disease years before causing damage to the nerve cells or even cells death still haven't been identified easily by a simple neuropsychological evaluation. Amyloid-beta ($A\beta$) peptide is a great help on this path. Accumulation and aggregation of amyloid-beta ($A\beta$) peptide in the brain extracellular space makes changes in the function of brain, especially in the electromagnetic activities and rhythms of the brain (Babiloni, et al., 2016). Following these changes the brain activity is changed and it affects the nerve cells signaling (Sadegh-Zadeh & Kambhampati, 2018). Research confirms that at the beginning of the secretion of amyloid-beta (Aβ) peptide in the extracellular of neurons, the brain rhythms have shown changes (Babiloni, et al., 2016).

8 References

Aattay, f. & Aberham, M., 1993. Modeling axon membranes for functional electrical stimulation. *IEEE Trans Biomed Eng,* pp. 1201-1209.

Abbracchio, M., Burnstock, G., Verkhratsky, A. & Zimmermann, H., 2009. Purinergic signaling in the nervous system: An overview. *Trends in Neurosciences,* Volume 32, p. 19–29.

Adrian, E. D., 1914. The all-or-none principle in nerve. *The Journal of physiology,* 47(6), pp. 460-474.

Ahmed, J. A., 1997. An intracellular study of the contrast-dependence of neuronal activity in cat visual cortex. *Cerebral Cortex,* 7(6), pp. 559-70.

Amthor, F., Oyster, C. & Takahashi, E., 1984. Morphology of on-off direction-selective ganglion cells in the rabbit retina. *Brain Res,* 298(Brain Res), p. 187–190.

Andlin-Sobocki, P., Jonsson, B., Wittchen, H.-U. & Olesen, J., 2005. Cost of disorders of the brain in Europe. *European Journal of Neurology,* pp. 1-27.

Andreas, J. & Bowser, R., 2017. Biomarkers in Neurodegenerative Diseases. *Neurodegenerative Diseases, Springer,* Volume 15, pp. 491-528.

Arcuri, C., 2017. The Pathophysiological Role of Microglia in Dynamic Surveillance, Phagocytosis and Structural Remodeling of the Developing CNS. *Front Mol Neurosci,* 10(191).

Arenas, A., Brenner, R. & C., F. R., 1986. Temporal slowing in the elderly revisited. *Am J EEG Technol,* Volume 26, pp. 105-114.

Ariano, M., 2005. Striatal potassium channel dysfunction in Huntington's disease transgenic mice. *Journal of Neurophysiology,* Volume 93, p. 2565–2574.

Arispe, N., C.Diaz, J. & Simakova, O., 2007. Aβ ion channels. Prospects for treating Alzheimer's disease with Aβ channel blockers. *Biochimica et Biophysica Acta (BBA) - Biomembranes,* 1768(8), pp. 1952-1965.

Arispe, N., Pollard, H. & Rojas, E., 1993. Giant multilevel cation channels formed by Alzheimer disease amyloid beta-protein [A beta P-(1-40)] in bilayer membranes. *National Acad Sciences,* 90(22), pp. 10573-10577.

Arispe, N., Rojas, E. & Pollard, H., 1993. Alzheimer disease amyloid beta protein forms calcium channels in bilayer membranes: blockade by tromethamine and aluminum. *Proceedings of the National Academy of Sciences,* 90(2), pp. 567-571.

Awasthi, M., 2017. Computational Approaches for Therapeutic Application of Natural Products in Alzheimer's Disease. *Computational Modeling of Drugs Against Alzheimer's Disease,* Volume 132, pp. 483-511.

Babilonia, C., 2009. Hippocampal volume and cortical sources of EEG alpha rhythms in mild cognitive impairment and Alzheimer disease. *NeuroImage,* p. 123–135.

Babiloni, C., 2016. Brain neural synchronization and functional coupling in Alzheimer's disease as revealed by resting state EEG rhythms. *Int J Psychophysiol,* Volume 103, pp. 88-102.

Bacak, B., Segaran, J. & Molkov, Y., 2016. Modeling the effects of extracellular potassium on bursting properties in pre-Bötzinger complex neurons.. *Journal of Computational Neuroscience,* 40(2), pp. 231-245.

Ballard, C., 2011. Alzheimer's disease. *Lancet,* Volume 377 , p. 1019–31.

Ballarini, T., 2016. Neuropsychiatric subsyndromes and brain metabolic network dysfunctions in early onset Alzheimer's disease. *Human Brain Mapping,* 37(12), p. 4234–4247.

Baravalleab, R., Rossocde, O. & Montani, F., 2017. A path integral approach to the Hodgkin–Huxley model. *Physica A: Statistical Mechanics and its Applications,* Volume 486, pp. 986-999.

Barnett, M. & Larkman, P., 2007. The action potential. *Practical Neurology,* Volume 7, p. 192–197.

Batistaa, C., Lopesa, S., Vianaa, R. & Batistab, A., 2010. Delayed feedback control of bursting synchronization in a scale-free neuronal network. *Neural Networks,* 23(1), p. 114–124.

Berridge, M., 2014 . Calcium regulation of neural rhythms, memory and Alzheimer's disease. *J Physiol,* 592(2), pp. 281-93.

Bondi, M., Edmonds, E. & Salmon, D., 2017. Alzheimer's Disease: Past, Present, and Future. *Journal of the International Neuropsychological Society,* 23(9-10), pp. 818-831.

Borgesa, R., 2016. Effects of the spike timing-dependent plasticity on the synchronisation in a random Hodgkin–Huxley neuronal network. *Communications in Nonlinear Science and Numerical Simulation,* Volume 34, p. 12–22.

Boundless, 2105. *Nerve Impulse Transmission within a Neuron: Action Potential.*

Braak, H. & Braak, E., 1991. Neuropathological stageing of Alzheimer-related changes. *Acta Neuropathologica,* 82(4), p. 239–259.

Brenowitz, S., Duguid, I. & Kammermeier, P. J., 2017. Ion Channels: History, Diversity, and Impact. *Cold Spring Harbor Protocols,* 2017(7).

Brette, R., 2007. Simulation of networks of spiking neurons: A review of tools and strategies. *Journal of Computational Neuroscience,* 23(3), pp. 349-398.

Brookmeyera, R., Johnsona, E., Ziegler-Grahamb, K. & Arrighic, M., 2007. Forecasting the global burden of Alzheimer's disease. *Alzheimer's & Dementia,* p. 186–191.

Brookmeyera, R., Johnsona, E., Ziegler-Grahamb, K. & Arrighic, M., 2007. Forecasting the global burden of Alzheimer's disease. *Alzheimer's & Dementia,* p. 186–191.

Burns, A. & Iliffe, S., 2009. Alzheimer's disease. *BMJ,* Volume 338.

Busche, M., 2008. Clusters of hyperactive neurons near amyloid plaques in a mouse model of Alzheimer's disease. *Science,* 321(5896), pp. 1686-9.

Canale, C., Oropesa-Nuñezac, R. & Dantea, S., 2018. Amyloid and membrane complexity: The toxic interplay revealed by AFM. *Seminars in Cell & Developmental Biology,* Volume 73, pp. 82-94.

Carlson, N. R., 2007. *Foundations of Physiological Psychology.* New York: Pearson.

Chandola, V., Banerjee, A. & Kumar, V., 2009. Anomaly detection: A survey. *ACM Computing Surveys (CSUR).*

Chappell, M. & Payne, S., 2016. The Action Potential. Physiology for Engineers. *Springer International Publishing,* Volume 13, pp. 33-41.

Chow, E. & Willsky, A., 1984. Analytical redundancy and the design of robust failure detection systems. *IEEE Trans. Automatic Control,* 29(3), pp. 603-614.

Cibils, D., 2002. Dementia and qeeg (alzheimer's disease). *Supplements to Clinical Neurophysiology,* Volume 54, pp. 289-294.

Clark, R., 1978. A simplified instrument failure detection scheme. *IEEE Trans. Aerospace and Electronic Systems,* 14(4), pp. 558-563.

Cleeremans, A., 2014. Connecting Conscious and Unconscious Processing. *Cognitive Science,* 38(6), pp. 1286-1315.

Coben, L., Danziger, W. & Berg, L., 1983. Frequency analysis of the resting awake eeg in mild senile dementia of alzheimer type. *Electroencephalography and clinical neurophysiology,* 55(4), pp. 372-380.

Cristina, P. et al., 2011. Ploia, Cristina, et al. "JNK plays a key role in tau hyperphosphorylation in Alzheimer's disease models.. *Journal of Alzheimer's Disease,* 26(2), pp. 315-329.

Cummings, J., Vinters, H., Cole, G. & Khachaturian, Z., 1998. Alzheimer's disease Etiologies, pathophysiology, cognitive reserve, and treatment opportunities. *Neurology,* pp. S2-S17.

Delgado, A., Hou, M. & Kambhampati, C., 2005. Neural observer by coordinate transformation. *IEE Proceedings,* 152(6), pp. 698-706.

Demuro, A., 2005. Calcium dysregulation and membrane disruption as a ubiquitous neurotoxic mechanism of soluble amyloid oligomers. *Journal of Biological Chemistry.*

Dodge, J., 1967. *A study of ionic permeability changes underlying excitation in myelinated nerve fibers of the frog,* New York: Rockefeller Institute, Ph.D. Dissertation. .

Dormand, J. & Prince, P., 1980. A family of embedded Runge-Kutta formulae. *Journal of Computational and Applied Mathematics,* 6(1), pp. 19-26.

E. Schneidman, B. F. &. I. S., 1998. Ion Channel Stochasticity May Be Critical in Determining the Reliability and Precision of Spike Timing. *Neural Computation,* 10(7), pp. 1679-1703.

Edwards, C., Spurgeon, S. & Patton, R., 2000. Sliding mode observers for fault detection and isolation. *Automatica,* 36(4), p. 541–553.

Engel, J., Pedley, T. & Aicardi, J., 2008. *Epilepsy: a comprehensive textbook.* Philadelphia: Lippincott-Raven.

Figueroa, V., 2014. Extracellular gentamicin reduces the activity of connexion hemichannels and interferes with purinergic Ca(2+) signaling in HeLa cells. *Frontiers in Cellular Neuroscience,* 4(8), p. 265.

Foran, E. & Trotti, D., 2009. lutamate Transporters and the Excitotoxic Path to Motor Neuron Degeneration in Amyotrophic Lateral Sclerosis. *Antioxidants and redox signalling,* 11(7), pp. 587-602.

Frank, E., 1994. Effect of Alzheimer's Disease on Communication Function. *Journal of the South Carolina Medical Association,* 90(9), p. 417–23.

Frank, P., 1990. Fault diagnosis in dynamic systems using analytical and knowledge-based redundancy. *Automatica,* Volume 26, pp. 459-474.

Frisoni, G., 2017. Strategic roadmap for an early diagnosis of Alzheimer's disease based on biomarkers. *The Lancet Neurology,* 16(8), pp. 661-676.

Frohlich, F. & Jezernik, S., 2005. Feedback control of Hodgkin–Huxleynerve cell dynamics. *Control Engineering Practice ,* Volume 13 , p. 1195–1206.

Frohlich, F. & Jezernik, S., 2005. Feedback control of Hodgkin–Huxleynerve cell dynamics. *Control Engineering Practice,* Volume 13, p. 1195–1206.

Gallagher, P., 2014. *alzheimers now costs the uk 26bn every year major new research suggests,* London: independent.

Gallaway, P., 2017. Physical Activity: A Viable Way to Reduce the Risks of Mild Cognitive Impairment, Alzheimer's Disease, and Vascular Dementia in Older Adults. *Brain Sci,* 7(22).

Gertler, J., 1991. Analytical redunduncy methods in fault detection and isolation. *Fault Detection, Supervision and Safety for Technical,* Volume 1, pp. 9-21.

Geula, C., 1998. Abnormalities of neural circuitry in Alzheimer's disease. *American Academy of Neurology,* pp. S18-S29.

Gijsbersa, L., Mölenberg, F., Bakker, S. & Geleijnsea, J., 2016. Potassium supplementation and heart rate: A meta-analysis of randomized controlled trials. *Nutrition, Metabolism and Cardiovascular Diseases,* 26(8), p. 674–682.

GlendaHalliday, 2017. Pathology and hippocampal atrophy in Alzheimer's disease. *The Lancet Neurology,* 16(11), pp. 862-864.

Gouaux, E. & Mackinnon, R., 2005. Principles of selective ion transport in channels and. *Science,* Volume 310, p. 1461–1465.

Gray, C. M., Konig, P., Engel, A. K. & Singer, W., 1989. Oscillatory responses in cat visual cortex exhibit inter-columnar synchronization which reflects global stimulus properties. *Nature,* Volume 338, p. 334–337.

Grewal, M. S. & Andrews., A. P., 2015. *Kalman Filtering: Theory and Practice with MATLAB.* 4 ed. s.l.:John Wiley & Sons.

Grubbs, F. E., 1969. Procedures for Detecting Outlying Observations in Samples. *Technometrics,* pp. 1-21.

Hampel, D., 2011. The future of Alzheimer's disease: The next 10 years. *Progress in Neurobiology,* Volume 95, pp. 718-728.

HAN, F., WIERCIGROCH, M., FANG, J.-A. & WANG, Z., 2011. EXCITEMENT AND SYNCHRONIZATION OF SMALL-WORLD NEURONAL NETWORKS WITH SHORT-TERM SYNAPTIC PLASTICITY. *International Journal of Neural Systems,* 21(05), pp. 415-425.

Hansel, D., Mato, G. & Meunier, C., 1995. Synchrony in Excitatory Neural Networks. *Neural computation,* 7(2), pp. 307-337.

Hardy, J. & Selkoe, D., 2002. The amyloid hypothesis of Alzheimer's disease: progress and problems on the road to therapeutics. *science,* 297(5580), pp. 353-356.

Ha, Y., Jeong, J., Kim, Y. & Churchill, D., 2016. Sodium and Potassium Relating to Parkinson's Disease and Traumatic Brain Injury. *The Alkali Metal Ions: Their Role for Life,* Volume 16, pp. 585-601.

Hazra, A., 2013. Inhibitory neuron and hippocampal circuit dysfunction in an aged mouse model of Alzheimer's disease. *PloS one,* 8(5).

He, B., 2005. Neural Engineering. In: *Neural Engineering.* Minneapolis: Plenum Publishers, pp. 157-347.

He, J.-H., 2006. A modified Hodgkin–Huxley model. *Chaos, Solitons & Fractals,* p. 303–306.

Hodge, V. J. & Austin, J., 2004. A Survey of Outlier Detection Methodologies. *Artificial Intelligence Review,* pp. 85-126.

Hodgkin, A. & Huxley, A., 1952 a. The Components of membrane conductance in the giant axon of Loligo. *The Journal of Physiology,* pp. 473-496.

Hodgkin, A. & Huxley, A., 1952. A quantitative description of membrane current and its application toconduction and excitation in nerve. *The Journal of Physiology,* 117(4), pp. 500-544.

Hodgkin, A. & Huxley, A., 1952a. Currents carried by sodium and potassium ions through the membrane of the giant axon of Loligo. *Physiol,* Volume 116, p. 49–472.

Hou, M., Busawon, K. & Saif, M., 2000. Observer design based on triangular form generated by injective map. *IEEE Transactions on Automatic Control,* 45(7), pp. 1350 - 1355.

Huxley, A. H. &. A., 1952a. Currents carried by sodium and potassium ions through the membrane of the giant axon of Loligo. *Physiol,* Volume 116, p. 449–472.

Hwang, I., Kim, S. K. Y. & Seah, C. E., 2010. A survey of fault detection, isolation, and reconfiguration methods. *IEEE Trans. on Control Systems Technology,* pp. 636-653.

Isermann, R., 2005. Model-based fault-detection and diagnosis – status and applications. *Annual Reviews in Control,* 29(1), pp. 71-85.

Isermann, R. & Balle, P., 1997. Trends in the application of model-based fault detection and diagnosis of technical processes. *Control engineering practice,* p. 709–719.

Izhikevich, E., 2003. Simple model of spiking neurons. *IEEE Transactions on Neural Networks,* 14(6), pp. 1569-1572.

Jensen, M., 2012. Mechanism of voltage gating in potassium channels. *Science,* 336(6078), pp. 229-233.

Jiang, F., 2017. Artificial intelligence in healthcare: past, present and future. *Stroke and Vascular Neurology,* 2(3).

Joshi, D., 2018. Mental health analysis using deep learning for feature extraction. *In Proceedings of the ACM India Joint International Conference on Data Science and Management of Data,* pp. 356-359.

Kang, Q., Huang, B. & Zhou, M., 2016. Dynamic Behavior of Artificial Hodgkin-Huxley Neuron Model Subject to Additive Noise. *IEEE Transactions on Cybernetics,* 46(9), pp. 2083-2093.

Kanno, Y. & Loewenstein, W., 1964. Low-resistance coupling between gland cells.Some observations on intercellular contact membranes and intracellular pace. *Nature,* Volume 201, p. 194–195.

Kashyap, C., Borkotoki, S. & Dutta, R. k., 2016. Study Of Serum Sodium And Potassium Level In Patients With Alcoholic Liver Disease Attending Jorhat Medical College Hospital - A Hospital Based Study. *International Journal of Health Sciences and Research (IJHSR),* 6(6), pp. 113-116.

Kemmetmüller, W., 2008. *Mathematical Modeling and Nonlinear Control of Electrohydraulic and Electrorheological Systems.* 1 ed ed. Herzogenrath, Germany: Shaker Aachen.

Keun, R. S., Quist, A. P. & Lal, R., 1998. Amyloid β protein-(1–42) forms calcium-permeable, Zn2+-sensitive channel. *Journal of Biological Chemistry,* 273(22), pp. 13379-13382.

Khalastchi, E. & Kalech, M., 2018. On Fault Detection and Diagnosis in Robotic Systems. *ACM Computing Surveys,* 51(1).

Kleer, J. d. & Williams, B. C., 1987. Diagnosing multiple faults. *Artificial Intelligence,* p. 97–130.

Komuro, H. & Kumada, T., 2005. Ca2+ transients control CNS neuronal migration.. *Cell Calcium,* Volume 37, p. 387–393.

Korbicz, J., Koscielny, J., Kowalczuk, Z. & Cholewa, W., 2012. *Fault diagnosis: models, artificial intelligence, applications.* s.l.:Springer Science & Business Media.

Kou, X. & Chen, N., 2017. Resveratrol as a Natural Autophagy Regulator for Prevention and Treatment of Alzheimer's Disease. *Nutrients,* 9(9), p. 927.

Kugi, A., 2001. *Non-linear Control Based on Physical Models: Electrical, Mechanical and Hydraulic Systems (Lecture Notes in Control and Information Sciences).* 1 ed ed. London, Great Britain: Springer.

Kumar, P., 2016. Ion Channels in Neurological Disorders. *Advances in Protein Chemistry and Structural Biology,* Volume 103, pp. 97-136.

Kumar, V., Abbas, A. & Aster, J., 2013. *Robbins Basic Pathology.* Philadelphia: Elsevier.

Kurachi, Y. & North, A., 2004. Ion channels: Their structure, function and control an. *The Journal of Physiology,* Volume 554, p. 245–247.

Labouriau, I. & Rodrigues, H. M., 2003. Synchronization of Coupled Equations of Hodgkin-Huxley Type. *Dynamics of continuous, discrete and impulsive systems; Series A Mathematical Analysis,* 10(1-3), pp. 463-476.

Labouriau, I. S. & Ruas, M. A. S., 1996. Singularities of equations of Hodgkin–Huxley type. *Dynamics and Stability of Systems,* 11(2), pp. 91-108.

Lawrence, T., Beers, W. & Gilula, N., 1978. Transmission of hormonal stimulation by cell-to-cell communication. *Nature,* Volume 272, p. 501–506.

Lee, J., 2017. Amyloid β Ion Channels in a Membrane Comprising Brain Total Lipid Extracts. *ACS Chem. Neurosci,* 8(6), p. 1348–1357.

Lewis, F., 2014. *The Trajectory of Dementia in,* London: Alzheimer's Research UK.

Lindemann, L. & Hoener, M., 2005. A renaissance in trace amines inspired by a novel GPCR family. *Trends Pharmacol,* p. 274–281.

Liu, T., 2012. Fasting activation of AgRP neurons requires NMDA receptors and involves spinogenesis and increasedexcitatory tone. *Neuron,* Volume 73, p. 511–522.

Li, W., Gui, W., Xie, Y. & Ding, S., 2010. Decentralised fault detection of large scale systems with limited network communications. *IET Control Theory,* 4(9), p. 1867–1876.

Lodish, H., 2000. *Molecular cell biology.* 4th ed ed. New York: W.H. Freeman.

Lorin, E. & Deborah, S., 2006. *Neuropsychology: Clinical and Experimental Foundations.* Boston: Pearson/Allyn & Bacon.

LuWang, M., Wen, J. & Dong, X.-W., 2016. *Implementation of Hodgkin-Huxley neuron model in FPGAs.* s.l., Asia-Pacific International Symposium on Electromagnetic Compatibility.

MA, B., 2008. Clusters of hyperactive neurons near amyloid plaques in a mouse model of Alzheimer's disease. *Science,* 321(5896), pp. 1686-9.

Madry, C., Haglerød, C. & Attwell, D., 2010. The role of pannexin hemichannels in the anoxic depolarization of hippocampal pyramidal cells. *Brain,* Volume 133, p. 3755–3763.

Mahmud, M. & Vassanelli, S., 2016. Differential modulation of excitatory and inhibitory neurons during periodic stimulation. *Frontiers in Neuroscience,* Volume 10.

Mantzavinos, V., Alexiou, A., Greig, N. H. & Kamal, M. A., 2017. Biomarkers for Alzheimer's Disease Diagnosis. *Current Alzheimer Research,,* Volume 14, pp. 1-6.

Matsuda, K., Hoshi, T. & SKameyama, 1958. Electrophysiology of the heart. *J. Exp. Med,* 66(8).

Mattson, M., 2004. Pathways towards and away from Alzheimer's disease. *Nature,* 430(7000), p. 631–639.

Mazur, J., 2006. Mathematical Models and the Experimental Analysis of Behavior. *Exp Anal Behav,* 85(2), p. 275–291.

McKhannab, G., 2011. The diagnosis of dementia due to Alzheimer's disease: Recommendations from the National Institute on Aging-Alzheimer's Association workgroups on diagnostic guidelines for Alzheimer's disease. *Alzheimer's & Dementia,* 7(3), pp. 263-269.

Melnik, R., 2015. *Mathematical and Computational Modeling: With Applications in Natural and Social Sciences.* 1 ed ed. New Jersey: John Wiley & Sons.

Mendez, M., 2017. Early-Onset Alzheimer Disease. *Neurologic Clinics,* 35(2), p. 263–281.

Mes¸e, G., Richard, G. & White, T., 2006. Gap junctions: Basic structure and function. *Journal of Investigative Dermatology,* Volume 127, p. 2516–2524.

Migliaccio, R., 2015. Mapping the Progression of Atrophy in Early- and Late-Onset Alzheimer's Disease. *J Alzheimers Dis,* 46(2), pp. 351-64.

Minkeviciene, R., 2009. Amyloid β-Induced Neuronal Hyperexcitability Triggers Progressive Epilepsy. *Journal of Neuroscience,* 29(11), pp. 3453-3462.

Montoliu-Gaya, L. & Villegas, S., 2018. Immunotherapy for neurodegenerative diseases: the Alzheimer's disease paradigm. *Current Opinion in Chemical Engineering,* Volume 19, p. 59–67.

Mylvaganam, S., Ramani, M., Krawczyk, M. & Carlen, P., 2014. Roles of gap junctions, connections, and pannexins in epilepsy. *Frontiers in Physiology,* Volume 5, p. 172.

NICE, 2018. *Dementia diagnosis and assessment,* London: National Institute for Health and Care Excellence (NICE) .

Nygren, A., 1998. Mathematical model of an adult human atrial cell: The role of K+ currents in repolarization. *Circulation Research,* 82(1), pp. 63-81.

Obreja, A.-R., Ross, P. & Bednar, P., 2017. Intelligent Systems in Health Care: A Socio-Technical View. *Reshaping Accounting and Management Control Systems,* Volume 20, pp. 221-236.

Odish, H., Berk, A. & Zipursky, S., 2000. *Molecular Cell Biology: Section 21.4Neurotransmitters, Synapses, and Impulse Transmission.* New York: W. H. Freeman.

Orellana, J., 2009. Modulation of brain hemichannels and gap junction channels by proinflammatory agents and their possible role in neurodegeneration. *Antioxidants & Redox Signaling,* Volume 2, p. 369–399.

Osipov, G., Kurths, J. & Zhou, C., 2007. *Synchronization in Oscillatory Networks.* 1st ed. New York: Springer.

Palop, J. & Mucke, L., 2009. Epilepsy and cognitive impairments in Alzheimer disease. *Arch Neurol,* 66(4), pp. 435-40.

Parton, L. et al., 2007. Glucose sensing by POMC neurons regulates glucose homeostasis and is impaired in obesity. *Nature,* Volume 449, p. 228–232.

Patel, V., 2017. *Office for National Statistics.* [Online] Available at:

https://www.ons.gov.uk/peoplepopulationandcommunity/birthsdeathsandmarriages/deaths/bulletins/deathsregisteredinenglandandwalesseriesdr/2015

[Accessed 30 12 2017].

Patton, R. & Chen, J. .., 1991. A review of parity space approaches to fault diagnosis. *Fault Detection, Supervision and Safety for Tech,* Volume 1, pp. 65-81.

Patton, R. & Chen, J., 1993. Optimal selection of unknown input distribution matrix in the design of robust observers for fault diagnosis. *Automatica,* 29(4), pp. 837-841.

Perez, C., Ziburkus, J. & Ullah, G., 2016. Analyzing and Modeling the Dysfunction of Inhibitory Neurons in Alzheimer's Disease. *PLOS ONE,* 11(12), pp. 1-24.

Perez, C., Ziburkus, J. & Ullah, G., 2017. Analyzing and Modeling the Dysfunction of Inhibitory Neurons in Alzheimer's Disease. *Biophysical Journal,* 112(3).

Pikovsky, A., Rosenblum, M. & Kurths, J., 2003. *Synchronization. A Universal Concept in Nonlinear Sciences.* 1 st ed. Cambridge : Cambridge .

Pikovsky, A., Rosenblum, M. & Kurths, J., 2003. *Synchronization: a universal concept in nonlinear.* 1 ed. Cambridge: Cambridge University.

Plonsey, R. & Barr, R., 2007. *Bioelectricity: A Quantitative Approach.* New York: Springer.

Poon, J., 2017. Model-Based Fault Detection and Identification for Switching Power Converters. *IEEE Transactions on Power Electronics ,* 32(2), pp. 1419 - 1430.

Prinz, P. & Vitiell, M., 1989. Dominant occipital (alpha) rhythm frequency in early stage Alzheimer's disease and depression. *Electroencephalography and Clinical Neurophysiology,* pp. 427-432.

Public-Health-England, 2017. *major causes of death and how they have changed.* [Online]

Available at: https://www.gov.uk/government/publications/health-profile-for-england/chapter-2-major-causes-of-death-and-how-they-have-changed

[Accessed 10 05 2018].

Q Cheng, P. V., Michels, J. & Belcastro, C., 2005. *Distributed fault detection via particle filtering and decision fusion.* Philadelphia, Proceedings of Information Fusion, p. 1239–1246.

Quintanilla, R., Orellana, J. & Bernhardi, R. V., 2012. Understanding risk factors for Alzheimer's disease: Interplay of neuroinflammation, connexin-based communication and oxidative stress. *Archives of Medical Research,* Volume 43, p. 632–644.

Raggi, et al., 2017. Health-related quality of life in community dwelling patients with mild-to-moderate Alzheimer's disease. *European Geriatric Medicine,* 8(2), pp. 158-163.

Raman, I. & Bean, B., 1999. Ionic Currents Underlying Spontaneous Action Potentials in Isolated Cerebellar Purkinje Neurons. *Journal of Neuroscience ,* 19(5), pp. 1663-1674.

Regev, K. & Weiner, H., 2017. Clinical Research in Neurology. *Clinical and Translational Science ,* pp. 555-571.

Reitz, C. & Mayeux, R., 2014. Alzheimer disease: epidemiology, diagnostic criteria, risk factors and biomarkers. *Biochemical Pharmacology,* 88(4), p. 640–51.

Rodriguesa, G., 2017. Mineral status and superoxide dismutase enzyme activity in Alzheimer's disease. *Journal of Trace Elements in Medicine and Biology,* Volume 44, pp. 83-87.

Roh, J., 2012. Disruption of the sleep-wake cycle and diurnal fluctuation of β-amyloid in mice with Alzheimer's disease pathology. *Sci Transl Med,* 4(150).

Rossetto, M., 2016. A note on the falsification of the ionic theory of hair cell transduction. *COMMUNICATIVE & INTEGRATIVE BIOLOGY,* 9(2).

Rossini, P. M., 2006. Conversion from mild cognitive impairment to Alzheimer's disease is predicted by sources and coherence of brain electroencephalography rhythms. *Neuroscience,* p. 793–803.

Sadegh Zadeh, S.-A. & Kambhampati, C., 2017. *All-or-None Principle and Weakness of Hodgkin-Huxley Mathematical Model.* London, 19th International Conference on Systems Biology and Bioengineering.

Sadeghzadeh-Nokhodberiz, N. & Poshtan, J., 2014. Belief consensus–based distributed particle filters for fault diagnosis of non-linear distributed systems. *Systems and Control Engineering,* 228(3), p. 1–15.

Sadegh-Zadeh, S.-A. & Kambhampati, C., 2017. All-or-None Principle and Weakness of Hodgkin-Huxley Mathematical Model. *International Journal of Mathematical and Computational Sciences,* 11(11).

Sadegh-Zadeh, S.-A. & Kambhampati, C., 2018. *A Computational Investigation of the Role of Ion Gradients in Signal Generation in Neurons.* London, Computing Conference 2018.

Sadegh-Zadeh, S.-A. & Kambhampati, C., 2019. Computational Investigation of Amyloid Peptide Channels in Alzheimer's Disease. *J ,* 2(1), pp. 1-14.

Sarangdhar, M., 2010. *A Computational Framework for Similarity Estimation and Stimulus Reconstruction of Hodgkin-Huxley Neural Responses,* HULL: THE UNIVERSITY OF HULL.

Sarangdhar, M. & Kambhampati, C., 2008. *Spiking Neurons: Is coincidence-factor enough for comparing responses with fluctuating membrane voltage?*. London, World Congress on Engineering.

Sarangdhar, M. & Kambhampati, C., 2011. Quantification of Similarity Using Amplitudes and Firing Times of a Hodgkin–Huxley Neural Response. *Electrical Engineering and Applied Computing,* Volume 90, pp. 687-698.

Scarpioni, R., Ricardi, M. & Albertazzi, V., 2016. Secondary amyloidosis in autoinflammatory diseases and the role of inflammation in renal damage. *World Journal of Nephrology,* 5(1), p. 66–75.

Scatton, B., 1986. Degeneration of Noradrenergic and Serotonergic but not Dopaminergic Neurones in the Lumbar Spinal Cord of Parkinsonian Patients. *Brain Research,* Volume 380, pp. 181 - 185.

Schrick, D. v., 1997. *Remarks on terminology in the field of supervision, fault detection and diagnosis.* HULL, s.n.

Serretti, A., 2017. Alzheimer's Disease And Neurotransmission Gene Variants. *European Neuropsychopharmacology,* 27(3), p. S438.

Sierpina, V. S. & Kreitzer, M. J., 2012. Life-Long Learning in Integrative Healthcare. *The Journal of Science and Healing,* Volume 8, pp. 210-212.

Silva, A., Belli, A. & Smith, M., 2016. Electrolyte and endocrine disturbances. In: A. Kofke, ed. *Oxford Textbook of Neurocritical Care.* Oxford: Oxford, pp. 375-386.

Silverthorn, D.-U., 2007. *Human Physiology: An Integrated Approach.* San Francisco: Pearson.

Singer, W., 1999. Neurobiology: Striving for coherence. *Nature ,* 397(4), pp. 391-393.

Sohn, J., 2013. Ion channels in the central regulation of energy and glucose homeostasis. *Frontiers in Neuroscience,* 7(85).

Soininen, H., 1992. Slowing of electroencephalogram and choline acetyltransferase activity in post mortem frontal cortex in definite Alzheimer's disease. *Neuroscience,* p. 529–535.

Stage, E., 2017. Brain Atrophy in Early and Late Onset Alzheimer's Disease and Suspected Non-Alzheimer's Pathophysiology. *Neurology,* 88(16), pp. P4-098.

Steinmetz, P., 2000. Attention modulates synchronized neuronal firing in primate somatosensory cortex. *Nature,* 404(9), p. 187–190.

Stern, E., Jaeger, D. & Wilson, C. J., 1998. Membrane potential synchrony of simultaneously recorded striatal spiny neurons in vivo. *Nature,* Volume 394, p. 475–478.

Stopfe, M., Bhagavan, S., Smith, B. & Laurent, G., 1997. Impaired odour descrimination on desynchronization of odour-encoding neural assemblies. *Nature,* 390(6), p. 70–74.

Strange, K., 2004. Cellular volume homeostasis. *Advances in Physiology Education,* Volume 28, p. 155–159.

Strange, P., 1992. *Brain Biochemistry and Brain Disorders.* New York: Oxford University Press.

Suh, J., 2017. Statistical Interpretation on Alzheimer's Disease. *International Research Journal of Advanced Engineering and Science,* 2(2), pp. 343-349.

Suresh, M., Fischl, B. & Salat, D. H., 2018. Factors influencing accuracy of cortical thickness in the diagnosis of Alzheimer's disease. *Alzheimer's Disease Neuroimaging Initiative (ADNI),* 39(4), pp. 1500-1515.

Takahashi, R., Nagao, T. & Gouras, G., 2017. Plaque formation and the intraneuronal accumulation of β-amyloid in Alzheimer's disease. *Pathology International,* 67(4), p. 185–193.

Takeda, S. & Morishita, R., 2017. Diabetes and Alzheimer's Disease. *Diabetes and Aging-related Complications,* pp. 101-111.

To¨mbo¨l, T., 1967. Short neurons and their synaptic relations in the specific thalamic nuclei. *Brain Research,* p. 307–326.

Trenor, B., 2017. Cardiac action potential repolarization re-visited: early repolarization shows all-or-none behaviour. *The Journal of Physiology,* 595(17).

Ullah, G., Demuro, A., Parker, I. & Pearson, J., 2015. Analyzing and modeling the kinetics of amyloid beta pores associated with Alzheimer's disease pathology. *PloS one.*

Vega, J., 2013. Role of gap junctions and hemichannels in parasitic infections. *BioMed Research International.*

Venkatasubramaniana, V., Rengaswamyb, R., Yinc, K. & Kavurid, S. N., 2003. A review of process fault detection and diagnosis: Part I: Quantitative model-based methods. *Computers & Chemical Engineering,* p. 293–311.

Verkhratsky, A. & Butt, A., 2013. Numbers: how many glial cells are in the brain?. In: *Glial Physiology and Pathophysiology.* s.l.:John Wiley and Sons, p. 93–96.

Verret, L., 2012. Inhibitory interneuron deficit links altered network activity and cognitive dysfunction in Alzheimer model. *Cell,* 149(3), p. 708–721.

Vinken, M., 2006. Connexins and their channels in cell growth and cell death. *Cellular Signalling,* Volume 18, p. 592–600.

Vitvitsky, V. M., 2012. Na+ and K+ ion imbalances in Alzheimer's disease. *Biochimica et Biophysica Acta (BBA)-Molecular Basis of Disease,* 1822(11), pp. 1671-1681.

Vladimir N., 2008. Cluster synchronization in oscillatory networks. *Chaos: An Interdisciplinary Journal of Nonlinear Science,* Volume 18, pp. 037106-1 - 037106-6.

Waldemar, G., 2007. Recommendations for the diagnosis and management of Alzheimer's disease and other disorders asscociated with dementia. *European Journal of Neurology,* 14(1), p. e1–e26.

Walkowska, A., 2016. Effects of high and low sodium diet on blood pressure and heart rate in mice lacking the functional Grainyhead-like 1 gene. *Physiological research.*

Waxman, S., 2012. Sodium channels, the electrogenisome and the electrogenistat: lessons and questions from the clinic. *The Journal of Physiology,* Volume 590, p. 2601–2612.

Weilinger, N., 2013. Ionotropic receptors and ion channels in ischemic neuronal death and dysfunction. *Acta Pharmacologica Sinica,* Volume 34, p. 39–48.

Whelton, P., 2016. Hyponatremia in the general population. What does it mean?. *PubMed,* 26(1), pp. 9-12.

White, T. & Paul, D., 1999. Genetic diseases and gene knockouts reveal diverse connexin functions. *Annual Review of Physiology,* Volume 61, p. 283–310.

Winkler, S., 2014. Comparative mathematical modelling of groundwater pollution. *Doctoral dissertation.*

World-Health-Organization, 2015. *Dementia.* [Online] Available at: http://www.who.int/mediacentre/factsheets/fs362/en/

Yang, H. & Saif, M., 1998. Observer design and fault diagnosis for state retarded dynamical systems. *Automatica,* 34(2), p. 217–227.

Yang, X. & Tang, Y., 2007. Efficient fault identification of diagnosable systems under the comparison model problem. *IEEE T Comput,* 56(12), p. 1612–1618.

Yang, Y., Mufson, E. J. & Herrup, K., 2003. Neuronal Cell Death Is Preceded by Cell Cycle Events at All Stages of Alzheimer's Disease. *The Journal of Neuroscience,* pp. 2557-2563.

Young, T., Kirchner, A., Wedd, A. G. & Xiao, Z., 2014. An integrated study of the affinities of the Aβ16 peptide for Cu(I) and Cu(II): implications for the catalytic production of reactive oxygen species. *Metallomics,* Volume 6, pp. 505-517.

Zhang, K., Jiang, B. & Cocquempot, V., 2008. Adaptive observer-based fast fault estimation. *International Journal of Control, Automation, and Systems,* 6(3), pp. 320-326.